

R-90.14

FINAL REPORT ON

LUNAR ORBITER VISUAL OBSERVATION INSTRUMENT SUBSYSTEM

CONTRACT NO. 950005

13 JANUARY 1961

FACILITY FORM 602

N65-88352
(ACCESSION NUMBER)
108
(PAGES)
CR-67152
(NASA CR OR TMX OR AD NUMBER)

(THRU)
None
(CODE)
(CATEGORY)

TO
JET PROPULSION LABORATORY
CALIFORNIA INSTITUTE OF TECHNOLOGY
PASADENA, CALIFORNIA

BY
ASTRO-ELECTRONICS DIVISION
RADIO CORPORATION OF AMERICA
PRINCETON, NEW JERSEY



TABLE OF CONTENTS

<u>Section</u>		<u>Page</u>
I.	INTRODUCTION	1
II.	SYSTEMS ANALYSIS	5
	A. Introduction	5
	B. Orbital Constraints	5
	C. General System Configuration	9
	1. Panoramic Scan System	9
	2. Stripping System	17
	D. Systems Constraints	25
	E. Systems Requirements	41
III.	COMPONENT ANALYSIS	45
	A. Communication System	45
	B. Electrostatic Storage Tape Camera	55
	C. Objective Lens	80
	D. Structure	86
IV.	SUMMARY	99

LIST OF ILLUSTRATIONS

<u>Figure</u>		<u>Page</u>
II-1	Orbital Parameters for Circular Orbits	6
II-2	Effect of 10% Circularity on Orbit	7
II-3	Orbital Separation at the Equator versus Altitude	8
II-4	Camera System Layout	11 & 12
II-5	Panoramic Scan Geometry	13
II-6	Maximum Resolution Versus Orbital Altitude at 200 T. V. lines/mm with 36 Inch, F/2.5 Lens	15
II-7	Camera Angle and Scan Angle Versus Altitude	16
II-8	Length and Width of Lunar Surface Imaged per Scan Versus Altitude	18
II-9	Time Between Scans Versus Altitude	19
II-10	Angular Scan Rate Over the Lunar Surface Versus Altitude	20
II-11	Tape Speed Versus Altitude for a 36 Inch Focal Length Lens	21
II-12	Storage Time Per Camera for 1500 Feet of Tape	22
II-13	Required Angular Field-of-View Versus Altitude for Alternate System	24
II-14	Maximum Resolution Versus Orbital Altitude at 100 T. V. lines/mm with 12 Inch, F/4 Lens	26
II-15	Angular Velocity of Image as a Function of Altitude	27
II-16	Variation of $\left(\frac{\Delta\omega_o}{\omega_o}\right)$ Versus Altitude	29
II-17	Geometry for Altitude Stabilization Errors	30

LIST OF ILLUSTRATIONS (Cont.)

<u>Figure</u>		<u>Page</u>
II-18	Image Twist Factor K_r as a Function of Roll Angle	32
II-19	Image Illumination Versus Object Latitude and Sun Angle for $F/4$ Lens	36
II-20	Image Illumination Versus Object Latitude and Sun Angle for $F/4$ Lens	37
II-21	Mosaic and Test Samples	39
III-1	Measured Sine Wave Response of a 0.01μ a Beam.....	49
III-2	RF Bandwidth Versus Modulation Index for (a) Uniform Modulating Spectrum, and (b) Modulating Spectrum of Vidicon	50
III-3	(a) Typical Pre-Emphasis Circuit, and (b) De- Emphasis Circuit	51
III-4	Transient Response of Circuit of Figure III-3. a to a Rectangular Wave, (a) Input Wave, (b) Output Wave	53
III-5	Typical Bridged "T" All Pass Network Used for Phase Correction	54
III-6	Electrostatic Storage Tape Camera	59
III-7	Two Speed, Two Motor Transmission	60
III-8	Experimental Electrostatic Storage, Return-Beam Readout Tube	64
III-9	EST Camera Enclosure	71
III-10	EST Camera System Block Diagram	73
III-11	Electron-Beam Film Recorder Block Diagram.....	74
III-12	EST Target and Component Test "Cube"	75

LIST OF ILLUSTRATIONS (Cont.)

<u>Figure</u>	<u>Page</u>
III-13 Response of Two Imaging Components Having the Same Limiting Resolution	77
III-14 Comparison of Theoretical Line-Wave Response of Obscured and Non-Obscured Optical Systems	79
III-15 Optical Schematics	81
III-16 Spectral Response Curves	83
III-17 Electrostatic Tape Camera Layout	84
III-18 Camera System Layout	87 & 88
III-19 Position of VOIS Package During Launch and Orbital Injection Phases	89
III-20 Scanning (Wobble) Mirror	91
III-21 Scanning Mirror Back Plate Mounting	92
III-22 Scanning (Elliptical) Mirror Details	93
III-23 Rear Mirror Drive and Support Details	94
III-24 (a) Acceleration - Velocity - Displacement Diagram, (b) Torque Curve Diagram	96
III-25 (a) Displacement Diagram, (b) Torque - Acceleration - Velocity Diagram	97

I. INTRODUCTION

The VOIS is designed to accomplish several functions. Of these functions, the mapping of the entire surface of the moon at a reasonably high resolution and the observation of selected areas of the lunar surface at higher resolution have the greatest priority. It is also desirable to accomplish stereoscopic or three-dimensional viewing of the lunar surface and correlation of the mapping information with other experiments included in the vehicle. The VOIS package will be an integral part of a spacecraft designed for this mission. It will be the primary experiment associated with the spacecraft and, as a result, will dictate the requirements of the spacecraft in the areas of:

- a. Guidance and Attitude Control
- b. Environmental Control.
- c. Auxiliary power supply.
- d. Communications

This report represents the results of the study program under Contract No. 950005. The purpose of the study was to determine the limitations of the selected system in accomplishing the desired mission while considering the constraints imposed upon the system by the interface requirements. At the initiation of the study program certain tolerances on the interface requirements were defined by JPL, and these are listed in Table I-1. In general, the study program was conducted in a parametric manner so that trade-off between VOIS capabilities and interface requirements might be accomplished.

The study program was divided into separate sections corresponding to the major subsystem components. These areas are:

- a. Systems Analysis.
- b. Communications System.
- c. Electrostatic Storage Tape Camera.
- d. Optical System.

The following sections of this report discuss the results of the study in each of these areas.

The electrostatic storage tape camera is utilized as the sensor for the system. The EST camera is an RCA development principally for space

application because of its advantages in this medium, some of which are as follows:

1. The tape itself is capable of inherently high resolution with the overall resolution being limited only by the electronic readout process. Even so, the system will offer a resolution capability of 200 TV lines/mm in the near future, rivaling photographic films for space application. The sensitivity and dynamic range of the EST permit imaging at low illumination levels with short exposures thereby alleviating image motion compensation problems.
2. The EST, though it has not been thoroughly tested for the radiation environment of space, has shown promising results when exposed to the equivalent of Van Allen radiation. No image or tape degradation was discernible in these tests.
3. The tape is erasable and reusable. Thus, for a continuing program only a limited amount of tape is required providing an imaging sensor throughout the lifetime of the system. Furthermore, the EST can be read-out several times without degrading the image stored on the tape.
4. There is no intermediate step required between imaging and read-out for transmission. The EST images and reads out without intermediate storage or data processing.
5. The EST is also capable of analog and digital storage offering a high density storage medium for other than imaged data.
6. Versatility of programming is also available with the EST since program variation is controllable by electronics.

Because of these characteristics the EST camera is especially suited for the VOIS and is the exclusive sensor considered in this study.

Table I-1

Preliminary Interface Characteristics

Payload Weight	300 - 500 pounds
Auxiliary Power	Several hundred watts
Orbital Characteristics	
Altitude (average)	100 - 500 km
Orbit Orientation	Polar \pm 1 degree
Circularity	1 - 10%
Transmission Characteristics	
frequency	2300 mc
R-F Bandwidth	\pm 2 mc
Ground Antenna Gain	50 db
Vehicle Antenna Gain	26 db
System Noise Temperature	400°K
Attitude Stabilization	Local Vertical (\pm 0.1 degree for three axes system)
Attitude Stabilization Rates	0.01 to 0.1 degrees/hour
Resolution	Highest obtainable (about 1 meter desired)
Lifetime	90 days

II. SYSTEMS ANALYSIS

A. INTRODUCTION

The basic system considered in this study program consists of an optical system, an electrostatic storage tape camera, and an s-band transmitter for relaying the images to the ground stations on earth. The optical image is projected on the electrostatic tape via a slit in the camera which is oriented at all times so that its longitudinal axis is normal to the image motion. The EST is moved past the slit so that its motion is synchronous with the image motion, thus producing on the tape a latent electrostatic image of the lunar surface. In the Interim Report, only a single system making use of panoramic scanning to obtain the required fields of view was presented. In this report two possible systems are presented. The primary system still makes use of the panoramic scan technique and is essentially the same as reported in the interim report. An alternate system is also proposed in which the scanning is produced by the motion of the vehicle in orbit. In this sense a continuous strip of the lunar surface is imaged on the EST for each orbit. The advantage of this system over the panoramic type system is that it eliminates the need for a scanning mirror and simplifies the ground data handling. However, the alternate system suffers from the requirement of wide angle fields-of-view and will not yield the maximum level of resolution with continuous coverage obtainable with the panoramic system. Both systems are described in the following sections.

B. ORBITAL CONSTRAINTS

The characteristics of lunar circular orbits in the altitude range from 100 to 500 kilometers were given in the interim report and are reproduced in Figure II-1. This analysis neglected perturbations to the orbit. Also presented in the previous report was the effect of 10% circularity on the orbital parameters of interest. This is shown in Figure II-2 of this report. One other parameter of interest is the amount the moon rotates under the orbit between successive passes of the satellite. This has been calculated for the lunar equatorial plane and is given in Figure II-3.

The effect of perturbations on the orbit over the operational life span of the satellite primarily affects the orbital eccentricity. The analysis presented in reference (1)* indicates that for nearly circular polar orbits the orbital inclination will change less than 1 degree from a polar orbit and that the eccentricity will change by less than a factor of e in one year. Making use

*Reference (1) "The Motion of a Satellite of the Moon", by Harry Lass; Jet Propulsion Laboratory Technical Release No. 34-56, dated 28 April 1960.

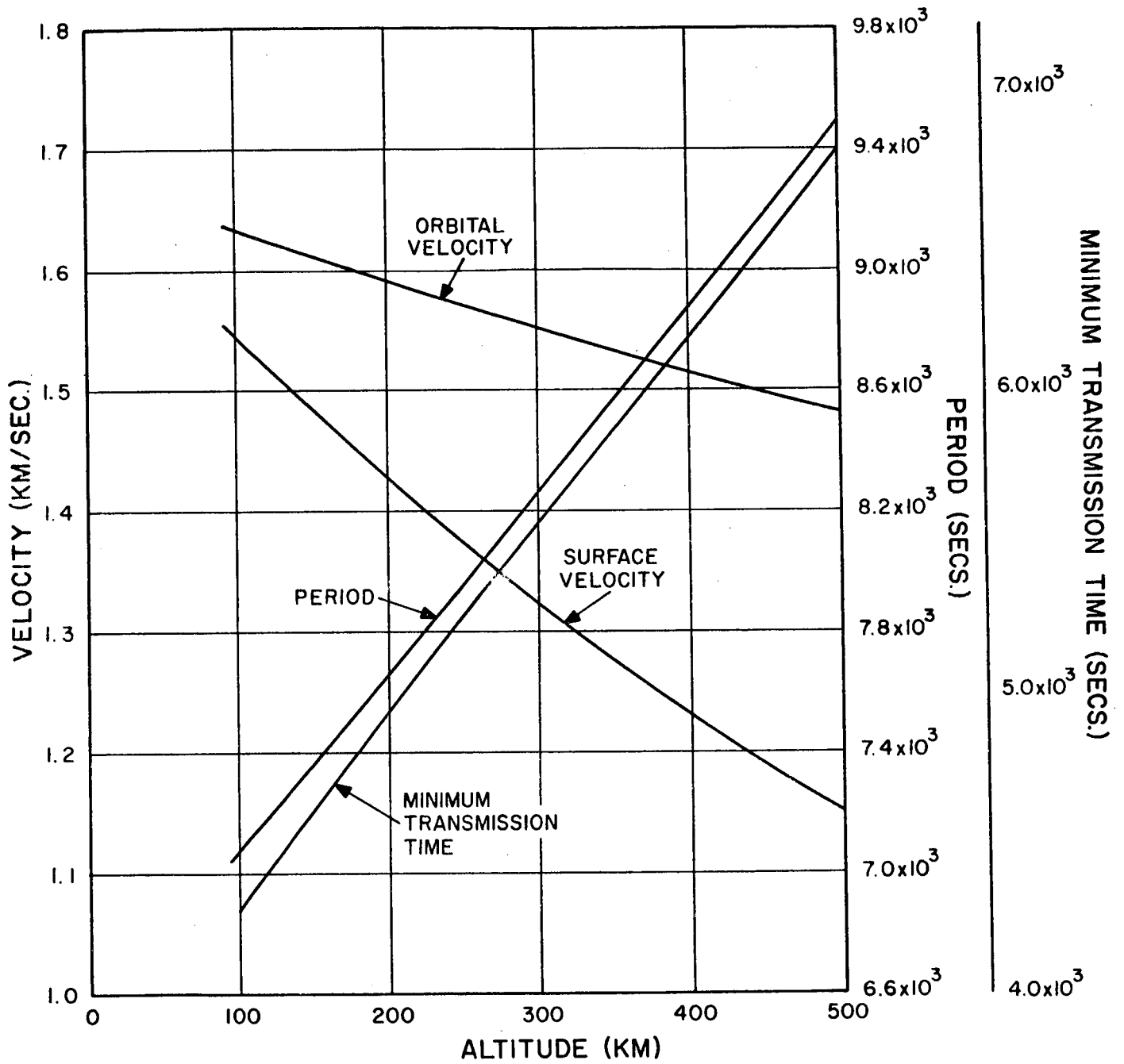


Figure II-1. Orbital Parameters for Circular Orbits

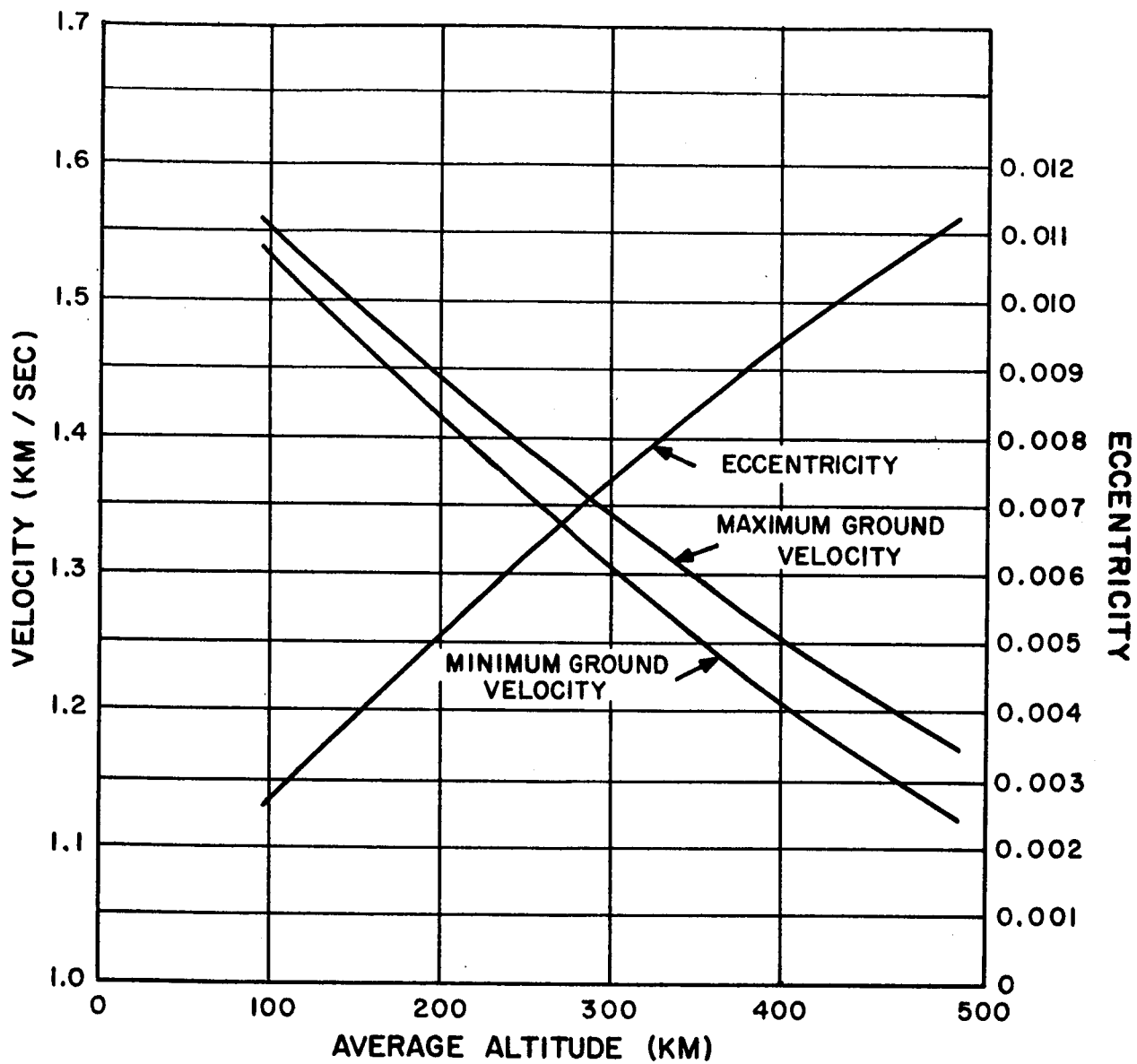


Figure II-2. Effect of 10% Circularity on Orbit

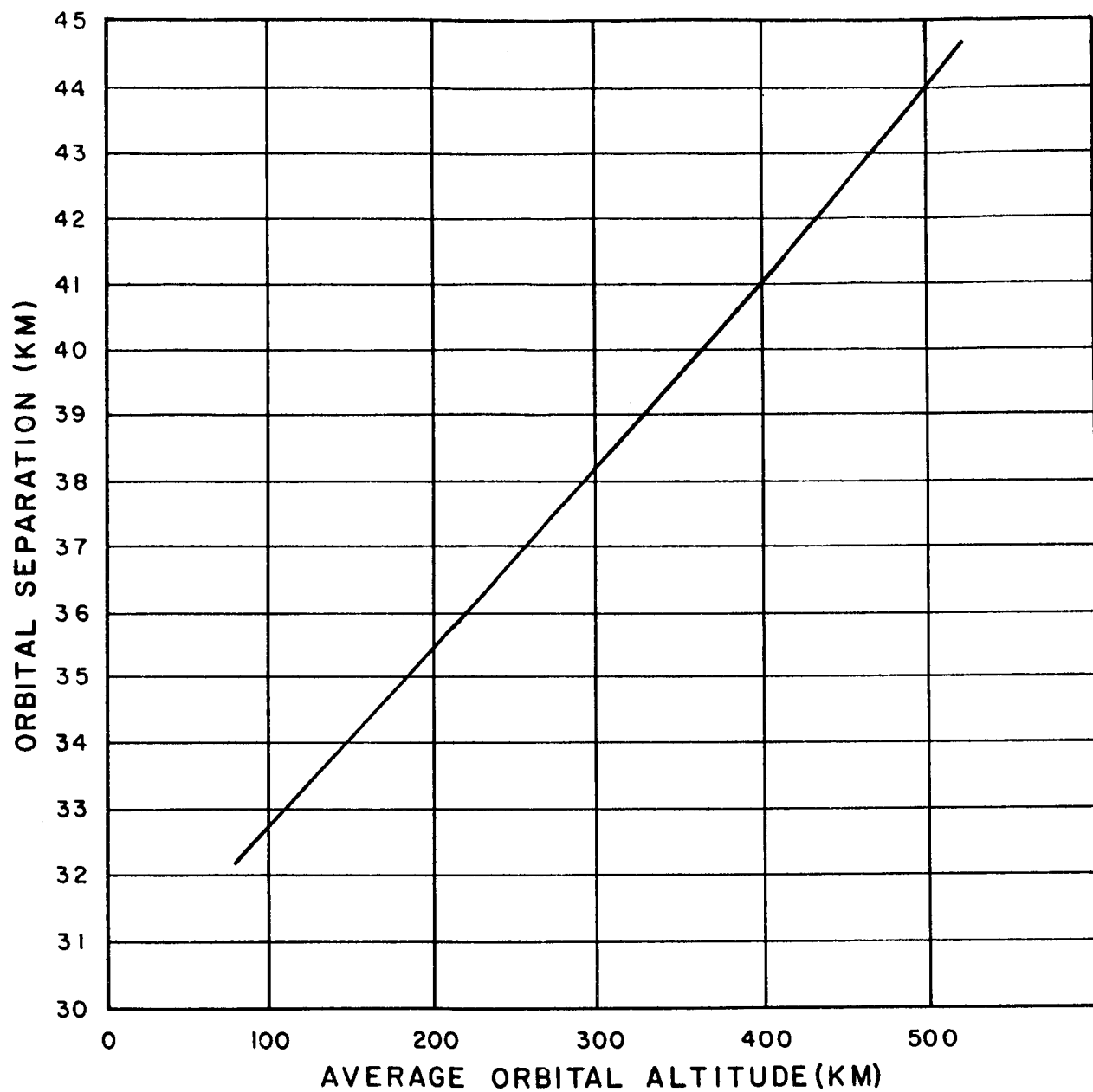


Figure II-3. Orbital Separation At The Equator Versus Altitude

of equation 49 in reference (1) the change in eccentricity over the 90 day operational lifetime may be calculated to be less than a factor of 1.25, or a 25% change in eccentricity. This effect will affect the system primarily in image motion compensation. However, because of the small change this is not expected to lead to an exceptional amount of image smear and can be controlled by varying the exposure time to compensate for it. The effect of image motion compensation is discussed later in this report.

C. GENERAL SYSTEM CONFIGURATION

1. Panoramic Scan System

The system described in the interim report covers the essentials of the panoramic scan system. The general philosophy of imaging at the maximum resolution capability of the system with readout at three levels of resolution remains the same as reported in the interim report. The following sections describe this system in more detail and with some modifications to the system discussed in the interim report.

a. Basic System Configuration

The general layout for this system is shown in Figure II-4. Its primary components consist of a scanning mirror, an f/2.5-36 inch focal length Baker Catadioptric lens system, and four 70 mm electrostatic tape cameras. Exposure control is maintained by pulling the tape passed a slit at a continuous speed consistent with the requirements of the system. The panoramic scan is accomplished across the subsatellite path. The lunar surface is thus imaged in a piecemeal fashion onto a continuous strip of electrostatic tape, the scanning mirror scanning over the necessary field-of-view and at the proper frequency to permit continuous mapping of the surface with a 10% overlap and sidelap between scans and orbits respectively. The system contains sufficient storage for several days of operation and the storage is reusable throughout the lifetime of the vehicle.

b. System Parameters

Consider the geometry shown in Figure II-5. Because of the fact that the vehicle is moving in orbit and the scanning mirror scans normal to the orbit the strip of the lunar surface mapped onto the tape will be canted to the direction of motion of the satellite.

From the geometry:

$$l = (l' - W \sin \xi) \cos \xi \quad (1)$$

where l = required orbital separation with 10% sidelap,

l' = length of the lunar surface swath imaged per scan,

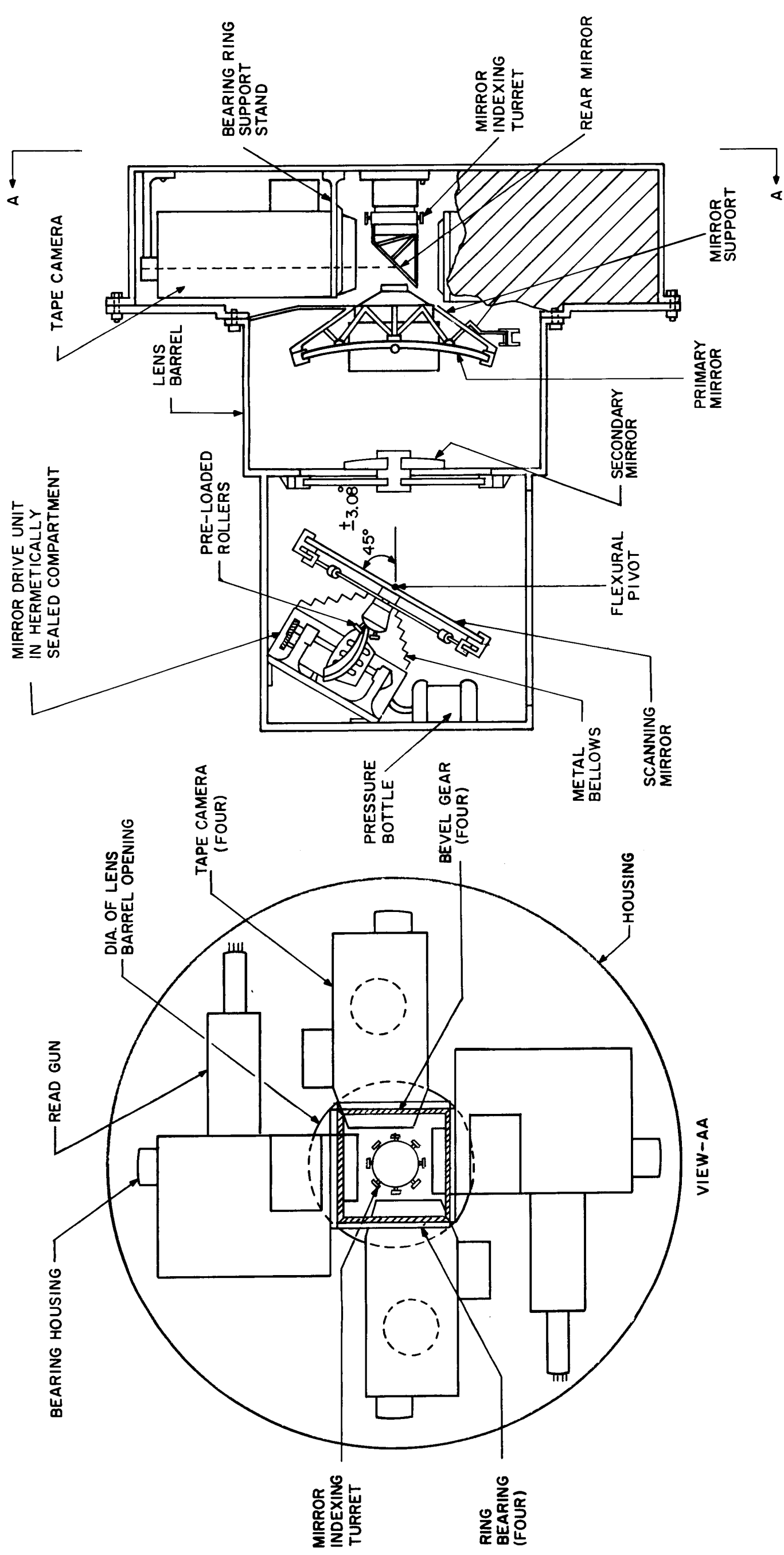


Figure 11-4. Camera System Layout

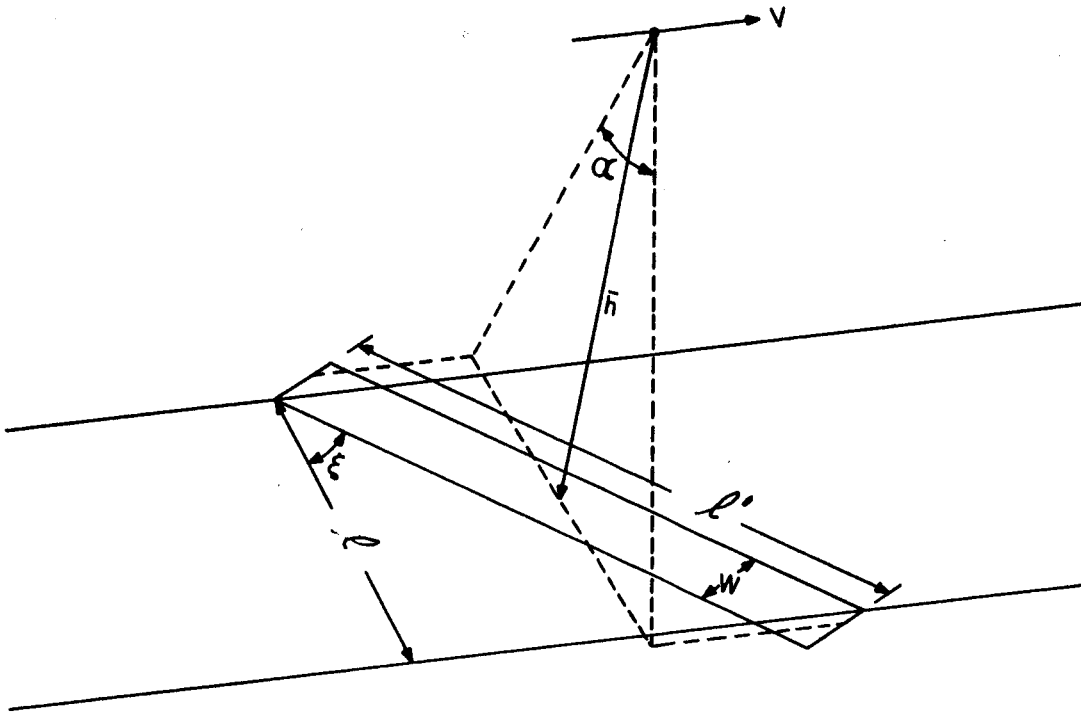


Figure II-5. Panoramic Scan Geometry

W = width of the lunar surface swath imaged per scan,

ξ = angle defined by the scanning velocity and the velocity of the vehicle over the lunar surface.

The total scan angle, α , is given by

$$\alpha = 2 \tan^{-1} \left[\frac{l + W \sin \xi}{2\bar{h}} \right] \quad (2)$$

where,

\bar{h} = average orbital altitude.

Assuming a 10% overlap between swaths (along a direction normal to the swath length) the distance moved over the lunar surface between swaths is given by

$$\Delta s = \frac{0.9W}{\cos \xi}$$

and the time between swaths, t_s , is given by

$$t_s = \frac{\Lambda_s}{V_s} = \frac{0.9 W}{V_s \cos \xi} \quad (3)$$

The time, t_s , will be composed of the time to scan through the required angle, α , for imaging plus the dead time (for flyback and accelerating to speed). Thus, if $\dot{\alpha}$ is the scanning speed of the mirror over the lunar surface during imaging then

$$\dot{\alpha} = \frac{\alpha}{0.9 t_s} \quad (4)$$

where a 10% dead time is assumed.

The image motion is composed of two components of angular velocity; one normal to the orbital plane generated by the scanning mirror, ω_x ; and one parallel to the orbital plane generated by the motion of the vehicle, ω_y . The total image motion then is:

$$\omega^2 = \omega_x^2 + \omega_y^2 \quad (5)$$

where

$$\omega_x = \omega \sin \xi = \dot{\alpha}$$

$$\omega_y = \omega \cos \xi = V_s / \bar{h}$$

Thus,

$$\frac{\dot{\alpha} \bar{h}}{V_s} = \tan \xi$$

and by substitution from equations 4 and 2 we obtain

$$\tan \xi = \left(\frac{2 \bar{h} \cos \xi}{0.81 W} \right) \tan^{-1} \left[\frac{1}{2 \bar{h}} (1 + W \sin \xi) \right] \quad (6)$$

Equation 6 may then be solved for ξ for a given altitude \bar{h} , optical focal length, f , and tape format size. Using a focal length of 36 inches and an active tape format of 57 millimeters the various parameters of the system are determined as a function of altitude.

The limiting resolution as a function of altitude is presented in Figure II-6. This is calculated for a 36 inch focal length lens and a limiting tape resolution (at readout) of 200 TV lines per millimeter.

Figure II-7 shows the camera angle, ξ , and the required angle of scan, α , for the same optical-tape format system. The camera is rotated about the optical axis of the system through an angle ξ with respect to the normal to the orbital plane for image motion compensation.

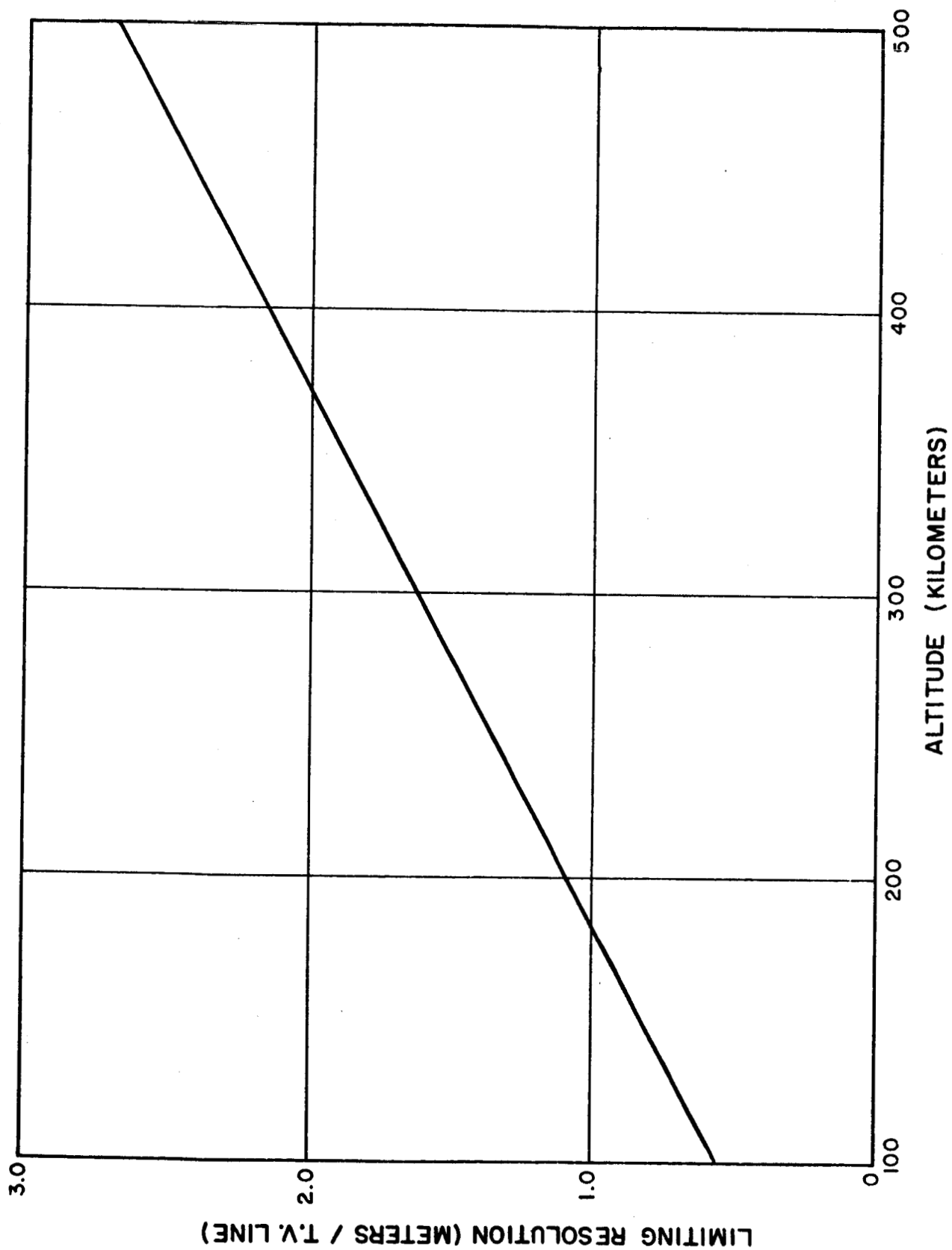


Figure II-6. Maximum Resolution Versus Orbital Altitude at 200 T.V. lines/mm With 36 Inch, F/2.5 Lens

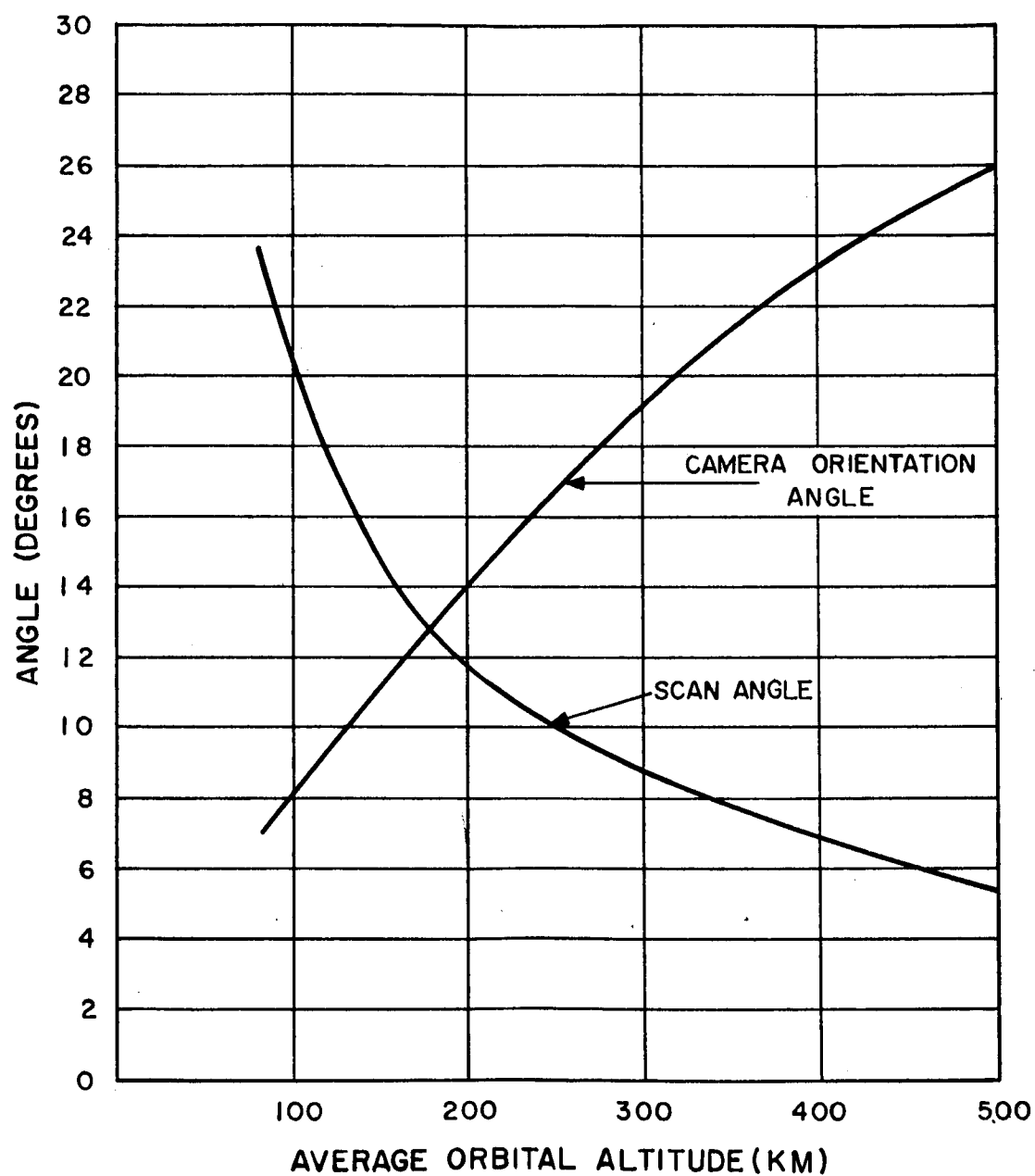


Figure II-7. Camera Angle and Scan Angle Versus Altitude

The length and width of the lunar surface imaged per swath are shown in Figure II-8. The time between scans is also shown as a function of altitude in Figure II-9. The angular scan rate over the lunar surface is shown as a function of altitude in Figure II-10.

The linear speed of the tape, v_T , required for image motion compensation can be obtained by:

$$v_T = f \omega \quad (7)$$

where

f = focal length of the lens system

and ω , defined by equation 5, is the angular velocity of the image. The computed tape speed for a 36 inch focal length lens is shown as a function of altitude in Figure II-11.

The available storage time may be computed on a basis of the tape speed, the total amount of tape per camera and assuming that imaging occurs over one-half the orbit. Although it is difficult to determine the maximum tape capacity for a camera it is estimated that tape transport systems utilizing 1500 feet of tape are feasible for this time period. Using this tape capacity the available storage per camera has been determined and is plotted as a function of altitude in Figure II-12.

2. Stripping System

Since the lunar surface is mapped by the scanning system in sections the processing of the received data at the ground station is more complicated. The scanning mirror introduces a moving part which is less desirable from a standpoint of vacuum operation and it introduces transient torques into the system which must be damped out by the stabilization equipment. Furthermore, the system is not too amenable to the requirement of stereo viewing of the lunar surface. Although these objections may be raised for the scanning system, in order to take advantage of the inherent high resolution capability of the electrostatic tape camera and to obtain imaging of the entire lunar surface at a maximum resolution, an optical system similar to the one proposed for the scan system is required. Such a system necessarily dictates a narrow instantaneous field-of-view and scanning is required for full high-resolution coverage. In general, refractive lens systems offer wider fields-of-view but at a sacrifice in resolution. In the VOIS system the requirement for mapping and for high resolution viewing of selected areas of the lunar surface dictates two levels of resolution. The two recommended levels of resolution differ by an order of magnitude so that a refractive lens system would be suitable for the mapping requirements. However, a reflective optical system similar to the system discussed for panoramic scanning would still be required to achieve the high resolution. On this basis the alternate system would make use of both types of optical systems.

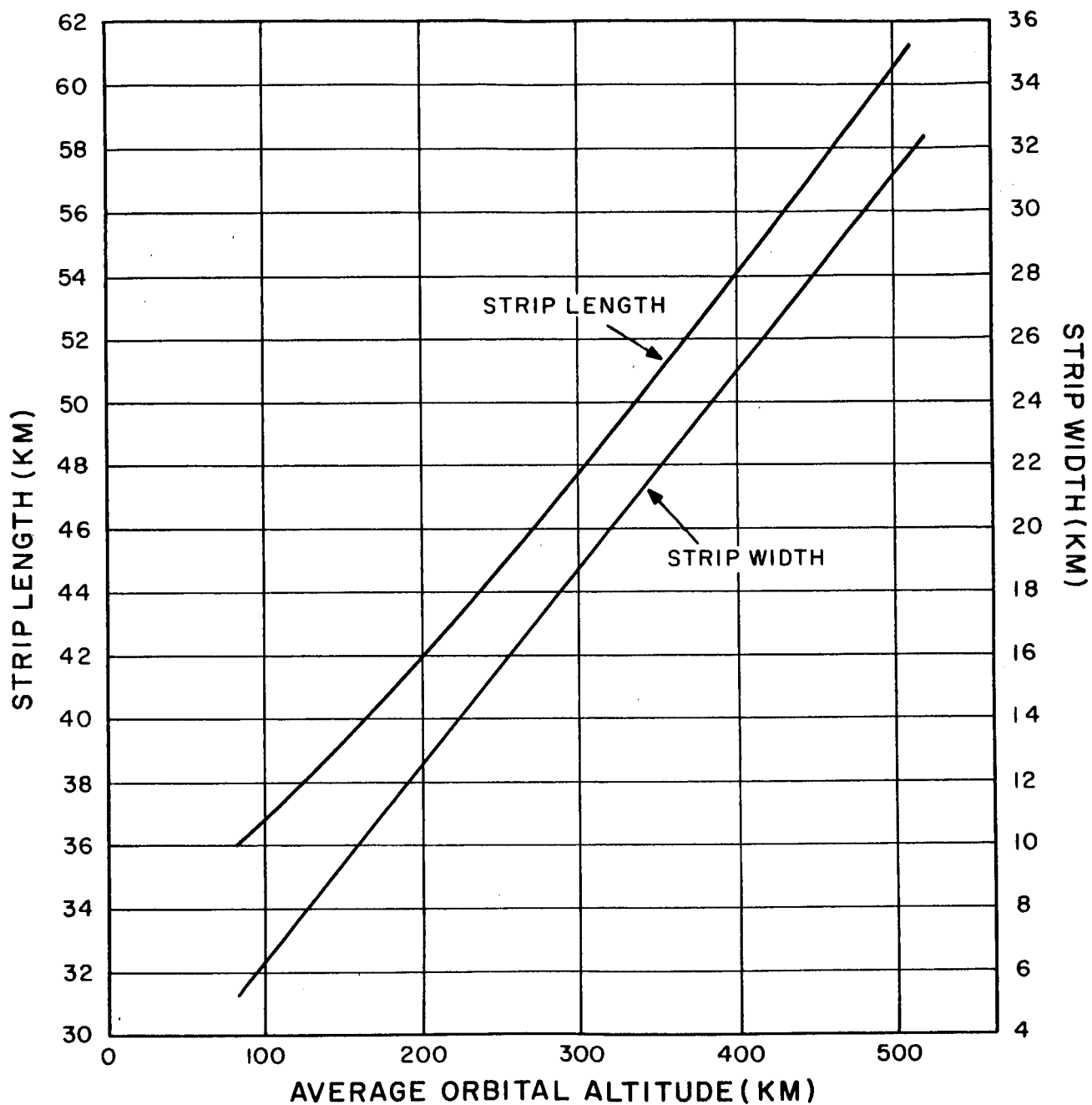


Figure II-8. Length and Width of Lunar Surface Imaged per Scan Versus Altitude

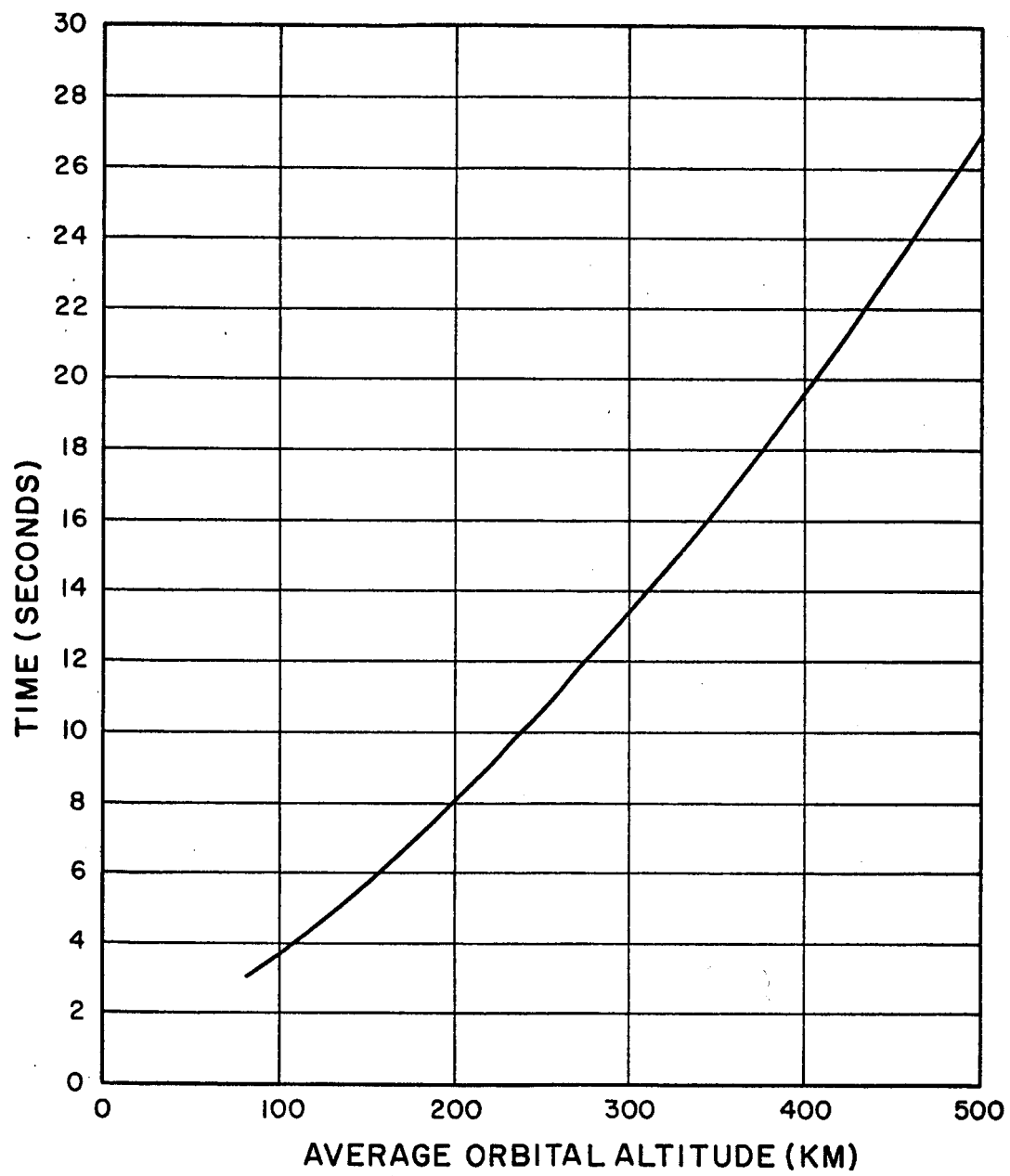


Figure II-9. Time Between Scans Versus Altitude

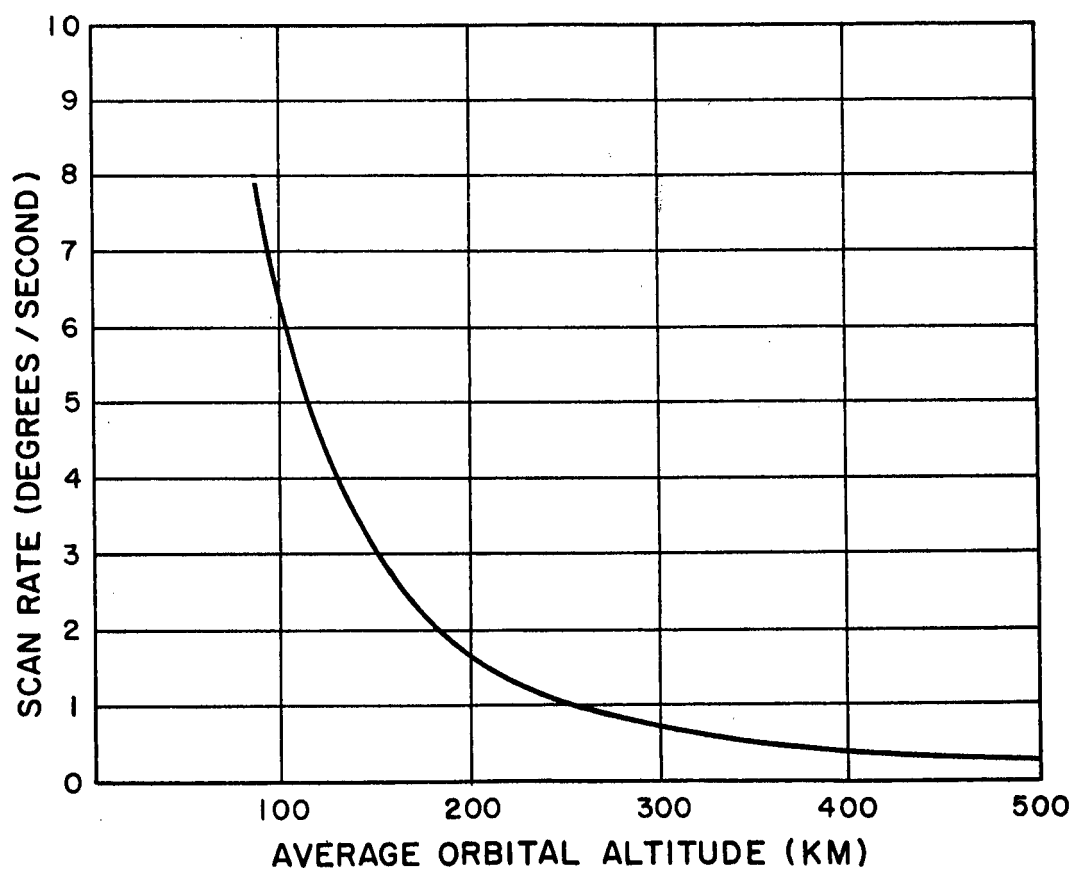


Figure II-10. Angular Scan Rate Over The Lunar Surface Versus Altitude

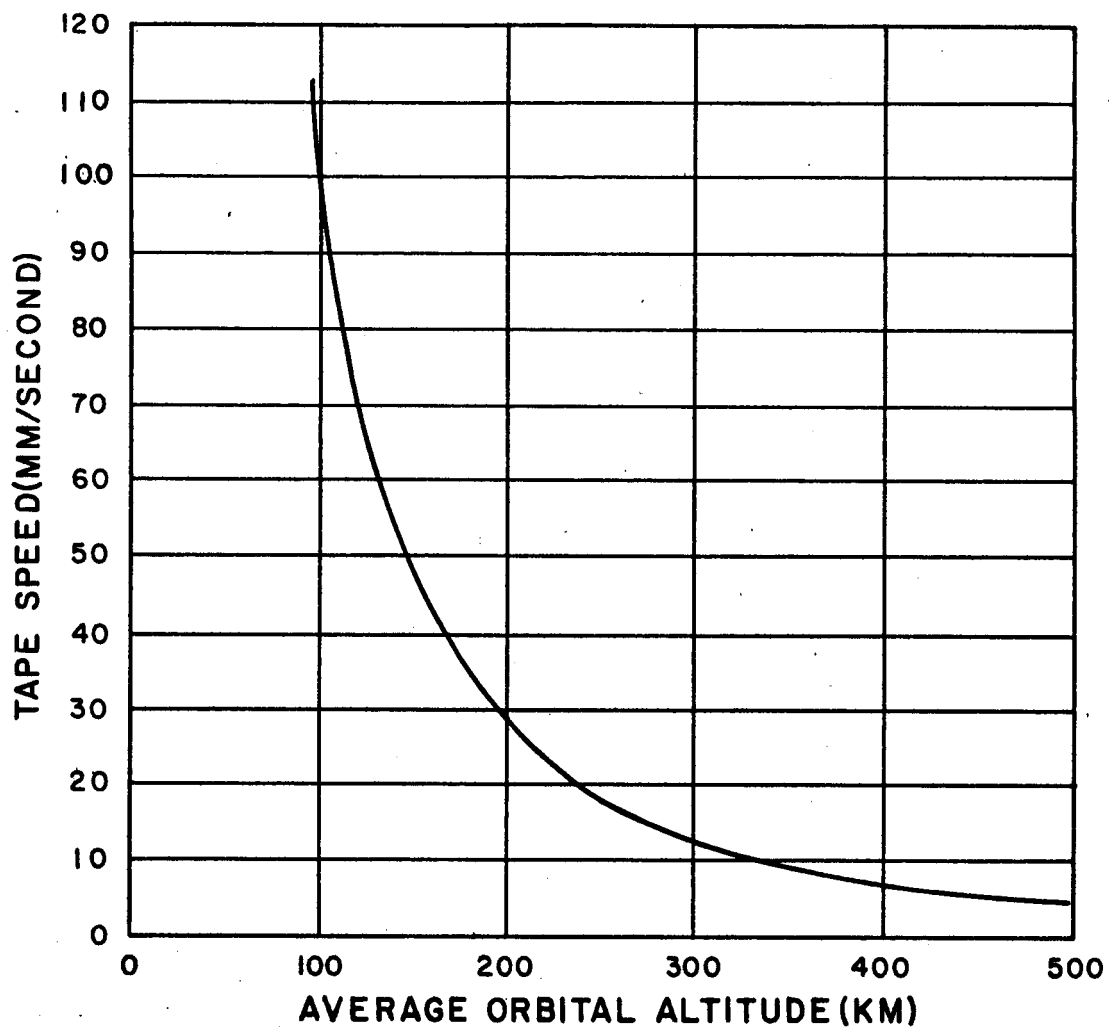


Figure II-11. Tape Speed Versus Altitude for a 36 Inch Focal Length Lens

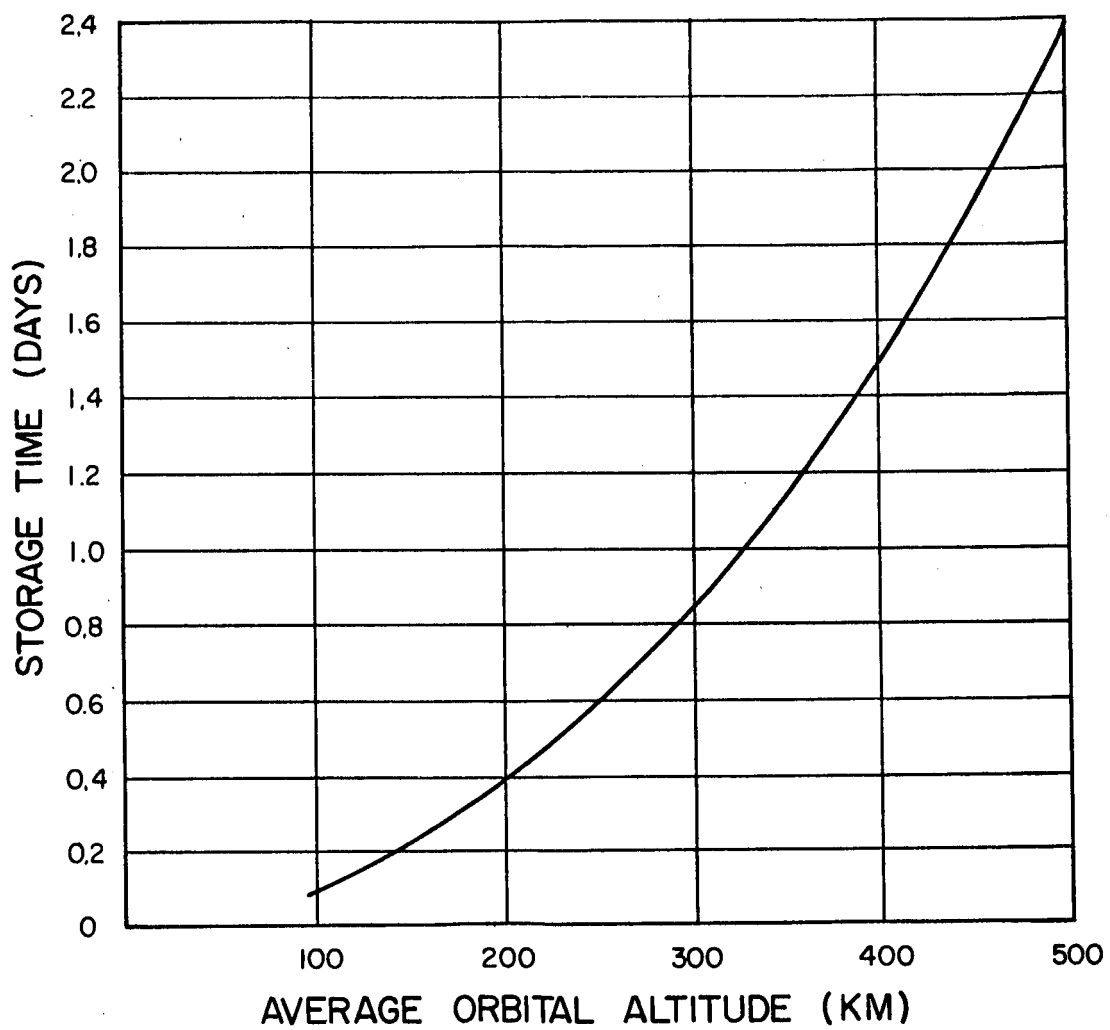


Figure II-12. Storage Time Per Camera for 1500 Feet of Tape

a. System Configuration

Two separate optical systems with separate electrostatic tape cameras are used for the alternate system. Both optical systems have their respective optical axes pointed along the subsatellite path, and imaging is accomplished on a slit-type camera with the motion of the vehicle generating the scan (i. e. scanning is done along the orbit producing a continuous strip of tape corresponding to a continuous strip of the lunar surface for each orbit).

The refractive system is composed of a 12 inch focal length lens with a focal-length-to-diameter ratio of approximately 4. The instantaneous field-of-view is approximately 11 degrees. The on-axis resolution of this system corresponds to approximately 100 T.V. lines/mm and is the limiting factor in resolution. Associated with this optical system are two 70 mm electrostatic tape cameras.

The reflective system is the same as described for the scan system with the exception that the scanning mirror is no longer used. This reflective system is composed of a 36 inch focal length lens with a focal-length-to-diameter ratio of 2.5. The instantaneous field-of-view is approximately 3.5 degrees. The on-axis resolution is greater than 200 T.V. lines/mm and the limiting resolution is that of the electrostatic tape (200 T.V. lines/mm). Associated with this optical system are two 70 mm electrostatic tape cameras.

The mapping system requires only one level of read out and this is equivalent to approximately 82 T.V. lines/mm for a 10 meter/T.V. line resolution. The high resolution system requires three levels of read-out which are the same as the scanning system read-out (approximately 200 T.V. lines/mm, 20 T.V. lines/mm, and 3 T.V. lines/mm). The first and third levels of readout resolution are utilized in the same manner as described for the scanning system (i. e. high resolution and indexing). The read-out at 20 T.V. lines/mm is used for stereo comparison with the mapping system.

The disadvantage of this system is that the high resolution component does not yield full coverage of the lunar surface. Therefore, some areas of interest will not be imaged at high resolution and cannot be viewed. However, since only a small percentage of the lunar surface can be transmitted back at high resolution during the operational lifetime of the vehicle this is not considered to be a tremendous detriment to the system.

b. System Parameters

With regard to the alternate system the most serious considerations are the required field-of-view for continuous mapping and the desired mapping resolution. Figure II-13 shows the required field-of-view

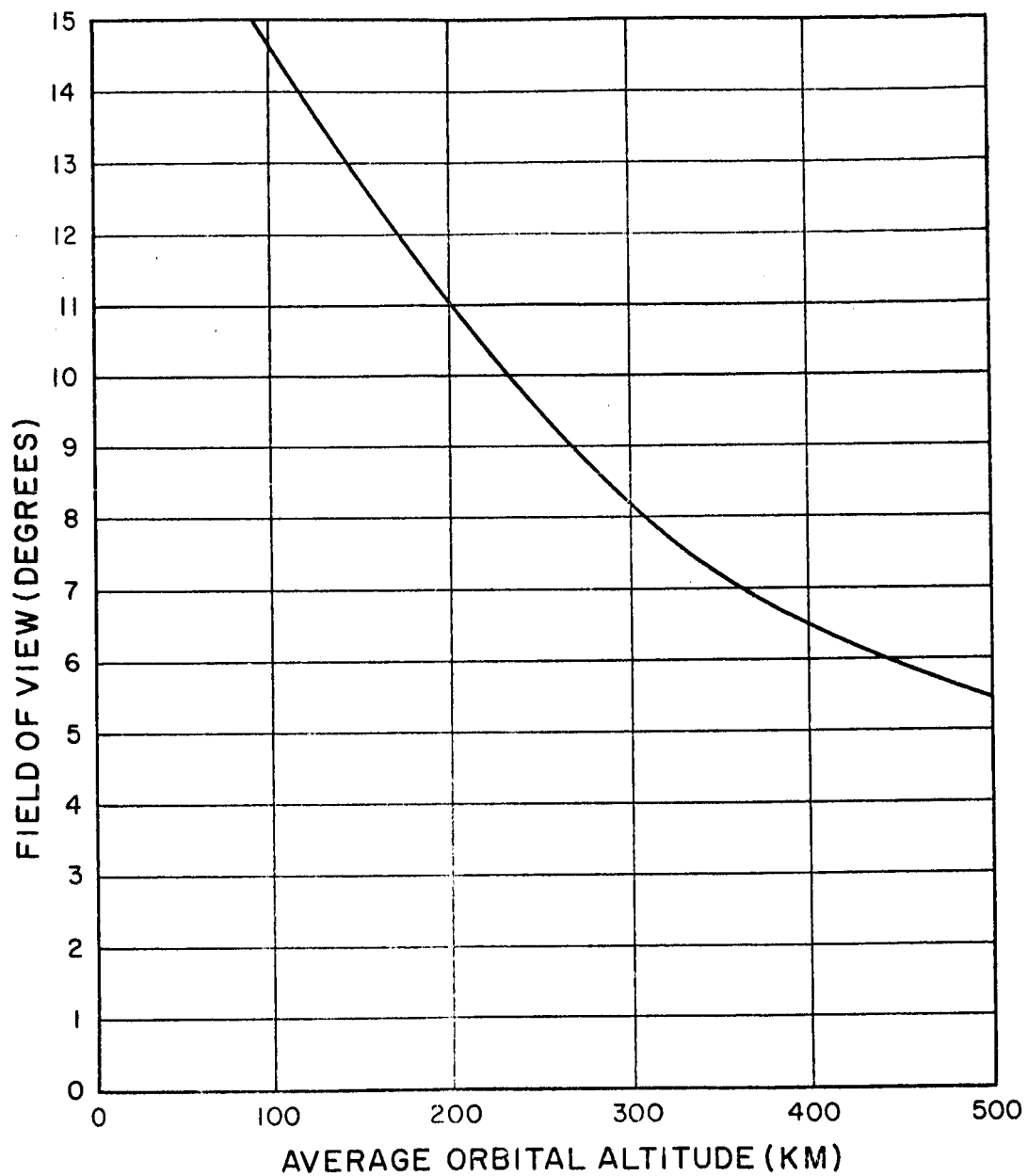


**Figure II-13. Required Angular Field-of-View Versus Altitude
for Alternate System**

as a function of altitude where a 10 percent sidelap is assumed. Figure II-14 shows the maximum resolution capability of the refractive optical system as a function of altitude. From these figures it is clear that to stay within the optical field-of-view of 11 degrees and to maintain a mapping resolution of 10 meters/T. V. line the altitude range suitable for these choices is from 200 to 300 kilometers. The following analysis assumes an altitude of 250 kilometers (mid-point in the range) for the alternate system.

The maximum resolution of the high resolution system at an altitude of 250 kilometers can be determined from Figure II-6 and is approximately 1.4 meters.

The image motion is generated by the motion of the vehicle over the lunar surface. The angular velocity of the image is given in Figure II-15 and at 250 kilometers altitude the angular motion at the nadir is 0.55×10^{-2} radian/second. The tape velocity for imaging may be computed from equation 7 and is found to be 1.68 mm/second for the mapping system and 5.03 mm/second for the high resolution system. The total storage time for one camera in the high resolution system assuming 1500 feet of tape and imaging over one-half the orbit is approximately 2.3 days. For the mapping camera only 500 feet of tape is required for the same storage time (2.3 days).

As was pointed out previously the high resolution camera will not give continuous coverage of the lunar surface because of its narrow field-of-view. The actual coverage at 250 kilometers is approximately 40 percent of that required for continuous coverage at the lunar equator. However, above a latitude of approximately 40 degrees continuous coverage for the high resolution system is possible. Furthermore, it is unlikely that the same portion of the lunar surface will be viewed by the high resolution system in these mid-latitudes on each successive rotation of the moon so that the expected coverage even at the equator should be greater than 40 percent throughout the vehicle lifetime.

D. SYSTEM CONSTRAINTS

1. Exposure Time and Image Immobilization

a. Panoramic Scan System

For a system utilizing a slit-type camera and a panoramic scanning of the lunar surface, image immobilization is obtained by pulling the tape past a slit in such a manner that the velocity of the tape exactly compensates for the image motion. The image motion has two components; that generated by the motion of the satellite in orbit and the motion generated

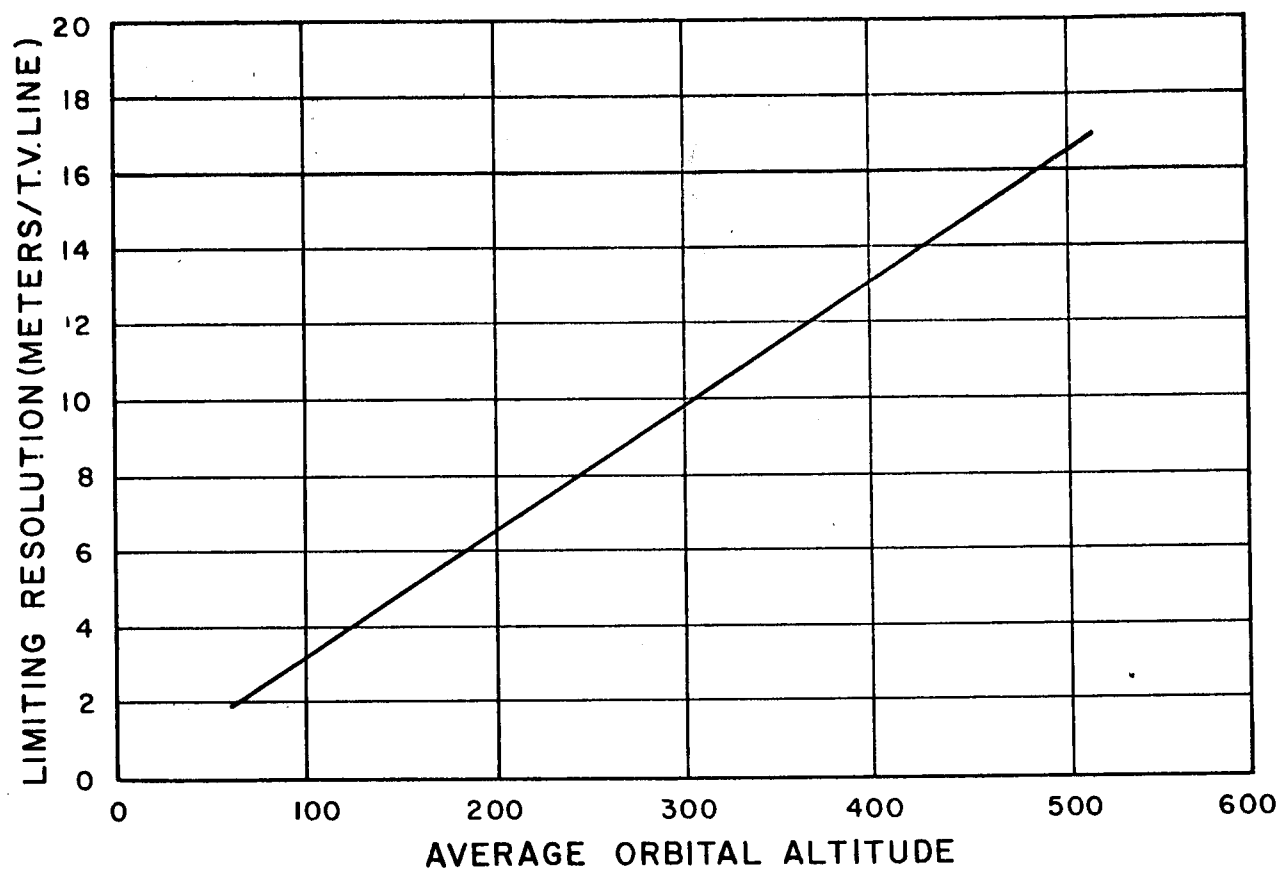


Figure II-14. Maximum Resolution Versus Orbital Altitude at 100 T.V. lines/mm with 12 Inch, F/4 Lens

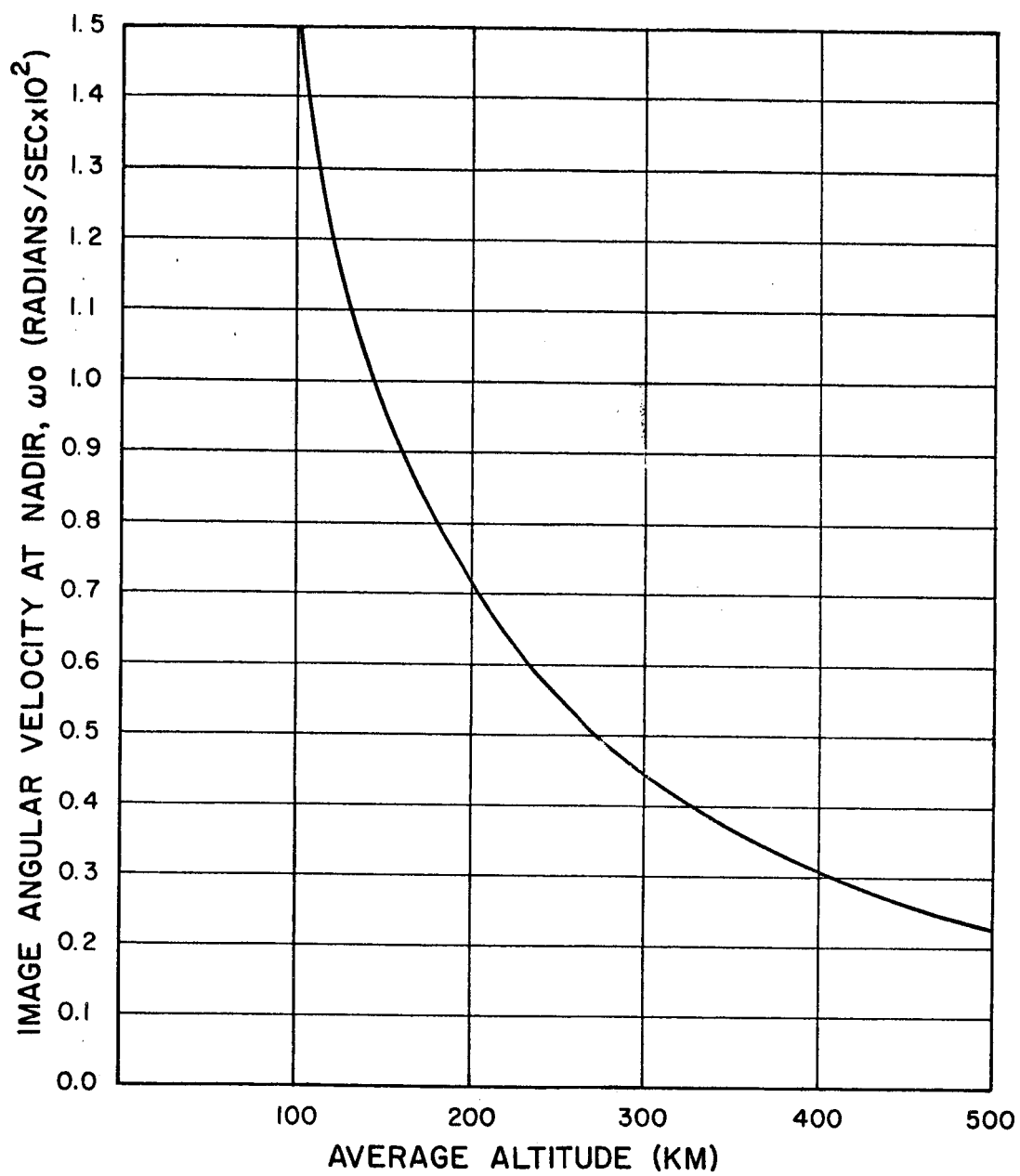


Figure II-15. Angular Velocity of Image as a Function of Altitude

by the scanning mirror. The first of these is parallel to the orbital plane and the latter normal to the orbital plane. Those parameters that will affect the image immobilization are:

- (1) Orbital speed, altitude and eccentricity
- (2) The moon's rotation
- (3) Maximum roll and pitch angles of the optical system
- (4) Residual angular rates from the stabilization system
- (5) Errors in camera alignment and tape speed.

In the interim report it was shown that the angular velocity of a point on the moon's surface as observed from the satellite is given by

$$\omega_i = \omega_o \cos^2 P \cos R$$

where

ω_o = angular velocity of the nadir point,

P = angle of pitch,

R = angle of roll.

In general, the angular velocity of the nadir point is given by

$$\omega_o = \frac{V_{\tan} R_m}{r (r - R_m)}$$

where

V_{\tan} = tangential velocity of the satellite in orbit,

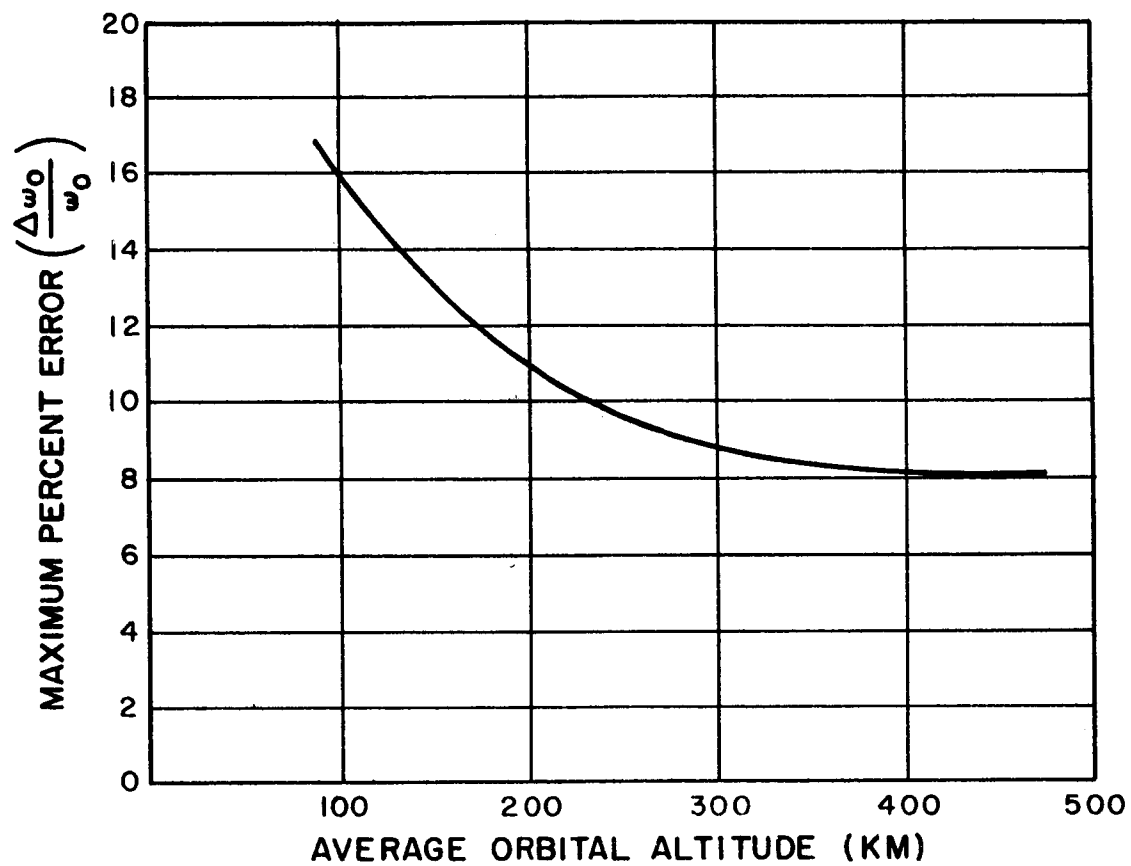
R_m = moon's radius,

r = radius of the orbit.

Neglecting second order terms the variation in ω_o can be determined to be

$$\frac{\Delta \omega_o}{\omega_o} = \pm \frac{\Delta v}{v} \pm \frac{\Delta R_m}{R_m} \pm \frac{\Delta r}{(r - R_m)} \pm \frac{\Delta R_m}{(r - R_m)}$$

The maximum variation $\frac{\Delta \omega_o}{\omega_o}$ is shown in Figure II-16 as a function of average orbital altitude for a 10% circularity and an average uncertainty in the



V_{ss}

$$\frac{V_s}{\Lambda} = \frac{V_{ss}}{f}$$

$$V_{ss} = V_s \frac{f}{\Lambda}$$

$$\omega_0 = \frac{V_{ss}}{h} = \frac{V_s f}{h \Lambda}$$

Figure II-16. Variation of $\left(\frac{\Delta\omega_0}{\omega_0}\right)$ Versus Altitude

moon's radius of 10 kilometers. The altitude variations considered here do not take into account that the orbit achieved may have an average altitude other than the desire done. The achieved average orbital altitude can be determined to a high degree of accuracy (other altitude errors would be much more pronounced) and adjustment of the tape speed and camera angle made to compensate for this change.

In addition to the error encountered by variations in the orbit, attitude stabilization errors will also contribute to residual image motion. These errors are of two types; the absolute angular errors in establishing the coordinate system and the residual angular rates. In general, the first of these will contribute primarily as a rotation of the image plane about the optical axis. Consider the geometry shown in Figure II-17. The angle of rotation about axis b due to an error e_y is given by

$$\Delta \psi = \frac{W}{S} \frac{\cos R}{\cos P} = \sin e_y \frac{\cos R}{\cos P}$$

The angle of rotation about axis b due to an error e_p is given by

$$\Delta \psi = \frac{h}{\cos P} \frac{\sin R}{\cos P} = \sin e_p \frac{\sin R}{\cos P}$$

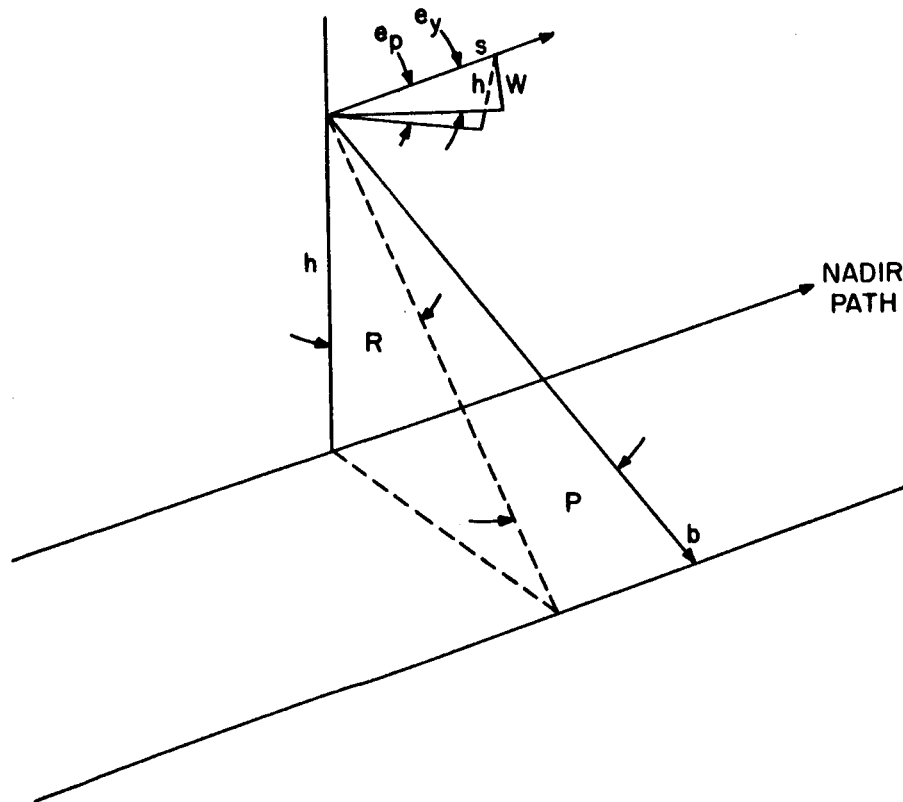


Figure II-17. Geometry for Altitude Stabilization Errors

The total image twist then is given by

$$\psi = e_y \frac{\cos R}{\cos P} + e_p \frac{\sin R}{\cos P}$$

assuming small angular variations of the stabilization system. Now for maximum twist $e_y = e_p$ and

$$\psi = \frac{e_y}{\cos P} \left[\cos R + \sin R \right] = \frac{K_R e_y}{\cos P}$$

The image twist factor, K_R , is shown as a function of roll angle in Figure II-18. The maximum twist occurs for the maximum pitch angle, P , which for the scanning system is approximately 1.8 degrees and can be neglected. Thus, for a 200 kilometer orbit the maximum roll angle is approximately 5.5 degrees and the maximum twist is given by

$$\psi_{\max} = 1.09 e_y$$

For an attitude error of 0.1 degrees this corresponds to

$$\psi_{\max} = 0.019 \text{ degrees}$$

Using this result it can be shown that the percent error contributed by an error of this magnitude in stabilization is less than 0.1 per cent.

In general, the synchronization of the scanning mirror and tape may be held to a tolerance of less than 0.4 per cent error in this component of image velocity. Residual angular rates from the stabilization system are assumed to be no greater than 1 degree/hour and this may propagate into the image plane alignment at a maximum ratio of 1.5 for each of the image plane axes. Table II. D. 1 gives a list of the maximum errors expected from this system for the two components of image motion.

For the case of a 200 kilometer orbit the previously determined values of ω_y and ω_x are:

$$\omega_x = 2.89 \times 10^{-2} \text{ rad/sec}$$

$$\omega_y = 0.72 \times 10^{-2} \text{ rad/sec}$$

Assuming that the errors listed in Table II. D. 1 add linearly (this is a maximum case) the errors for the image motion components are

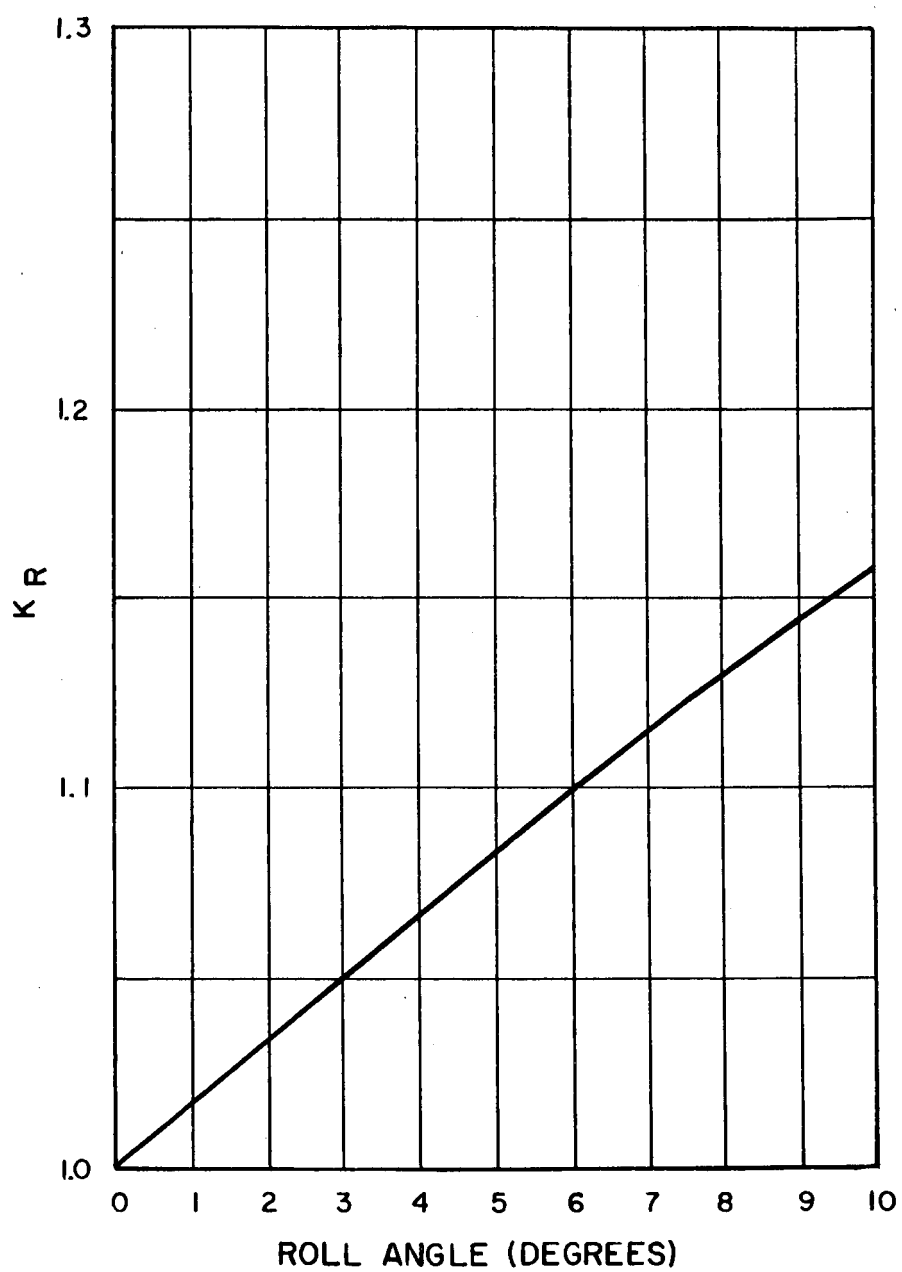


Figure II-18. Image Twist Factor K_R as a Function of Roll Angle

$$\Delta\omega_y = 94.2 \times 10^{-5} \text{ rad/sec}$$

$$\Delta\omega_x = 14.55 \times 10^{-5} \text{ rad/sec}$$

Thus, the major error in image motion compensation is caused by the variation of the orbital altitude due to a non-circular orbit and the variation of the moon's average radius; both of these effects being comparable in magnitude. Approximately 80% of the total error can be attributed to these factors.

From an altitude of 200 kilometers an object of 1.1 meters subtends an angle of 5.5×10^{-6} radians, corresponding to a distance on the electrostatic tape of 5×10^{-3} mm for 200 TV lines/mm (maximum resolution). The linear tape speed is shown in Figure II-11 and is

$$v_T = 27.2 \text{ mm/sec.}$$

To determine the exposure time and, as a result, the slit width, it is necessary to determine the maximum allowable error in image motion compensation.

Table II. D. 1

List of IMC Errors at 200 Kilometers Altitude

	ω_x	ω_y
Variation of Orbital Parameters		$11\% \omega_y$
Synchronization of Mirror and Tape	$0.4\% \omega_x$	
Variation of Image Motion from Average over Field-of-view		$0.3\% \omega_y$
Residual Angular Rates	$7.5 \times 10^{-6} \text{ rad/sec}$	$7.5 \times 10^{-6} \text{ rad/sec}$
Moon's Motion (maximum at the equator)	$2.3 \times 10^{-5} \text{ rad/sec}$	

If it is required that image misalignment be less than one-quarter the separation between T. V. lines during the exposure time, t , the component of image angular velocity causing smear will be

$$\Delta\omega = \frac{5.5 \times 10^{-6}}{4 t}$$

or

$$t = \frac{5.5 \times 10^{-6}}{4 \Delta\omega}$$

For 200 kilometers

$$\begin{aligned}\Delta\omega &= \sqrt{(94.2)^2 + (14.6)^2} \times 10^{-5} \text{ rad/sec} \\ &= 95.3 \times 10^{-5} \text{ rad/sec.}\end{aligned}$$

and

$$t = 1.44 \text{ milliseconds}$$

In general, the allowable smear tolerance without too much degradation in image quality can be as much as one-half a T. V. line which would permit an exposure time of approximately 3 milliseconds. Furthermore, the errors were assumed to add linearly and the computed errors in IMC are a maximum. Thus, a 3 millisecond exposure time is feasible. The slit width, Δx , can be computed from

$$\Delta x = v_T t = .082 \text{ mm}$$

which is well above the diffraction limitation of the slit.

b. Alternate System

The alternate system involves two optical systems. The high resolution system is the same as that for the panoramic scan system and the image immobilization errors will be approximately the same with the exception of the errors associated with the scanning mirror. Thus, the exposure time computed for the previous case (3 milliseconds) will be approximately the same. The slit width computed in the same manner as before is 0.015 millimeters.

For the mapping system the IMC errors are approximately the same with the exception of the errors associated with the scanning mirror. Thus, the total angular rate error will be approximately 95×10^{-5} rad/sec. Utilizing the same analysis as before for exposure time but realizing that the object size is 10 meters instead of 1.1 meters as before, the calculated exposure time is, based on one-quarter TV line image smear,

$$t = \frac{5 \times 10^{-5}}{4 \Delta\omega} = 13 \text{ milliseconds}$$

The slit width for the mapping system computed as before is 0.022 millimeters.

2. Image Illumination

The illumination level associated with the lunar surface was analyzed in the interim report. The image illumination was found to be

$$E_I = \frac{T B_o}{4 (f/\#)^2} \text{ foot-candles}$$

where B_o is in foot-lamberts;

T is the transmission factor of the lens; and

$f/\#$ is the focal length-to-diameter ratio of the lens.

Also, if E_s is the incident illumination from the sun; θ is the sun angle of the object; and R is the albedo of the object,

$$B_o = R E_s \cos \theta$$

Figure II-19 is a plot of the illumination, assuming $E_s = 13,000$ foot-candles, $f/\# = 2.5$, and $T = 60\%$. Figure II-20 is a plot of the illumination, assuming $E_s = 13,000$ foot-candles, $f/\# = 4$ and $T = 60\%$. The illumination level is plotted for the two extreme values of R and for various positions of the sun with respect to the orbital plane at the moon's equator. Also shown in these figures are the minimum illumination levels for the present and future predicted capabilities of the electrostatic tape assuming the exposure times computed in the previous sections.

3. System Resolution Levels

The proposed system of readout for the VOIS involves three levels of resolution, since the level of resolution affects the time and power required for transmission of the imaged data. In the interim report the recommended three levels of resolution were

High resolution $\simeq 1$ meter/TV line,

Mapping resolution $\simeq 10$ meters/TV lines,

Pointing or Indexing resolution $\simeq 100$ meters/TV line.

Since this time further analysis has revised the pointing resolution to approximately 60 meters. The reason for including the Pointing resolution in the system was covered in the interim report and, briefly, it is to allow for complete readout of storage in a reasonably short time so that the earth station can determine which portions of the storage should be read out at high resolution. An analysis has been conducted during this final period to determine if the recommended pointing resolution is sufficient so that comparisons of stored data at this level can be made and areas selected based on such a comparison.

An experiment was designed so that nine subjects were given images of nine different sample areas at three different levels of resolution. The

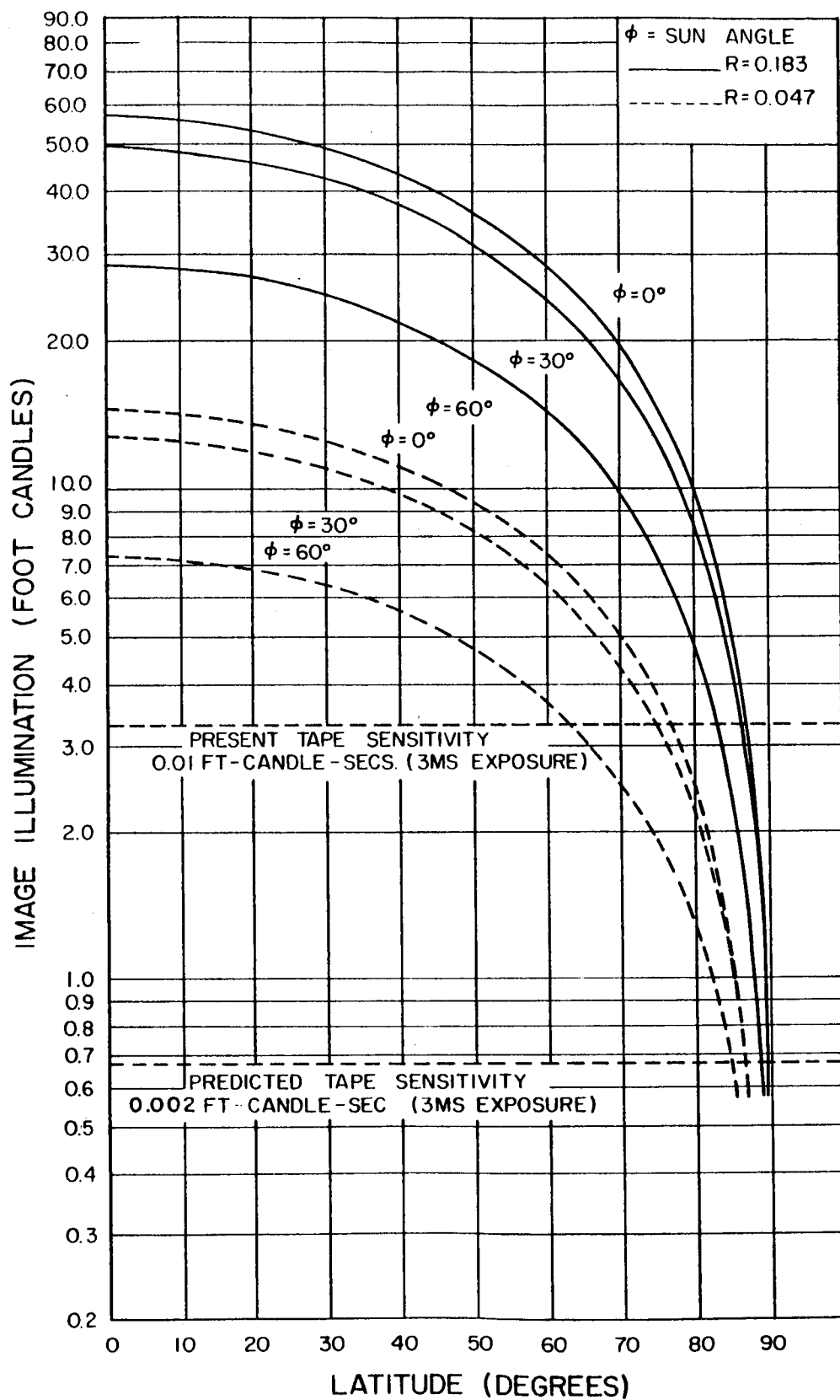


Figure II-19. Image Illumination Versus Object Latitude and Sun Angle for F/2.5 Lens

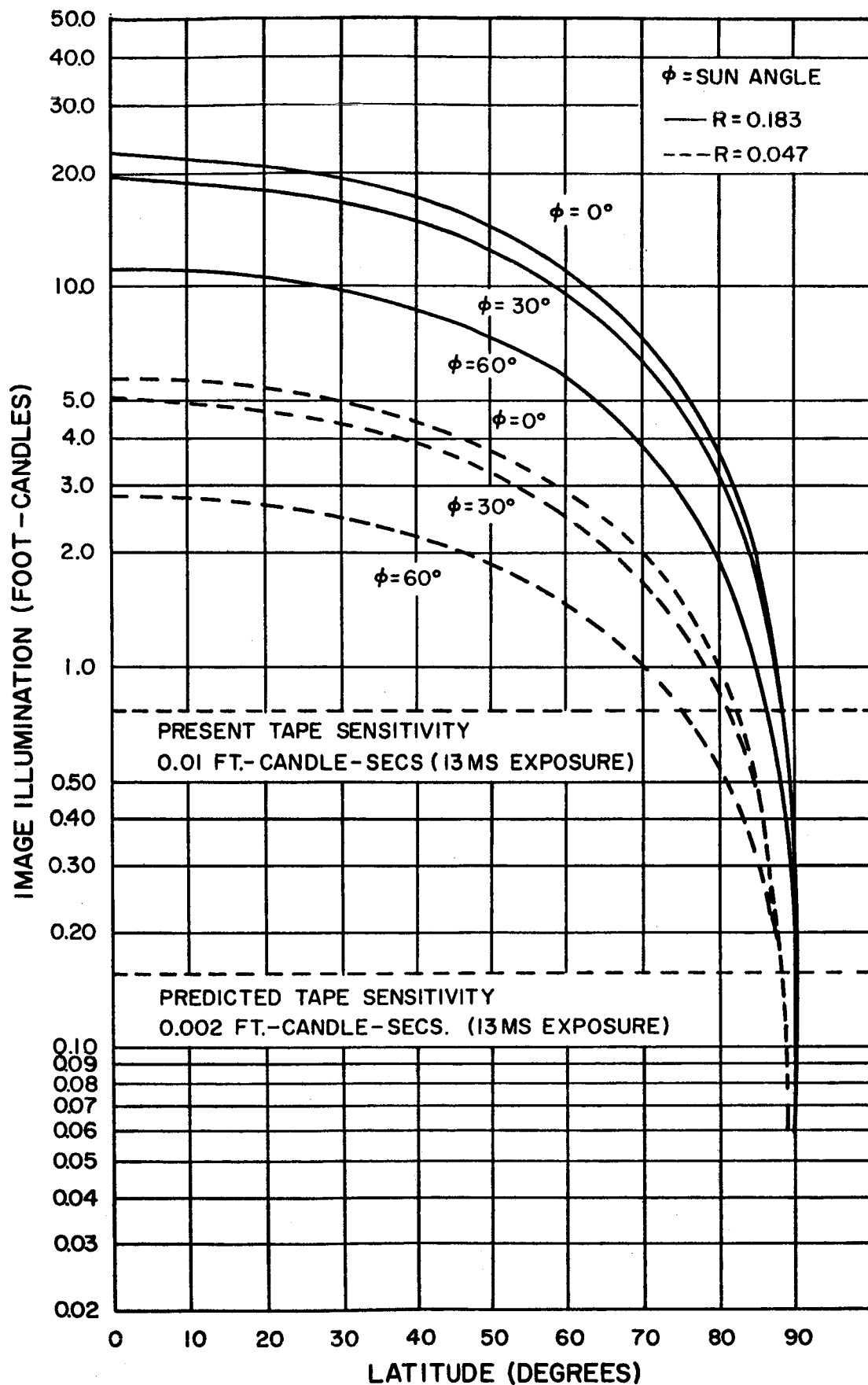


Figure II-20. Image Illumination Versus Object Latitude and Sun Angle for F/4 Lens

subjects were asked to match the sample areas with a mosaic simulating portions of three orbital passes over the lunar surface. The mosaic was produced at a resolution approximating the recommended mapping resolution. The pictures used in the experiment were part of a flight survey over the mountainous area southeast of San Diego, California, and were obtained from the Aero Service Corporation of Philadelphia, Pennsylvania. They were made at a scale of 62000:1 and were composed of nine by nine inch photographs. Each of these photographs were processed through the RCA simulator to give the proper resolutions. The resolution levels were:

Mosaic resolution \simeq 7 meters/TV line

Sample resolution (1) \simeq 14 meters/TV line

Sample resolution (2) \simeq 28 meters/TV line

Sample resolution (3) \simeq 58 meters/TV line

Figure II-21 shows one photograph of the mosaic and the three sample resolutions.

The instructions given to each of the subjects were as follows:

Instructions

1. The purpose of this experiment is to test the effect of resolution on the ability of a person to correlate various areas imaged at various levels of resolution. It should be emphasized that the individuals ability is not being tested but simply the effect of resolution. In order to have valid statistical data a number of persons will be tested within the same experiment. In this respect it is important that the experiment not be treated lightly particularly since the results of the test will be included in a final report with recommendations for a given resolution level. This experiment is to simulate the conditions that might exist in a lunar satellite mapping the surface of the moon.
2. The mosaic you see simulates a portion of three orbital passes over the moon's surface and you will note that there is approximately two-thirds overlap between the passes.
3. The samples you will be given have been taken from this mosaic and represent different areas and levels of resolution.
4. Your objective is to align the samples with the matching areas on the mosaic. You may find that the match is not exact since photographic

AREA SAMPLES



Mosaic-Resolution ~ 7 Meters/T.V. Line



Resolution (1) ~ 14 Meters/T.V. Line



Resolution (2) ~ 28 Meters/T.V. Line



Resolution (3) ~ 58 Meters/T.V. Line

Figure II-21. Mosaic and Test Samples

paper has a tendency to stretch and shrink in the processing. Furthermore, the samples were passed thru the T. V. simulator and some distortion naturally accrues from this. However, the match should be close enough and only small variances noted.

5. Speed is important but you should take as much time as necessary since accuracy of orientation will weigh heavily in the experimental results. In this respect the orientation of the samples was not chosen in any special manner.
6. You will be given the samples face down and when I say "go" you will turn the sample over and commence trying to find the matching area. When you have done so indicate orally by saying "now" and hold the sample at that position. After you have indicated the match there will be no chance to change your mind and the result will stand.
7. Initially you will be given as much time as you feel necessary to examine the mosaic. You will also be given two sample areas to permit you some practice. These will not count in the overall experiment.
8. As a final instruction it is imperative that you do not discuss the test with anyone else since the other people to take the test will come from AED and any discussion will necessarily bias the experiment.

The results of the experiment indicated that within the limitations of the experiment the resolution levels used did not affect, significantly, the ability of a subject to locate the sample area on the mosaic with its proper orientation. In the experiment a trend was noticeable, in that on the average it took longer to locate the matching areas at the lowest level of resolution. However, the differences were not sufficient to establish any overall significance in the experiment. It was also noted that the variation in subjects and the selected sample areas were highly significant which is to be expected.

It should be pointed out that the experiment did not exactly simulate the VOIS system. The operational lifetime of the VOIS is 90 days over which period the sun angle for a given portion of the lunar surface will vary considerably. The experiment conducted for this study did not take this into account. Furthermore, far more data will be available to the ground controllers of the VOIS than was available to each of the test subjects. In spite of these differences it is concluded that the resolution levels recommended are feasible for the operational techniques proposed for the VOIS.

With regard to the effect of resolution on image content several study programs have been conducted in the past by RCA for various Defense

agencies. In general, it was found that for linearly extended objects and geometrical patterns variations in resolution produced less of an effect than such parameters as contrast variation and overall signal-to-noise ratio of the system. Reference 2* gives the results of one such program. Details of the program cannot be given here because of the classification.

E. SYSTEM REQUIREMENTS

a. Environmental Control

The major requirement for environmental control is in the areas of radiation and thermal control. Although the vibrational and acceleration problems associated with launch and injection into lunar orbit are serious, particularly with regard to the large optical system, the Perkin-Elmer Corporation assures that the optical system can be designed to withstand such an environment and maintain collimation. However, thermal control once the vehicle is in orbit is required. The large optical system will maintain its characteristics over a temperature range of 20 degrees \pm 5 degrees centigrade. Other portions of the VOIS require thermal control within the range of 0 to 50 degrees centigrade. Thus, the controlling factor here is the optical system. It is possible that the range of temperatures over which the optical system maintains its characteristics may be extended by redesign of the supporting members so that thermal variations across the optical tube would produce compensating effects. This requires more study before the final tolerances on thermal control can be established.

The problem associated with the radiation environment is another which will require further study and in some cases experimental determination before final tolerances can be established. The electrostatic tape has been subjected to low energy radiation which was equivalent to the Van Allen energy levels in a preliminary type of test. No tape or image degradation was discernible. However, the major radiation problem which the VOIS is faced with is the radiation produced by solar flares. In general, heavy particles with high energies (energies as high as 100 MEV have been estimated) accompany these flares out to at least the earth's radius from the sun. Moreover, the frequency of such flares would indicate that several would occur during the operational lifetime of the VOIS. Under these circumstances of such penetrating radiation and because of the preliminary nature of the previous experiment with the electrostatic tape, a more thorough test should be devised to determine the sensitivity of the tape to radiation.

*Reference (2) "Combat Surveillance Data Link Family Study," Report #3 on Contract #DA 36-039-SC 78344, DA Project No. 30-38-01-001 for the U.S. Army Signal Research and Development Laboratory, Fort Monmouth, N.J. Classified Confidential.

Radiation effects will also affect the design of the optical system since non-browning glass will be required for the lens elements.

b. Attitude Stabilization

The image motion compensation analysis allowed a tolerance of ± 0.1 degrees error in stabilization with residual angular rates of less than 1 degree/hour. These tolerances are within reasonable bounds and can be relaxed somewhat without affecting the overall system characteristics. If these tolerances quoted above are obtainable the stabilization system is within the requirements of the VOIS.

c. Power Requirements

The total peak power requirements for the VOIS will be approximately 350 watts. The average power requirement will be approximately 150 watts. The power requirements are as follows:

Transmitter:	Peak	50 to 100 watts
Camera:	Peak	150 watts/camera
	Average	75 watts/camera
Tape Transport:	Peak	30 watts/camera
	Average	10 watts/camera
Control Circuitry:	Average	5 watts.

d. Program Control Function

The required control functions for the ground station for the VOIS are as follows:

- (1) Tape speed and camera angle.
- (2) Total time for imaging.
- (3) Automatic "on-off" for cameras during remote operations.
- (4) Camera selection for imaging (4 cameras).
- (5) Camera selection for read-out (4 cameras).
- (6) Generation of imaging intervals.
- (7) Read-out Program.

- (a) Mode I - Mapping Program
 - (1) Imaging - reel A to reel B
 - (2) Read-out at mapping resolution- reel B to reel A.
 - (3) Playback at high resolution - reel A to reel B.
 - (4) Rewind - reel B to reel A.
- (b) Mode II - High Resolution Program
 - (1) Imaging - reel A to reel B.
 - (2) Playback at pointing resolution - reel B to reel A.
 - (3) Playback at high resolution - reel A to reel B.
 - (4) Rewind - reel B to reel A.
- (8) Exposure Control
- (9) Clock Program Control

To accomplish all these functions an internal program control circuit will be required. This will involve a clock to generate the necessary pulses and pulse rates for the various portions of the system and a storage mechanism for remote control of the VOIS. The system has sufficient storage time for programming from a single earth station for continuous operation. It is estimated that a bit rate of approximately 500 bit/second which corresponds to an audio bandwidth for the command control system of 0.75 kilocycles/second will be required. Programming for one days operation would require approximately ten minutes.

III. COMPONENT ANALYSIS

A. COMMUNICATION SYSTEM

1. Introduction

The interim report discussed those aspects and considerations of the lunar satellite communication equipment that might effect or modify the "VOIS" package design study. The object of the interim report was to show that the proposed "VOIS" system would result in a reasonable communication system, considering state-of-the-art techniques projected to 1964.

This report will present a summary of those communications considerations thought to be important in the "VOIS" parametric design study.

2. Transmitter Modulation Techniques

Various possible modulating techniques such as FM, PCM, and orthogonal PCM were suggested and briefly analyzed in the interim report. The analysis of the modulation techniques was based upon considerations of minimum transmitter power, weight, size, complexity, and maximum reliability and efficiency for the satellite equipment as well as compatability with ground equipment. A frequency modulated system was considered the best choice even though the orthongonal PCM system, (such as digilock) might require less transmitter power. However, the orthogonal coding for the wide baseband VOIS package would result in very high pulse rates; for example, for the 500 -kc VOIS baseband, a pulse rate of 8 MC is required for orthogonal coding and a 16 MC RF bandwidth.

A further advantage for the FM system is that pre-emphasis of the VOIS baseband frequencies can be used to reduce the transmitter power by approximately 1.7 DB. Considering all of these factors, FM is the better choice.

A comparison of VOIS parameters and DSIF capabilities for 1964 as they are now understood can be made to show the basis for the communication considerations of the VOIS design study. This comparison is made in Table I.

The VOIS parameters shown in Table I are altered slightly from those listed on page 35 of the Interim Report. These changes were made to accomodate the savings in power afforded by pre-emphasis which essentially allows the received baseband circuits to operate in the presence of a degraded signal to noise ratio. This subject is discussed in more detail in paragraph 5. The effect, however, is a reduction in IF bandwidth and a subsequent

reduction in optimum transmitter power. Also note that the baseband frequency has been reduced from 576 KC to 500 KC.

The system margin of 9 DB is an assumed value to account for various system losses in order that the estimation of the overall system requirements would be more realistic. The receiver threshold of 6 DB is discussed later in this report.

A comparison of S-Band power sources was made in the Interim Report in order to show what developments might be reasonable by 1964. A review of this work is necessary because some experience and design information has accrued from the development of a satellite TWT amplifier-transmitter at RCA-AED. The results of this new information are shown in Table II. Tube types mentioned in the Interim Report exemplify the present state of the art. Improved versions of these tubes may be necessary to satisfy the lunar mapping mission reliability requirements. It is also understood that a 25 watt klystron transmitter development has been undertaken by JPL to satisfy the DSIF 1964 projection of required transmitter power.

3. Receiver Techniques

An important factor in receiver design is the receiver threshold, which is the minimum ratio of carrier power to noise power which will result in a video picture of sufficient quality. The lower threshold will require less transmitter power. In the Interim Report a carrier-to-noise threshold of 6 DB was assumed. This threshold may be achieved by either a phase-locked detector or a Chaffee-type receiver. A conventional but high quality limiter-discriminator combination has a noise threshold of 10 DB. This threshold value has been measured empirically by RCA-AED and is also the value of threshold commonly reported in the literature. For TV pictures of good quality it is not feasible to operate much below the noise threshold level because the impulse type noise that is generated below threshold in the limiter discriminator is very objectionable. Further, an increase in receiver threshold from 6 DB to 10 DB does not increase the required transmitter power by 4 DB because the optimum RF bandwidth must be reduced at the higher value of threshold, (to maintain the baseband signal to noise ratio). It has been calculated that 4 DB increase in threshold requires 3 DB more transmitter power and a reduction in carrier bandwidth from 2.4 MC to 1.93 MC. The actual receiver threshold achieved for the VOIS ground equipment involves considerations beyond the scope of this present report, however, the savings in transmitter power seem to indicate that an effort to achieve a receiver threshold near 6 DB would be worth while. Therefore, this value of threshold has been assumed in the VOIS communications system parameters.

Table I. Comparison (where applicable) of Projected DSIF Capabilities for 1964 and Suggested Operating Points for VOIS

<u>VOIS Assumptions</u>		<u>DSIF Capabilities Projected to 1964</u>
Signal-to-noise-ratio in RF bandwidth	6 DB	_____
Output-signal-to-noise ratio (baseband)	24 DB rms to rms	_____
Baseband frequency	500 KC	1 MC
IF bandwidth	2.4 MC total	reported to be 4 MC total
Modulation index	1.4	_____
Receiver noise temperature	100°K	100°K
System noise temperature	400°K	_____
Free space attenuation	211.4 DB	_____
Ground antenna gain	50 DB	50 DB
Satellite antenna gain	26 DB	reported to be 26 DB
System margins	9 DB	_____
Antenna pointing allowance	2 DB	
RF losses in satellite plumbing	2 DB	
Polarization losses	0 DB	
System margins in- cluding deterioration	5 DB	
Atmospheric losses	<u>0 DB</u>	
TOTAL	<u>9 DB</u>	
Preemphasis saving in power	1.7 DB	_____
Transmitter power	15 watts	25 watts

Table II. Results of Calculation of Satellite Transmitters Capable of Satisfying VOIS System Requirements

<u>12 watt transmitter</u>	<u>triode or tetrode</u>	<u>twt amplifier-transmitter</u>
tube weight (lb.)	. 25	7
cavity weight (lb.)	2. 0	
power supply weight (lb.)	5	5
modulator weight (lb.)	3	1
Structure weight	<u>2</u>	<u>3</u>
total weight (lbs.)	12. 25	16
power gain	10 DB (final stage)	36 DB saturated gain
primary power input (28 VDC)	75 watts	65 watts
tube dimensions (in.)	2 x 1 3/4	21 x 2 x 1 3/4

Another consideration in receiver design is the impulse type noise generated in "FMFB" receiver or a phase locked receiver as their respective "thresholds" are approached. In the FMFB type receiver the modulation index of the IF carrier has been reduced to a small value so the threshold in the normal sense does not appear. However, as the carrier power decreases and approaches the noise power there are finite intervals of time during which the noise power exceeds the signal power because of the gaussian nature of thermal noise. Since the limiter usually used in an FMFB system has constant output power the noise tends to suppress the signal, resulting in impulse-type noise in the output. This effect becomes prominent very quickly for a carrier to noise ratio in the vicinity of 6 DB, and a probability of noise peaks exceeding signal strength of the order of 0. 1%. Impulse type noise is also generated when the voltage controlled oscillator of a phase locked receiver or FMFB receiver fails to follow the signal modulation. Provided the phase detector in the phase locked loop remains operating on its linear characteristic, and there is only one bandwidth determining circuit in the FMFB loop, the behavior of the two systems are very similar. The question as to whether or not either or both of these circuits can be designed to achieve a 6 DB threshold for a 500 KC baseband, and a modulating index of 1. 4 and still yield a video picture of sufficient quality can only be answered completely by a more detailed design. Specifically, the character of the noise, whether thermal or impulsive is important as is the information content of the picture, and its purpose, (i. e. , pleasure or information).

4. Pre-emphasis

The sine wave frequency response of a typical vidicon tube is shown in Figure III-1 if the abscissa is converted from optical line pairs to frequency. If the modulating input spectrum to the vidicon is uniform, that is uniform power per cycle, then the frequency spectrum modulating the transmitter is as shown.

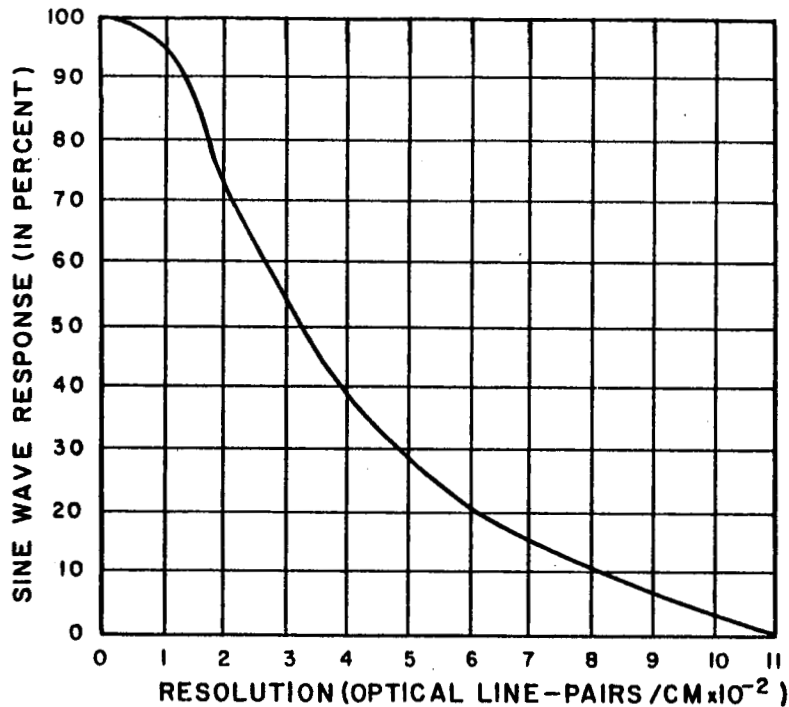


Figure III-1. Measured Sine Wave Response of A $0.01\mu a$ Beam

If the transmitter is modulated by a uniform frequency spectrum with a cut off

$$f_c = b, \quad (1)$$

where b = highest baseband frequency

then for a modulating index δ , the resulting RF spectrum has RF sidebands of significant power within the band B , where

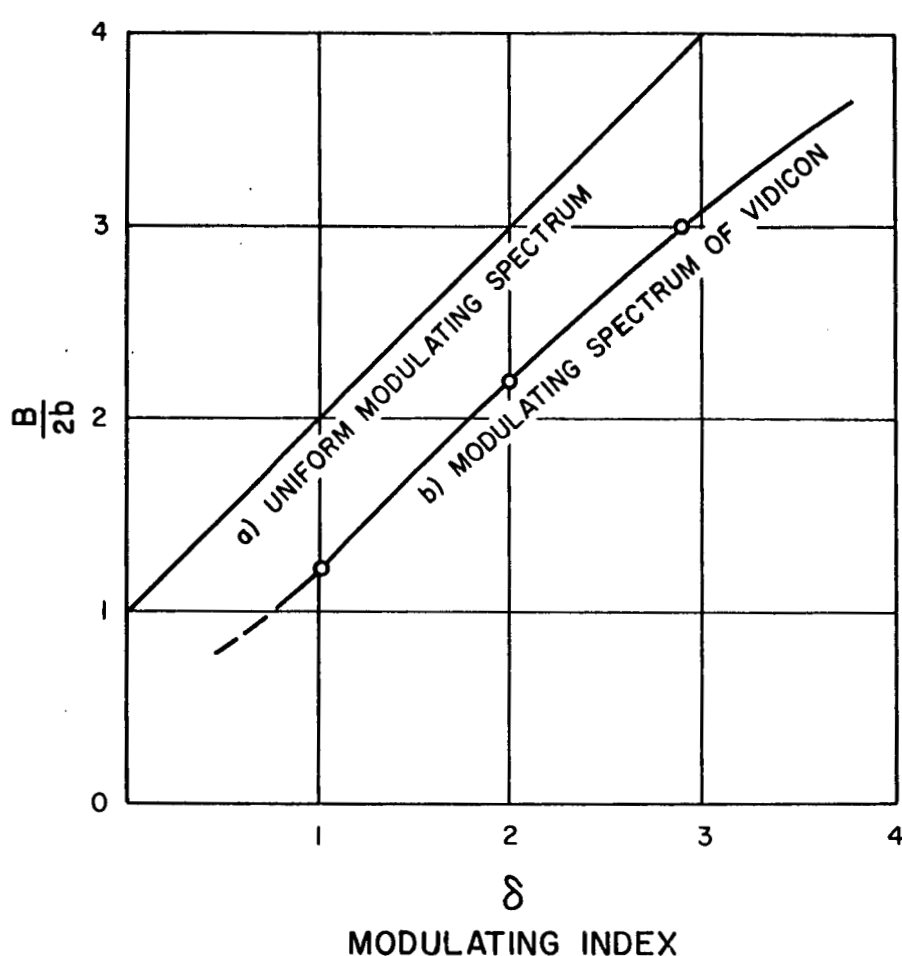
$$B \simeq 2b(1 + \delta) \quad (2)$$

For the proposed operating parameters

$$\delta = 1.4$$

$$b = 500 \text{ KC, so that} \quad (3)$$

$$B \simeq 2.4 \text{ MC}$$



$\frac{B}{2b}$ VS δ FOR TYPICAL VIDICON
TUBE SPECTRUM MODULATOR
A FM TRANSMITTER

B =RF BANDWIDTH
 b =BASEBAND
 δ =MODULATOR INDEX = $\frac{F_d}{b}$
 F_d =ONE HALF THE PEAK
TO PEAK DEVIATION

NOTE: THE CRITERIA DEFINING USEFUL SIDEBAND POWER ARE THOSE
SIDEBAND POWERS GREATER THAN 10% OF THE UNMODULATED
CARRIER POWER. THIS IS NOT A GOOD DEFINITION FOR $\delta \ll 1$
BECAUSE SIGNIFICANT INFORMATION MAY BE NEGLECTED.

Figure III-2. RF Bandwidth Versus Modulation Index for (a) Uniform Modulating
Spectrum, and (b) Modulating Spectrum of Vidicon

Now, if the spectrum similar to the vidicon frequency response is used to modulate the transmitter the RF bandwidth B , given by equation 2 is no longer valid because the higher frequency components (of reduced amplitude) do not fully modulate the transmitter. Actually, the significant sidebands existing at the extremes of the RF bandwidth are actually higher order sidebands of the lower modulating frequencies, and not higher order sidebands of the higher modulating frequencies. Assuming the case that defines equation (2), only those sidebands greater than 10% of the unmodulated carrier are considered significant, the actual side band frequencies for the vidicon type baseband spectrum may be calculated at single frequencies and the resultant spectrum obtained by superposition. If this is done the curve of Figure III-2 results, indicating that for a 500 KC baseband and a modulating index of 1.4, the actual RF spectrum is only 1.6 MC instead of the 2.4 MC calculated from equation (2).

Pre-emphasis is a technique whereby the high frequency signal components of the modulating wave are accentuated. In the receiver, after baseband detection, a de-emphasis circuit attenuates the high frequency signal components to their original values relative to the amplitude of the low frequency components. However, in the process the high frequency noise components are attenuated also, so that the baseband signal to noise ratio is increased. A typical pre-emphasis circuit is shown in Figure III-3A, and a typical de-emphasis circuit in Figure III-3B.

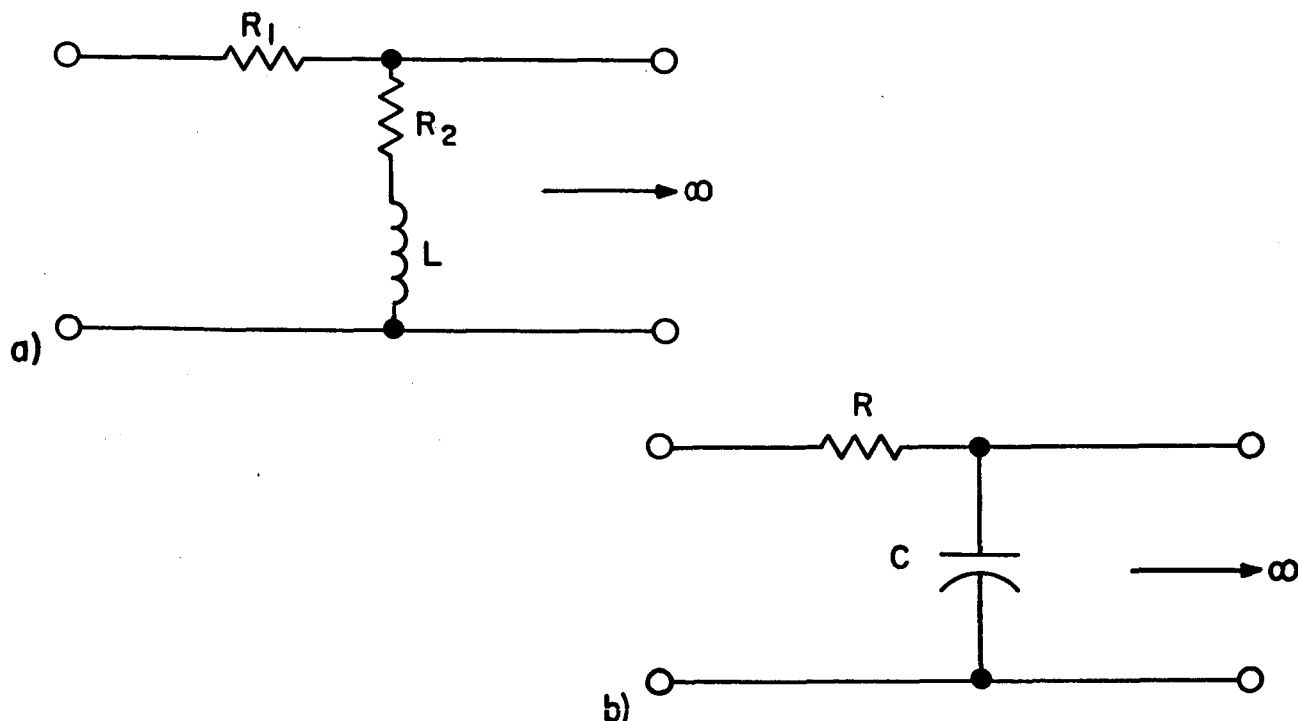


Figure III-3. (a) Typical Pre-Emphasis Circuit, and (b) De-Emphasis Circuit

The power transfer function of the circuit of Figure 3B is:

$$|H(j\omega)|^2 = \frac{1}{1 + \omega^2 \tau^2}, \tau = RC \quad (5)$$

$$\omega = 2\pi f$$

Now, for an FM detector with a rectangular baseband filter cutoff frequency equal to b , the baseband noise power N is proportional to:

$$N \approx \int_0^b f^2 df \quad (6)$$

For the case where the circuit given by equation (5) is inserted in the baseband circuit, the noise power N' is then proportional to:

$$N' \approx \int_0^b \frac{f^2}{1 + 4\pi^2 T^2 f^2} df = \frac{1}{4\pi^2 T^2} \left[b - \frac{1}{2\pi T} \tan^{-1} 2\pi bT \right] \quad (7)$$

With these equations, the improvement in signal to noise ratio, using pre-emphasis may be calculated. For a 500 KC baseband, and $\tau = 1 \times 10^{-6}$, a 7 DB improvement in baseband signal to noise ratio can be achieved. This results in a gain in carrier signal to noise ratio of 1.7 DB which is the value tabulated in Table 1. The 1.7 DB gain is achieved by the addition of passive circuits to the satellite transmitter.

These calculations assume certain conditions which should be carefully denoted. Signal to noise ratio is usually defined as the ratio of the power of a single frequency sinusoid to the average power of the noise in the defined bandwidth. For a uniform signal spectrum there is no ambiguity. However, a problem of definition and interpretation arises when the signal power varies with frequency, (a non-uniform spectrum), as is the case above. In the calculations on pre-emphasis, the 1.7 DB saving in carrier power was obtained by assuming a signal power (a low frequency sinusoid) that fully modulated the transmitter. As a result, the single frequency signal to noise ratio decreases with increasing signal frequency. For a given baseband signal to noise ratio the presence of noise will manifest itself in different ways depending on the baseband frequency spectrum, which in turn, will depend not only on the vidicon characteristics, but on the character of the information, the picture content. (For instance, the difference in information content between a picture of a dried up ocean bed and a non-eroded mountain top). The calculations have been done in the customary manner, and the results are indicative of what might be expected.

Several conditions must be satisfied before pre-emphasis can be used, however. These conditions stem from the nature of TV signals. In voice transmission (voice, music, etc.), the ultimate sensor, the ear, is found to be relatively insensitive to phase distortion. Hence, simple pre-emphasis and de-emphasis circuits may be used. In commercial television audio, de-emphasis time constants of 75 microseconds are used to good advantage. In video transmission unfortunately, the situation is more complex because the intelligence is essentially in the form of rectangular pulses. An elementary type of distortion is shown in Figure III-4 and is essentially caused by the non-linear phase characteristic of the pre-emphasis characteristic. Of course, the intelligence may be recovered without distortion if the product of the transfer functions of the transmitter pre-emphasis circuit and receiver de-emphasis circuit is a constant. One can derive many combinations where this

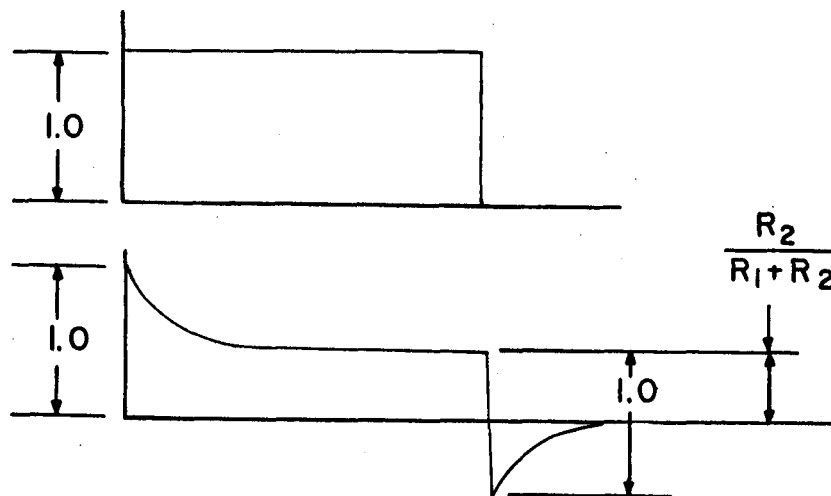


Figure III-4. Transient Response of Circuit of Figure III-3.a to a Rectangular Wave, (a) Input Wave, (b) Output Wave

is true for certain bandwidths, and the circuits in Figures 3a and 3b are examples. Unfortunately, the waveform distortions arising from the phase non-linearities frequently over-modulate the transmitter ^{*1} or result in sidebands beyond the bandwidth capability of the communications channel so that distortion can be very severe. The problem is difficult to analyze because of the complexity of video signals and empirical solutions are frequently used, once the transmitter parameters are known. One approach is to use all pass

*1 Television Standard and Practice, N. T. S. C. McGraw Hill 1943

"bridged T" or "ladder networks" to correct the phase characteristic and reduce the overload "peaks", an example of one type of phase correction network is shown in Figure III-5*2.

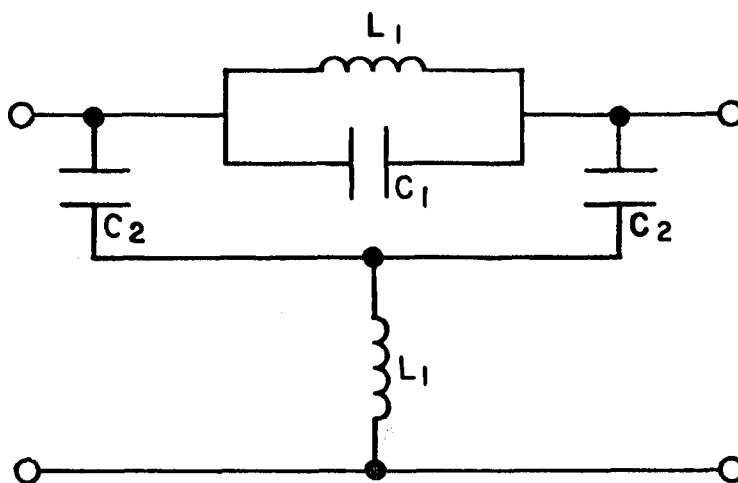


Figure III-5. Typical Bridged "T" All Pass Network Used for Phase Correction

5. Signal to Noise Ratio Considerations

Signal to noise ratio is discussed in detail elsewhere in this report because the optical system, camera and data storage system, ground data handling facilities and techniques, and the characteristics of the communications system all effect the signal to noise ratio of the output data.

In discussing the communication systems interface requirements, some general remarks and observations may be made. Specifically, the signal to noise ratio discussed in the interim report and the final report has assumed to be gaussian in form, that is, thermal noise. For a system where this is the case, a signal to noise ratio of 24 DB rms to rms, (33 DB peak to peak to rms), for the picture characteristics discussed in this report, (lines per millimeter, resolution, information character etc.), results in a picture having an information content that is limited essentially by the resolution and not by the signal to noise ratio. On the other hand, if one considers a picture with an 18 DB rms to rms (27 DB peak to peak to rms) signal to noise ratio the resultant picture has the characteristic "grainy" appearance caused by

*2 Notes on Delay Equalization, G. L. Fredendall, Engineering Memorandum PEM-407, RCA Laboratories, Princeton, N. J.

background noise, (thermal noise). Therefore, the optimum output signal to noise ratio is in the vicinity of 24 DB. This is the value chosen for the design study.

The effects of impulse noise on the information content of a picture is more difficult to define since the effects depend not only on the characteristics of the noise but on the picture and information characteristics. For example, although impulse noise is very objectionable in commercial TV pictures, and in audio too, to some extent, the "line" character of the lunar maps may make this type of noise less objectionable due to the "integration" carried on by human observers. Therefore, if the limiting receiver noise is essentially impulsive in character as one might expect from a phase-locked oscillator that is periodically falling out of lock, the desired signal to noise ratio would have to be reevaluated, perhaps empirically.

B. ELECTROSTATIC STORAGE TAPE CAMERA

1. Introduction

The electrostatic storage tape camera section of the Interim Report was divided up into a discussion of the basic principles of operation, a discussion of EST properties, a discussion of camera design, and a discussion of EST techniques applicable to electrical signal recording. The information presented in these discussions will not, for the most part, be repeated here. The purpose of this section of the Final Report is to qualify and complete the discussions of the Interim Report. Specifically, the specification, description and discussion of the final camera design(s) and a discussion of efforts related to the proposed VOIS camera design are presented.

The EST properties discussed in the Interim Report include storage time, resolution, sensitivity, spectral response, signal-to-noise ratio, gray-level response, and radiation resistance. A description of the writing flood gun was given in the resolution discussion. A comprehensive discussion of return-beam readout -- including the considerations required by the three levels of resolution -- is given in Section III. B. 3 of this report. An attempt to accurately correlate photographic and television terms and parameters (the objective being a more satisfactory description of the resolution capabilities of EST) would constitute a major effort beyond the scope of the present contract. However, the discussion of Section III. B. 6, based on the work in this area of O. Schade, should indicate the considerations to be made in evaluating various systems.

Theoretical and experimental investigations of highly sensitive EST are being performed by the Astro-Electronics Division for the classified programs discussed in Section III. B. 5 of this report. An analysis of the gray-level response was just begun in the last week of the final period; it is hoped

that this effort will be continued. Sufficient radiation resistance data on EST is still not available; radiation tests are planned, however, for the near future.

The camera design discussion in the Interim Report was intended to indicate the main areas of concern. The proposed mechanical and electrical designs are presented in Sections III. B. 3 and 4, respectively, of this Final Report.

2. Continuous Tape Evaporator

A comprehensive discussion of the electrostatic storage tape camera -- with emphasis on the basic principles of operation and the important properties of EST -- was given in the Interim Report. The VOIS package proposed herein and its suggested alternate design incorporate four EST cameras, each camera containing 1500-2500 feet of tape. The Astro-Electronics Division, anticipating the needs of future satellite systems, has been engaged in an RCA-supported program for producing long lengths of EST. A discussion of this project is included below.

In review, EST construction consists of depositing, in the order named, a transparent conducting layer or signal plate, a photoconducting layer, and an insulating layer on a flexible transparent base. On either side of the sensitive area of the tape is a conducting strip that serves as an electrical contact to the signal plate. At present short lengths of EST are being produced manually; a three-foot length of 70-mm tape was made in this manner in December, 1960. With respect to the progress being made under the present EST research and development programs (see Section III. B. 5), the need for longer lengths of tape will soon appear.

In the winter of 1958, the Astro-Electronics Division began work on an EST manufacturing process. The initial effort involved the research and design of a prototype continuous tape evaporator. This machine was to reproduce and then modify the manual procedures for making EST. The progress of this effort is noted below.

At present the evaporator can coat 10-foot lengths of 70-mm tape with a conducting layer. Indications are that the gold and copper mixture will make an effective signal plate. A modification of the feed apparatus will permit 50-100-foot coatings by February, 1961.

The conducting strip is also of copper and gold. Rolling contact tests on the machine-deposited strips are now being performed. If excessive wear is noted, other methods of obtaining a conducting strip will be sought. Fifty to 100-foot strips could be achieved in the continuous tape evaporator by mid-year, 1961. In any case, the electrical contact to the signal plate is not expected to be a serious problem.

Bulk evaporations of antimony trisulfide and selenium are being attempted in the evaporator. If successful deposition of photoconductor is achieved in this manner, then 50-100-foot lengths of tape could be coated by February, 1961. If boat-feed evaporation is required, then long-length deposition of photoconductor will be delayed to mid-year, 1961.*

With respect to the insulating layer, there may be a strong limitation to the length attainable in the prototype machine. Short lengths of tape bearing discharge-deposited styrene layers should be attainable by March, 1961. The time schedule for longer lengths of tape coated with polystyrene depends on the results of current tests.

The flexible base being used in all of the above procedures is 4-mil, 70-mm Cronar tape, duPont's movie-film base. This tape has served as a successful base for all the strips of EST made to date, and is expected to be the substrate for all future lengths of EST.

To summarize, each of the procedures for manufacturing EST on a prototype basis is expected to be developed by mid-year, 1961. The combined process should produce 10-100-foot lengths of EST in the evaporator by July, 1961. Conservative estimates of the time required to make continuous lengths of tape, including the pull-down and set-up times, indicate that 50 feet of EST could be produced in two working days.

The quality of the tape to be produced (in the prototype evaporator) during the first half of 1961 is not expected to be compatible with the high quality requirement of VOIS. An investigation of EST quality -- with emphasis on obtaining optimum target geometry and uniformity -- is now under way at the Princeton location of the Astro-Electronics Division. This effort is expected to be increased after the completion of quality tests to be run in March, 1961. Modifications of the prototype machine are expected to result from the investigation.

The state of the present program, coupled with the progress expected in the areas concerned with tape quality, points to the desirability of considering the design and construction of a large-capacity continuous tape evaporator. The design of the prototype machine was intended to be compatible with that of a large-capacity evaporator. The new machine would also incorporate the design changes suggested by the quality investigation.

The large-capacity machine would be expected to produce high-quality EST -- suitable for use in the VOIS cameras -- in lengths exceeding 1000 feet. Lengths of tape in the 1500-2500-foot range would naturally have

* Since the writing of this report, successful bulk evaporations of Sb_2S_3 were achieved in the continuous tape evaporator. Tape lengths of up to 35 feet displayed clean and uniform coatings; this method seems readily applicable to 1000 foot evaporations.

to include some splices. Thin splices which would not disturb EST camera operation now seem feasible; they would also be engineered into the new machine.

At present it is estimated that considerable funding would be required for a large-capacity continuous tape evaporator. Both RCA and a government agency are considering supporting this expansion of the present program. If the present plans are realized, then the design and construction of a new machine would begin in March, 1961, and would be completed and ready for EST production early in 1962.

3. Mechanical Design

The camera housing is an enclosure which contains the electrostatic storage tape and its transport mechanism and the imaging (flood) electron gun. The readout electron gun is mounted on one wall of the housing and extends outward. A window in another wall admits the optical rays from the lens system so as to form an image on the tape at the imaging focalplane (see Figure III-6).

One-thousand, five-hundred feet of electrostatic tape are stored in the housing. The tape is in the form of 70 mm movie film and the tape base is .005" thick Cronar. The tape is stored on and exchanged between two 12" diameter reels. For economy of space the two reels are mounted coaxially. The tape leaving one reel passes around a series of rollers before entering the second reel. The rollers introduce a twist into the tape at two sections and lead the tape out of the plane of one reel and into the plane of the other reel. The two reels are torqued in opposite directions by constant tension spring mechanisms. This torquing system produces a tape tension which is essential for maintaining flatness in the two focal planes, and also develops a frictional grip between the tape drive capstan and the tape.

A capstan frictional drive is used to move the tape rather than a positive sprocket drive because of the need for smooth tape motion during the imaging process. Sprocket teeth used for driving will introduce some jitter to the tape motion and degrade the image resolution. The capstan is required to drive the tape at two speeds: 1.1 inches/second (28 mm/second) during imaging and mapping resolution readout, and 39.4 inches/second (1 meter/second) during pointing resolution readout. The two speed mechanism consists of two independent motors coupled to the planetary pulley system, shown in Figure III-7. The speed of the output shaft of such a system may be expressed by the equation

$$N_3 = RN_1 + (1 - R) N_2$$

where N_3 = output speed

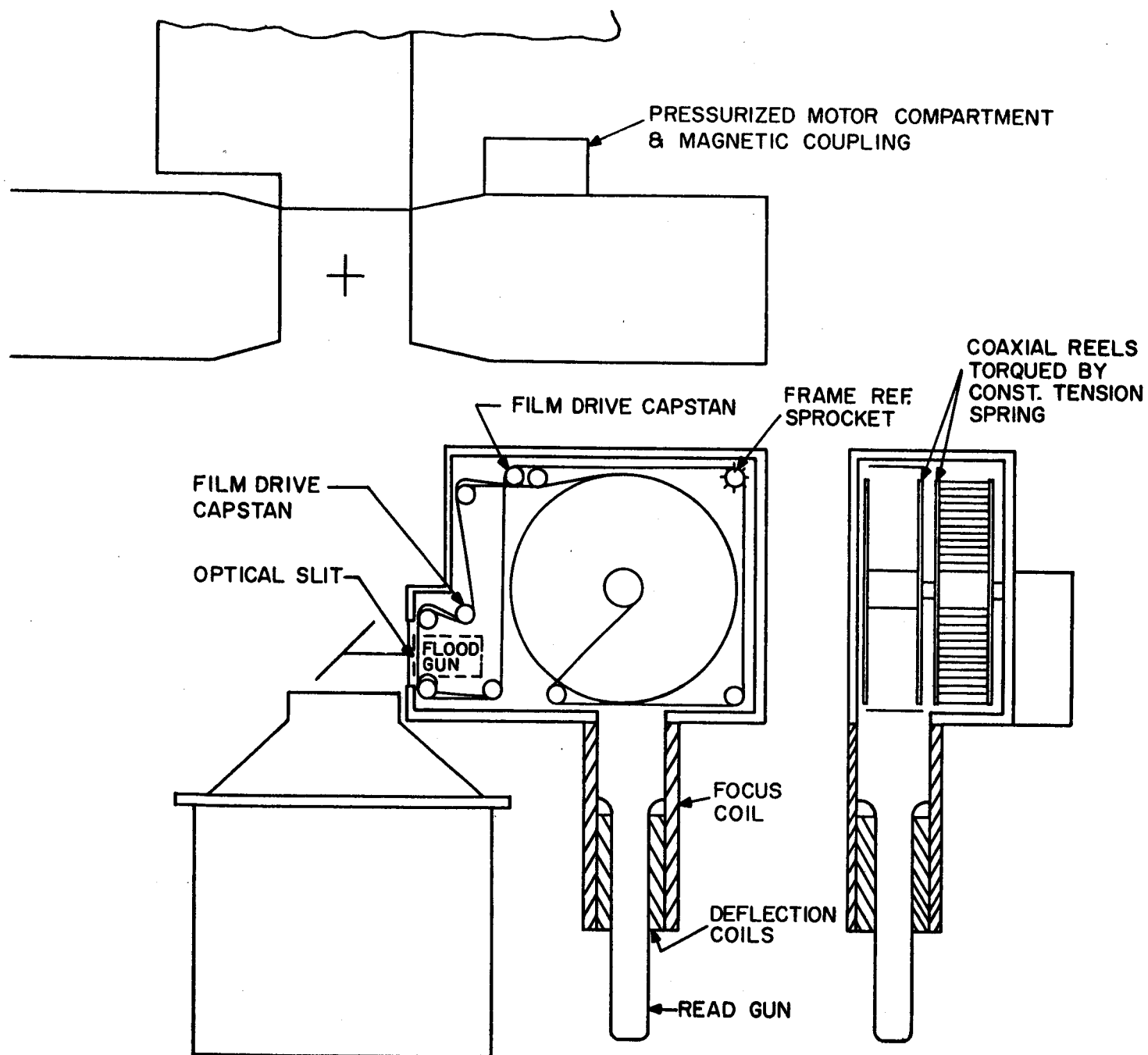


Figure III-6. Electrostatic Storage Tape Camera

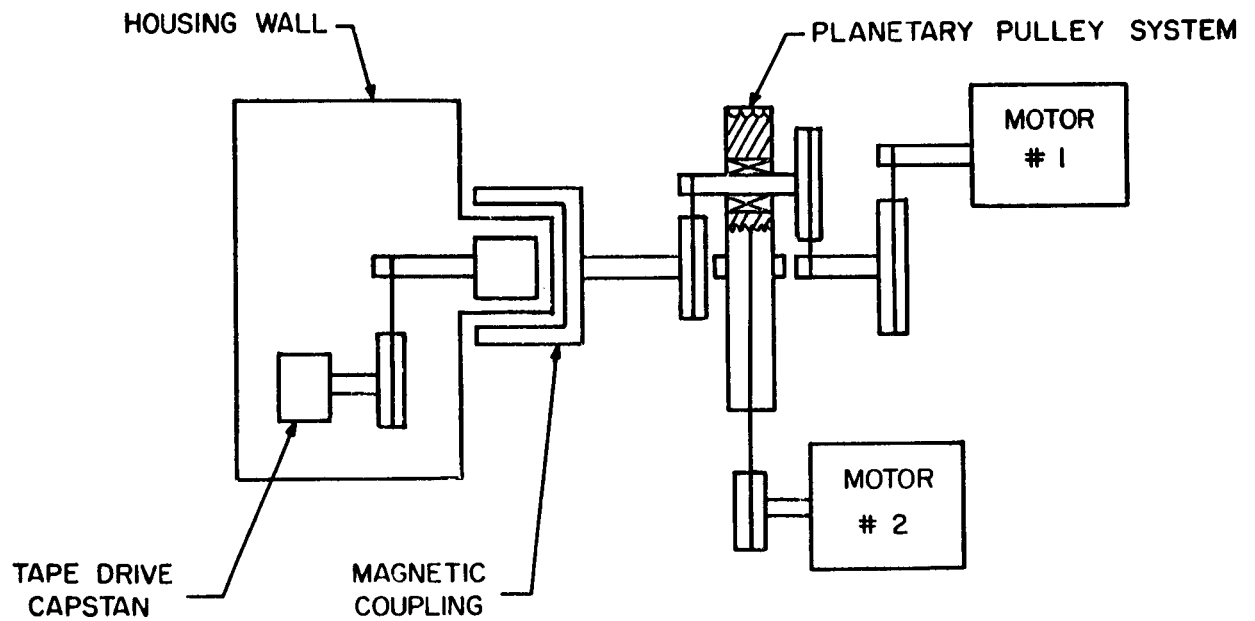
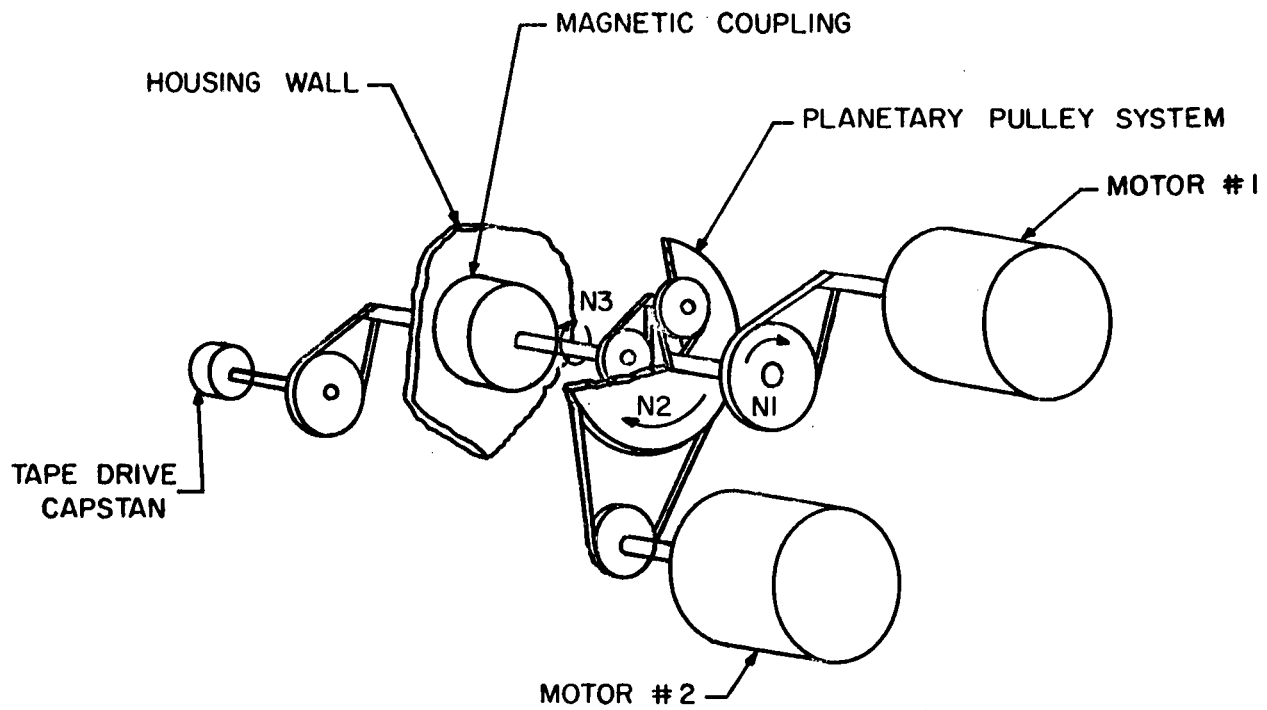


Figure III-7. Two Speed, Two Motor Transmission

N_1 = input speed from motor #1

N_2 = input speed from motor #1

R = reduction ratio when N_2 is zero

This system, powered by two constant speed motors, will provide as many as four different speeds by: (1) driving motors #1 and #2 in the same direction, (2) driving motors 1 and 2 in opposite directions, (3) driving motor 1 only, (4) driving motor 2 only. As proposed here, the two speeds will be obtained by energizing either motor #1 only or motor #2 only. The planetary belt system will use endless Mylar belts which permit very compact pulley arrangements, and result in smooth low-compliance drives.

The two motors and the planetary pulley system are located in a pressurized housing adjacent to the tape housing. This is done because of the problems of lubricating high-speed bearings in a vacuum, and also the troublesome effects of outgassing of any organic materials in the motor. The output shaft motion of the planetary system is transmitted into the tape housing through a magnetic coupling. The shaft motion of the magnetic coupling inside the tape housing is coupled to the tape drive capstan by an additional mylar belt stage. This last stage is used to increase the effective torque capacity and stiffness of the magnetic coupling.

The two motors will be hysteresis - synchronous motors driven by AC power from a transistorized power converter. The low speed motor will draw 4 watts and the high speed motor will draw 30 watts. The AC power will be nominally 400 cycles, however, it will be adjustable within narrow limits by a variable oscillator. This will permit correcting the scanning speed in accordance with any errors in orbital altitude.

During the imaging process the tape, driven by the capstan, moves past a slit in the optical focal plane and past the electron flood gun in exact synchronization with the scanning motion of the image. As part of the previously described route the tape follows, between its exit from one reel and entrance into another, the tape moves past the slit at an angle to the plane of the camera body. This angle will be selected so that the transverse component of the tape motion will match the transverse image motion due to satellite velocity. The resulting image will now be stored without smear.

During the readout process the tape will be driven past the read gun for mapping and pointing resolution. The electron beam will scan horizontally while the mechanical movement of the tape will provide continuous vertical scanning. During the high resolution readout the tape will be immobilized and a limited length of tape will be electronically scanned horizontally and vertically. The vertical scanning rates are 1 Meter/second for pointing resolution, 28 mm/second for mapping resolution, and 1/4 mm/second for high resolution.

Although the tape is driven by a capstan rather than a sprocket because of the need for a smooth drive, an idler sprocket wheel is engaged and rotated by the sprocket holes in the tape. The idler sprocket wheel rotates a commutator as part of a counting circuit and provides a reference on the tape length and frame number at the readout station. The high tape speed for pointing resolution will also be used for rapid advance or rewind of the tape for reading out discrete frames.

The camera housing will be a welded stainless steel assembly, hermetically sealed under high vacuum. A titanium getter pump will be incorporated in the housing. This will permit periodic ionic pumping of the vacuum in case of any gradual loss of vacuum due to outgassing during testing, storage, or transportation. Once in orbit, however, a small rupture disc in a wall will be punched out by a solenoid impact. This will insure that the vacuum in the tape chamber is the same as the outer environment. The pressurized chamber containing the motors and transmission will be made of aluminum, as will most of the mechanical and structural elements within the tape housing. The ball bearings which must operate under vacuum, however, will either be made of Stellite and run dry, or else of stainless steel, lubricated with a dry lubricant. All insulating components within the tape housing will be of inorganic materials.

It is estimated that the weight of each camera housing will be approximately 80 lbs., exclusive of any optical elements.

4. Camera Design: Electrical

For the electrical design of the VOIS camera system the main concern is with performing readout at the levels of resolution designated pointing, mapping and high resolution. The latter is defined as 200 TV lines/mm; the mapping resolution is expected to be 20 TV lines/mm; and the pointing resolution shall be down by approximately another order of magnitude (3 TV lines/mm).

For mapping and pointing resolution readout, the tape motion will be continuous past an electron gun; the image stored as a charge pattern on the tape will be scanned horizontally by the electron beam. The required tape speeds and horizontal scan rates are calculated below. For high resolution readout tape "frames" will be brought into stationary position, or indexed, in front of an electron gun; selected areas of the "frames" will be scanned horizontally and vertically by the electron beam. Each strip "frame" will be approximately a 2 1/4 inch x 2 1/4 inch square, defined by the active tape width (57 mm). The scan rates for this readout are also calculated below.

If L = horizontal scan rate in TV lines/second,

S = tape speed (or vertical scan rate) in mm/second,

R = readout resolution (assuming equal resolution in the horizontal and vertical directions) in TV lines/mm, and

K = vertical utilization or Kell factor (accounting for the imperfect registration of the imaging and readout processes),

then $L = KRS$.

If B = video bandwidth in cycles/second,

W = active tape width in mm, and

k = retrace or flyback time factor,

then $2B = kRWL = (kKW)R^2S$.

For a 10% flyback time $k=1.1$. The Kell factor has been determined experimentally and analytically; its value is $\sqrt{2}$. The active tape width of 70-mm EST is 57 mm. Substituting these values into the above expression yields

$$2B = 88.8R^2S.$$

Thus, for constant bandwidth the tape speed is inversely proportional to the packing density R^2 (in bits/mm² of tape). For the VOIS camera system full utilization of the available video bandwidth is desirable; this conserves transmission time. Assuming an available bandwidth of 500 kcs, the expression for the tape speed (or vertical scan rate) can be written

$$S = \frac{1.13 \times 10^4}{R^2}$$

From this expression the vertical scan rate required for the high resolution readout ($R^2 = 4 \times 10^4$) is calculated to be 0.28 mm/second; the horizontal scan rate is $1.6 \times 10^4/R = 80$ TV lines/second. The tape speed required for the mapping resolution ($R^2 = 400$) is calculated to be 28 mm/second. Since this is the same tape speed required for imaging (at the average orbital altitude of 200 kilometers) the mechanical design of the EST transport is greatly simplified. The horizontal scan rate required for mapping is 800 TV lines/second.

For constant bandwidth the tape speed increases as the resolution decreases. Thus the minimum possible pointing resolution is dictated by the maximum permissible tape speed. Very conservative estimates indicate that a 1-meter/second EST speed will be state-of-the-art with respect to high tape-positioning accuracy by 1962 - 63. Thus the pointing

resolution is calculated to be approximately 3 TV lines/mm; the horizontal scan rate required for pointing is 5000 TV lines/second.

As discussed and analyzed in the Interim Report, high velocity return-beam readout is the technique to be employed at each resolution level. To determine the operating characteristics of high velocity return-beams the Physical Research Group designed and built special test apparatus. Several electrostatic storage tubes have already been fabricated and tested.

These tubes consist of storage targets deposited on 1-inch vidicon faceplates and mounted in 3-inch image orthicon bulbs. Standard RCA 5820 Image Orthicon electron guns, optics and multipliers were employed by these test devices. In addition to these tube parts, target shields were incorporated to restrict the return of secondary electrons to the scanned area of the target. (In the EST cameras these shields will prevent erasure of adjacent pictures by secondary electrons produced during the writing procedure.)

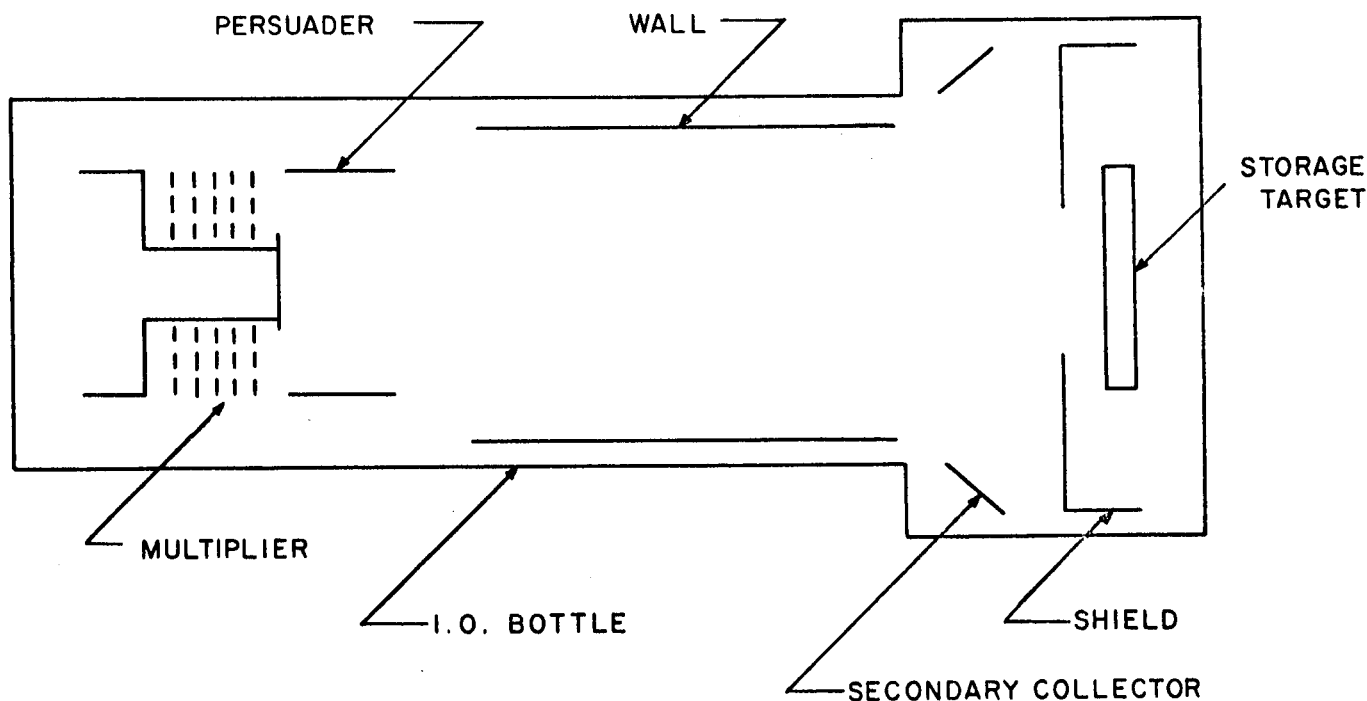


Figure III-8. Experimental Electrostatic Storage, Return-Beam Readout Tube

Figure III-8 is a diagram of an experimental electrostatic storage, return-beam readout tube.

The stored pictures read out during these tests were, in general, of good quality. Gun and electrode design modifications will of course be required for high resolution EST camera application, but preliminary tests produced the following set of operating voltages:

	<u>Electrode</u>	<u>Operating Voltage</u>
Multiplier	Dynode 2	450 volts
	Dynode 3	600
	Dynode 4	900
	Dynode 5	1200
	Collector	1250
G ₂		300
Persuader		260
Wall		300
Secondary Collector		120
Shield		250
Target	Prepare	205
	Write	260
	Read	240.

Further tests suggested shield and target voltage changes. With respect to gray-scale and background effects, better pictures were obtained at:

Shield		150 volts
Target	Prepare	100
	Write	200
	Read	150.

For all these return-beam tests the primary beam current was estimated to be 10^{-7} ampere.

Another important request of the initial experiments was an evaluation of the "redistribution effect." The tests indicated that either there was no significant redistribution of secondary electrons or the redistribution process acted in such a manner as not to degrade the picture resolution.

At present several methods -- each employing either one or two electron guns -- of obtaining EST camera readout at the three levels of resolution look promising for 1962-63 implementation. Two of these methods are recommended for further investigation and are discussed immediately below.

The single-gun method is the simplest in concept. A wide-deflection-angle, high-resolution gun is employed for the 200-TV line/mm readout. The gun will probably be quite similar to the positive-grid guns now being built and tested by the Astro-Electronics Division. The high resolution capability is expected to be maintained over the entire 2 1/4 inch x 2 1/4 inch format, the minimum scannable area being arbitrarily chosen as 1000 TV lines x 1000 TV lines (corresponding to a 1 km x 1 km area on the moon surface). This gun shall require 4 1/2-inch image orthicon deflection components (probably standard). Readout at the mapping and pointing resolutions is effected by successive defocussing of the high resolution beam. The latter is easily accomplished by mismatching the electrostatic and magnetic fields; the scanning rates and tape speeds are correspondingly adjusted. (This method is simpler and more efficient than that requiring filtering of the high resolution readout signal.) Writing, of course, is performed with a separate flood gun.

The second method, although employing two electron guns for reading, is inherently more reliable than the first. High resolution readout is accomplished with the same electron gun as above. Readout at the mapping and pointing resolutions is performed with a second gun. The electron-beam would be electrostatically focussed and deflected. Low power consumption and mechanical simplicity are outstanding features of this second gun. Defocussing from the mapping to pointing resolution condition and adjustment of the scanning rates and tape speeds are easily effected. The General Electrodynamics Corporation is now marketing a TV pickup tube employing return-beam readout and electrostatic focus and deflection; the electron beam is capable of resolving 20 TV lines/mm.

With respect to the electrical power requirements of the VOIS camera system, the table below indicates the peak-power requirements of the individual camera circuits. The values of power are current estimates of the 1962-63 state-of-the-art:

<u>Camera Circuit</u>	<u>Effective Peak-Power</u>	
Deflection Generator,		
Vertical:	33v @ 1.50a	50w
Horizontal:	33v @ 1.50a	50w
Sync. Generator:	33v @ 0.06a	2w
Focus & Alignment		
Current Generator:	33v @ 0.30a	10w

<u>Camera Circuit</u>	<u>Effective Peak-Power</u>	
Video Amplifier		
and Processor:	33v @ 0.60	20w
Auxiliary Equipment		
<u>(DC/DC Converters, etc.)</u>		<u>18w</u>
Total Peak-Power per Camera		150w.

On the basis of these tabulated figures, the average operating power requirement per VOIS camera is estimated to be between 50 and 75 watts.

The vertical deflection, sync. generator, and video processing circuits are expected to be completely transistorized. The 5000-TV line/second horizontal scan rate required for pointing will probably necessitate the use of tubes in the horizontal deflection circuit. The design and development of EST camera circuits similar to those suggested for the VOIS camera system is proceeding at the Astro-Electronics Division. This effort is a necessary phase of the overall EST camera program discussed in Section III. B. 5.

5. Related Efforts

At present there are four EST research and development programs being conducted by the Astro-Electronics Division. As described in Section III. B. 2 above, an RCA-supported program for producing long lengths of EST is underway at the Princeton location. The three major government-sponsored programs mentioned briefly in the Interim Report are discussed more fully below.

Research on EST and EST devices for satellite use is being conducted for the Wright Air Development Division under Contract No. AF-33(616)-6365. The efforts supported by the Television Photo Tape project include development of special-purpose photoconductive layers, determination (by extensive measurements) of storage target characteristics, design and testing of electron-optical components, experimentation with mechanical parts, and development of vacuum techniques. Much of the work is directly applicable to VOIS, and the pertinent results of the research performed under this contract for the past 20 months have influenced the camera discussions in the Interim and Final Reports on VOIS. Because of the Secret classification of the project specific references to the Television Photo Tape contract are not permitted.

An EST camera for meteorological satellite applications is being developed for the National Aeronautics and Space Administration under Contract No. NAS 5-434 (unclassified). The final subsystem is intended to produce high resolution, good contrast pictures of specified, limited areas of the earth. The optical system of the flyable camera will take panoramic pictures by scanning the earth's surface in a direction perpendicular to the motion of the satellite. This is the same scanning procedure proposed for VOIS.

The following specifications and parameters, which pertain to the final subsystem for the NASA camera, are basic to the present camera development program:

Size: Less than 2.5 cubic feet (external electronic controls).

Weight: Less than 50 pounds.

Power: Less than 20 watts (24.5-volt primary supply).

Output:

Impedance: 1000 ohms.

Amplitude: 10-volt peak, including 0.2-volt horizontal sync. in the negative (or black) direction.

Video bandwidth: 670 kcs.

Digital data storage: To about 50 binary codes on tape between pictures, with information on time, pitch, yaw and roll angles and rates of primary concern.

Tape:

Overall width: 35 mm.

Overall length: 50 feet per orbit, 150 feet total.

Tape length per picture: About 13 inches.

Exposed tape per picture: About 12 inches.

Sensitivity: At least 0.1 foot-candle-second for white light.

Storage capability: 30 pictures per orbit, 90 pictures total.

Resolution (optical): 0.1 mile for 600-mile altitude.

Gray scale: 10 steps of $\sqrt{2}$.

Readout time: About 3.3 minutes per orbital picture.

Optical System:

Effective focal length: 7.2 inches \pm 5%.
Speed: f/3 maximum or as required.
Transmission: At least 0.7.
Field of view: 98° normal to the trajectory.
Spectral response: Peaked between 5000 and 7000 Å.

Associated Circuitry:

DC/DC converters drawing on a 25-volt primary supply of 1% regulation.
Video amplifiers.
Time base oscillators and deflection circuits.
Synchronous AC power supply.
Timing device.
Digital converters.

The Phase I activities of the contract are not intended to result in flight hardware. The design of the laboratory models of the EST camera, however, is expected to be compatible with the above specifications and with the packaging and environmental limitations. Thus, the tape transports will be in vacuum enclosures, whereas the mechanical parts of the optical system will be in pressurized vessels. Torque transfer will occur through shielded, magnetic couplings.

The program for the development of the camera and its associated equipment is concerned with three main items: the EST camera (including the camera tube, circuitry and optics), the display and calibration device (providing a permanent record of the camera output), and the EST, itself. Work in these areas has been in progress since July, 1960. The results of the efforts to date are included in the camera discussions of the Interim and Final Reports on VOIS.

Finally, a research and development program for a high resolution EST camera is being sponsored by the Wright Air Development Division under Contract No. AF-33(616)-7284. The contract calls for the development of a breadboard model of a complete camera and ground-recording system to demonstrate the feasibility of certain image storage and readout techniques. It is expected that sufficient data will be available by the end of the program to permit the design of a prototype, high-quality image storage and transmission system suitable for use in an earth satellite. Three basic divisions of the project were established as follows: EST camera design and fabrication, electron-beam film recorder design and fabrication, and component and system testing and analysis.

The following specifications represent the EST camera design goals:

Tape:

Overall width: 70 mm.

Frame size: 2 1/4 inch x 2 1/4 inch.

Storage capacity: 20 frames.

Quality: Less than 25 defects smaller than 0.2 mm;
variation in output signal over surface less
than 10% (for at least six frames); less than
10% degradation in signal during 1000 exposure
cycles.

Sensitivity: 0.01 foot-candle-second; 0.1 foot-candle-second
peak highlight exposure.

Spectral response: 5000 to 9000 Å (essentially red), with
peak between 6000 and 8000 Å.

Resolution: Immediate, 40 TV lines/mm measured at 50%
response; after 2-hour storage, 30 TV lines/mm
measured at 50% response.

Associated circuitry:

Scanning bandwidth: 6 mcs.

Scanning frequency: 2 kcs (corresponding to 100
TV line/mm).

Scanning linearity: 2% overall.

Deflection amplifier.

Video amplifier.

Focus current regulator.

Sync. generator.

Power supplies.

The tape camera enclosure was designed to be compatible with a vacuum environment. The structure -- a rectangular chamber of stainless steel -- houses a sophisticated tape transport mechanism, a flood gun for writing, and access parts for an optical system, a readout gun and a vacuum pump. The enclosure -- pictured without its flood gun in Figure III-9 -- was completed by the Astro-Electronics Division in December, 1960. Tests are now in progress to determine the ability of the chamber to maintain satisfactory vacuum.

With respect to the associated camera circuitry, work on the deflection generator and amplifier, transistorized sync. generator, focus current regulator, and associated power supplies has been completed. The design of the breadboard model of the transistorized video amplifier was

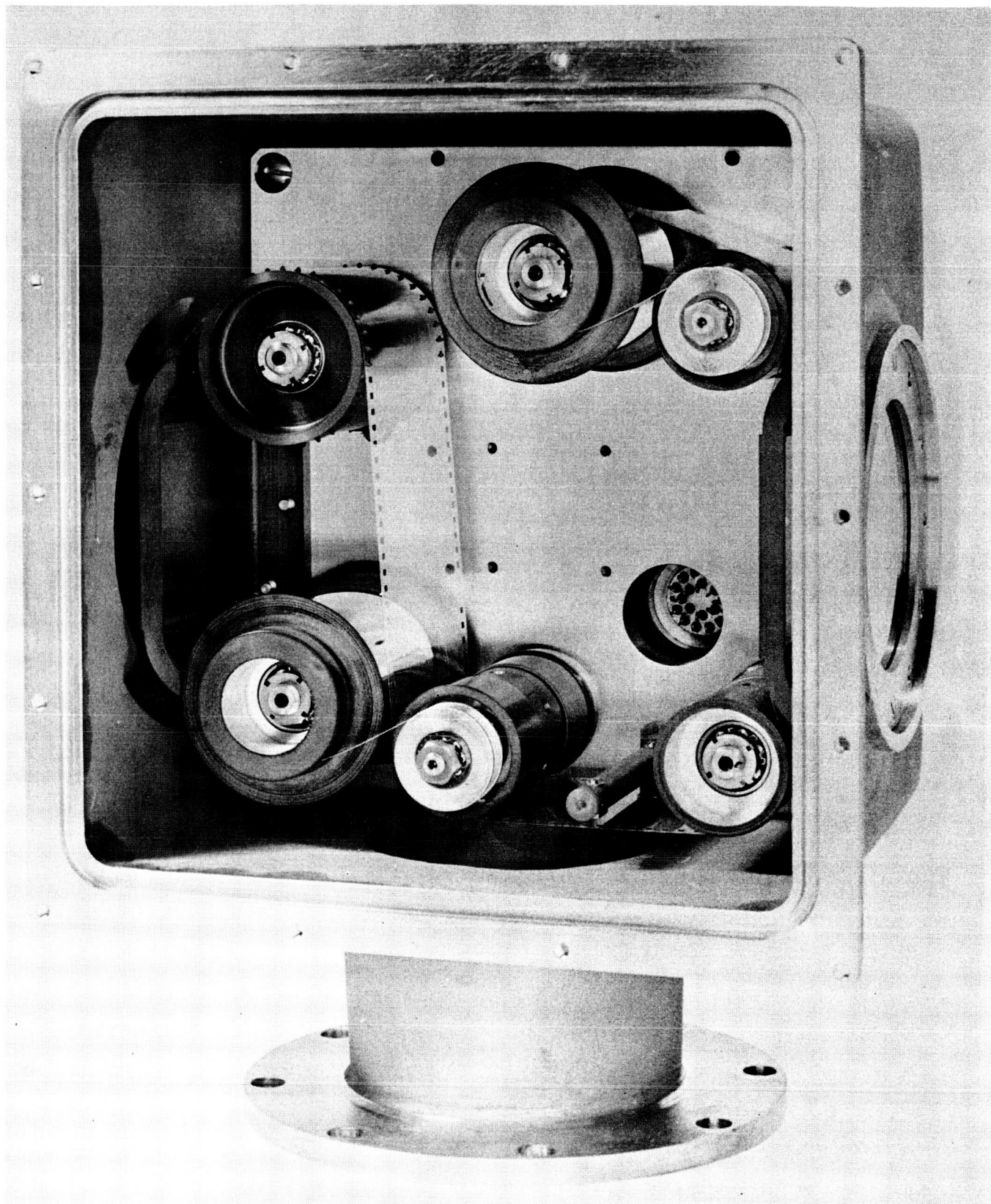


Figure III-9. EST Camera Enclosure

completed in December, 1960. A block diagram of the overall system (including the camera and its associated circuitry) is presented in Figure III-10. Unless unforeseen difficulties arise preliminary testing of the over-all system will begin by the end of 1960.

The development of high resolution image pickup and storage devices necessitates the development of compatible receiving and recording systems. Conventional systems incorporate standard kinescope display of the data and permanent record by ordinary photographic means. The present limit of kinescope resolution, however, is about 3000 TV lines/picture height. This limit has several sources: the electron beam used to excite the phosphor, the grain and internal halation associated with the phosphor itself, and the limitations of available lenses.

In 1960, the Astro-Electronics Division successfully demonstrated the feasibility of a "new" high resolution recording technique which previously had application only in the fields of electron microscopy and cathode ray oscillography. An image was formed directly on photographic film by electron-beam bombardment. This technique -- incorporated in the electron-beam film recorder being developed for the Wright Air Development Division -- eliminates the phosphor and lens limitations previously imposed on the recording systems.

The enclosure for the electron-beam film recorder -- which features a high resolution, high voltage triode electron gun -- will be completed by the end of 1960. The recorder chamber and associated circuitry (in block diagram form) are pictured in Figure III-11. Work on the electronic circuits will essentially be completed in December, too. Preliminary testing of the recorder system is expected to begin in mid-January, 1961.

The development of an EST camera system implies the determination of basic system characteristics and limitations. Present and future laboratory tests will determine component and system aperture responses, sensitivity, signal-to-noise performance, storage and operating characteristics, mechanical performance, interface requirements, and equipment stability. Test facilities have been established at the RCA Space Center for this purpose.

The main test fixture, which was completed in the latter part of December, will permit the testing of EST samples, flood guns, readout guns and electron multipliers. The test "cube" -- pictured in Figure III-12 -- provides a vacuum environment for the camera components; the structure is independent of the EST camera system.

The results of the effort supported under Contract No. AF-33(616-7284 are included in the camera discussions of the Interim and Final Reports on VOIS. Specific reference to the project engineering reports and status letters is not permitted under the Confidential classification recently imposed on these communications.

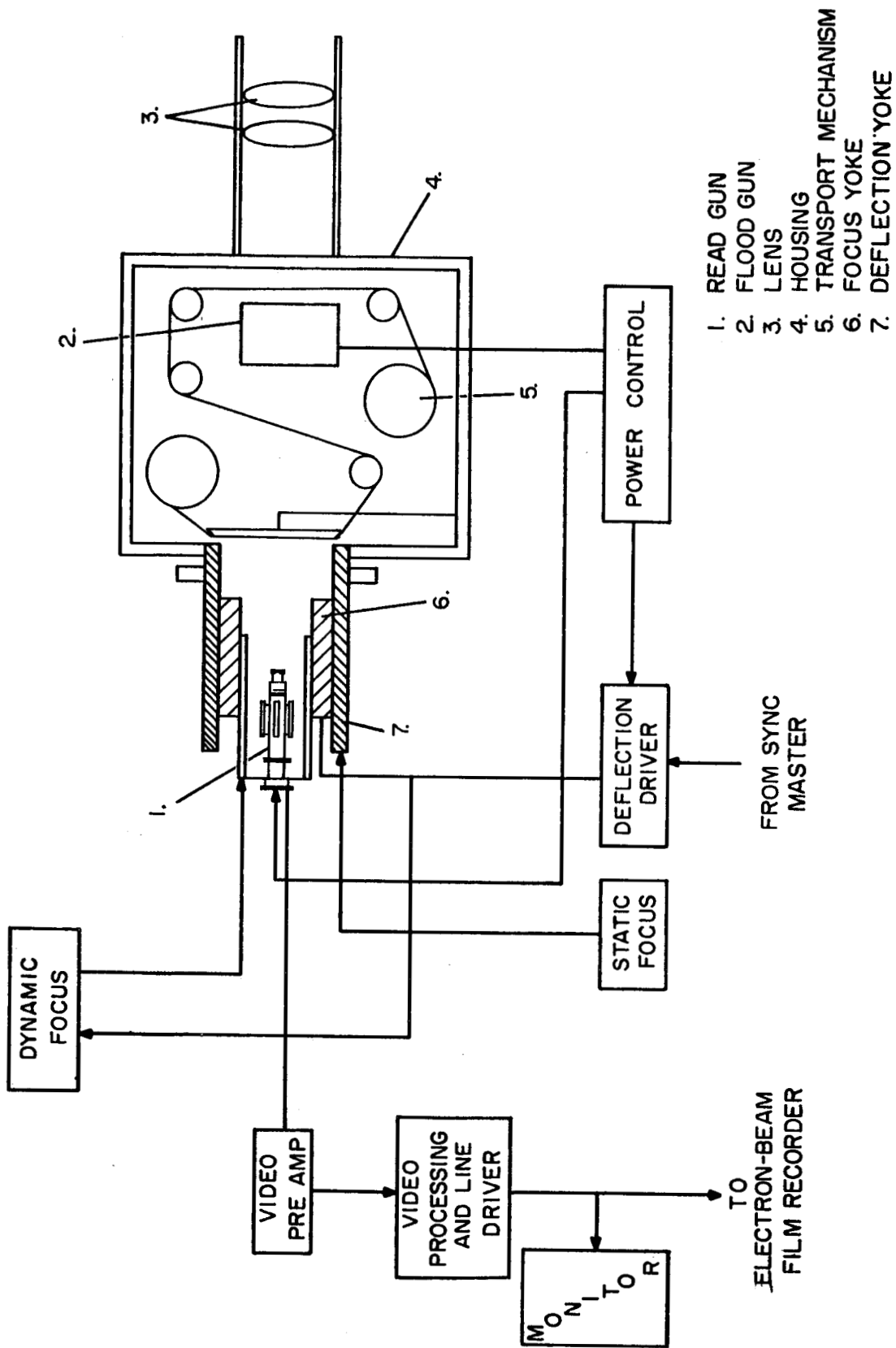


Figure III-10. EST Camera System Block Diagram

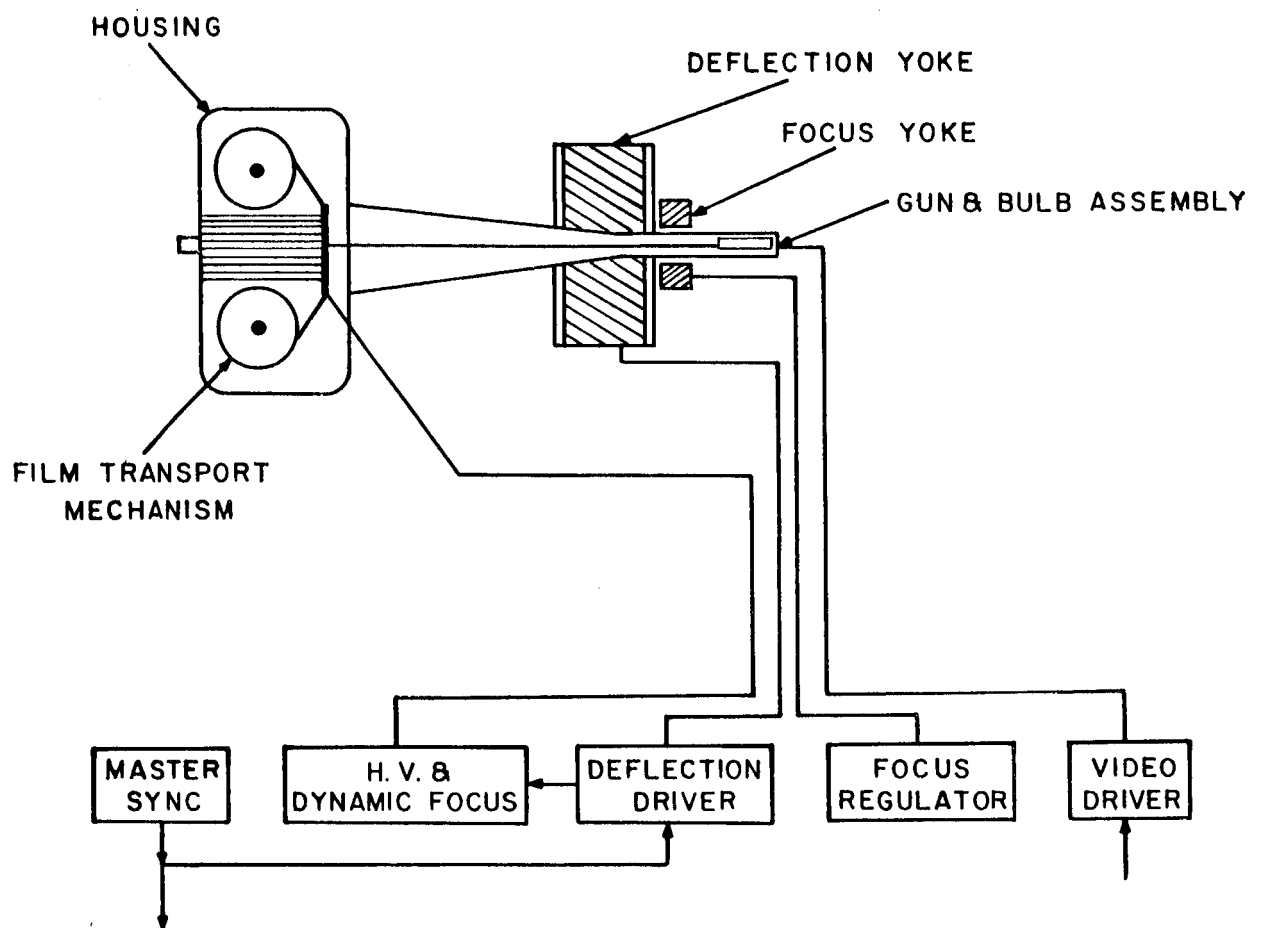


Figure III-11. Electron-Beam Film Recorder Block Diagram

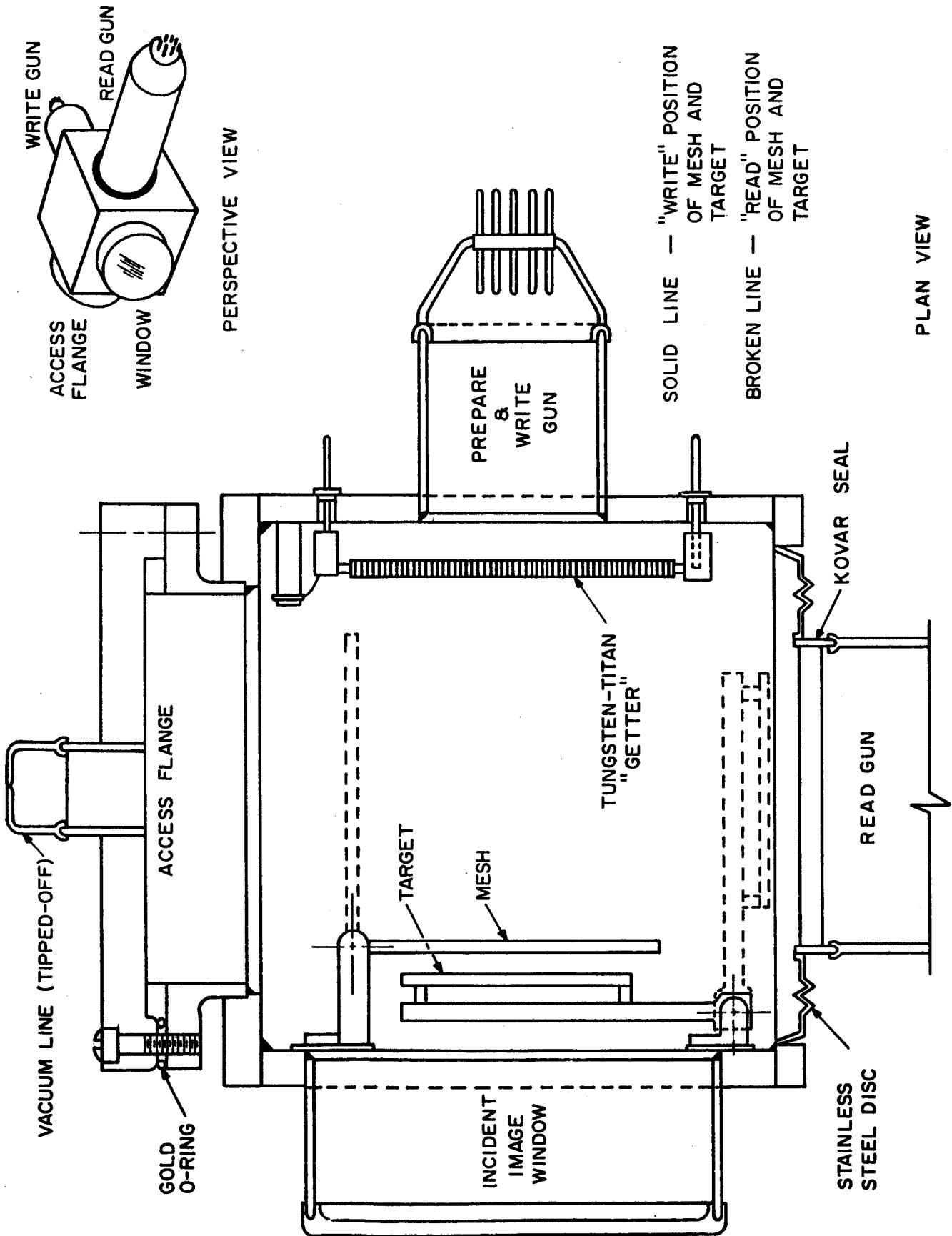


Figure III-12. EST Target and Component Test "Cube"

The mutual benefits derived (by the sponsoring agencies) under the coordination of the four EST research and development programs cannot be overestimated. In general, the progress of a phase of one program can be traced directly to the progress of a number of phases of the other programs. The salutary effect that these four EST programs would have on a VOIS research and/or development program should be obvious from the above discussion.

6. Resolution Criteria

The entire process of optical imaging was analyzed by O. H. Schade of the Radio Corporation of America (Harrison, New Jersey). * The system of evaluation which he developed is particularly applicable to imaging systems constructed of cascaded processes. The discussion below pertains to Schade's development of criteria for determining system resolution.

Perfect imaging implies perfect point-to-point transfer of information from object to image. In reality, however, any imaging process loses information because of the integration from an object area (rather than a point) to an image point. Thus in a light-optical system, the resolution of optical information is limited by diffraction (as determined by the geometry of the system) and, more severely, by aberrations. In a television system the resolution is limited by the electron-beam spot size at the target.

The resolution capabilities of an imaging process, as defined by its aperture response, can be determined in several ways: by measuring the area distribution of the information in the image of a point source, by measuring the transient response or reproduction of a sharp edge, or by measuring the relative response to repetitive object patterns of varying spatial frequency. When the object pattern in the latter method varies sinusoidally in intensity, the result is the sine-wave response or steady-state frequency response of a low-pass filter.

The functions associated with the above methods of determination are computable from one-another. For example, consider the radially symmetric intensity distribution for the point-image, $F(x, y)$. The integral $T(x) = \int_{-\infty}^{\infty} F(x, y) dy$ is a line-transmittance function whose Fourier transform is just the sine-wave response:

* O. H. Schade, "Image Gradation, Graininess and Sharpness in Television and Motion Picture Systems." J. of SMPTE. Part I: "Image Structure and Transfer Characteristics." 56, pp 137-177 (Feb. 1951). Part II: "The Grain Structure of Motion Picture Images -- An Analysis of Deviations and Fluctuations of Sample Numbers." 58, pp 181-222 (Mar. 1952). Part III: "The Grain Structure of Television Images." 61, pp 97-164 (Aug. 1953). Part IV: "Image Analysis in Photographic and Television Systems (Definition and Sharpness)." 64, pp 593-617 (Nov. 1955).

$$r \tilde{\psi}(N) = \frac{1}{A} \int_{-\infty}^{\infty} T(x) \cos(\pi Nx) dx,$$

where $A = \int_{-\infty}^{\infty} T(x) dx$, N is the television line-number, and r indicates that the function is normalized to unity for $N = 0$.

The sine-wave response is probably the most convenient, complete expression of the resolution capabilities of an imaging process. For a system of cascaded processes the sine-wave response for the system at a line number N is the product of the component responses at that line-number:

$$r \tilde{\psi}_{\text{sys}}(N) = r \tilde{\psi}_1(N) \cdot r \tilde{\psi}_2(N) \cdot r \tilde{\psi}_3(N) \dots$$

The importance of minimizing the number of imaging stages in the system design can be readily seen from the above expression.

In general, specification of resolution in terms of "limiting resolution" is not adequate. The line-number at which response is just detectable is made ambiguous by the noisiness of the system. Aperture response and signal-to-noise ratio, on the other hand, are distinct measures of image quality.

Actually, processes having the same limiting resolution may have significantly different capabilities for information transfer. This is illustrated in Figure III-13:

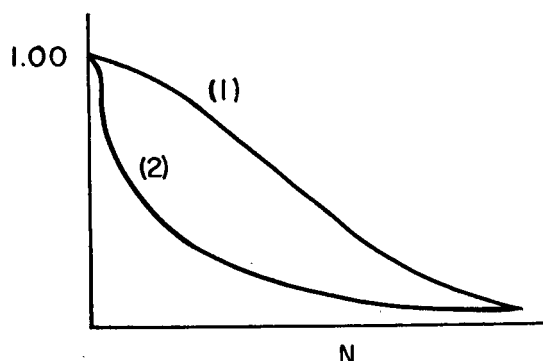


Figure III-13. Response of Two Imaging Components Having the Same Limiting Resolution

Response (1) could be obtained with a Gaussian point-image. Response (2) is the sine-wave response for a point-image with a relatively sharp central peak and a wide diffusion disc. The geometries of the two point-images were adjusted to establish an arbitrary percent response at the same line-number. It should be clear that response (2) is inferior to response (1) because of the relatively low response of the former for intermediate values of N .

Limiting resolution can be used as a comparison criterion for imaging processes when their response curves display similar shapes. Thus photographic films and phosphors (which have the same general grain structure) can be compared in terms of limiting resolution, but the criterion is not valid when comparing photographic-film with an electron-optical process. Limiting resolution also impedes any analysis of cascaded processes.

The one number that accurately specifies the aperture response of an imaging process is N_e , the equivalent line-number. It is the cut-off line-number for a rectangular (100%) sine-wave response having the same capabilities for information power transfer as the sine-wave response to which it corresponds. With respect to mathematical definition, N_e is the power integral of the sine-wave response:

$$N_e = \int_0^{\infty} r \tilde{\psi}(N)^2 dN.$$

Systems having the same value of N_e produce equivalently sharp images even though their component stages are different. This has been demonstrated by Schade in pure photography-television comparisons. The N_e of a system can be computed from the known aperture responses of its components:

$$\left(\frac{1}{N_e}\right)_{\text{sys}}^2 = \left[\left(\frac{1}{N_e}\right)_1^2 + \left(\frac{1}{N_e}\right)_2^2 + \left(\frac{1}{N_e}\right)_3^2 + \dots\right].$$

When all the responses are Gaussian, the above expression is exact. Errors of less than 5% result from more general responses.

The proposed VOIS camera system consists, essentially, of three cascaded apertures: the optical system, the electrostatic tape, and the reading electron-beam. With respect to the final picture record, the system N_e is further reduced by the ground reproducer (e. g., an electron-beam film recorder). The N_e of the optical system, as computed from the sine-wave response (for 50% obstructed) pictured in Figure III-14, is approximately 111 TV lines/mm. The N_e of EST is approximately 300 TV lines/mm. The N_e of the reading process, as calculated from the measured sine-wave response of a 0.01 microampere beam (see Figure III-11 of the Interim Report), is approximately 46 TV lines/mm. Thus the N_e of the VOIS camera can be computed:

$$\left(\frac{1}{N_e}\right)_{\text{cam}}^2 = \left(\frac{1}{N_e}\right)_{\text{opt}}^2 + \left(\frac{1}{N_e}\right)_{\text{EST}}^2 + \left(\frac{1}{N_e}\right)_{\text{read}}^2$$

$$= \left(\frac{1}{111} \right)^2 + \left(\frac{1}{300} \right)^2 + \left(\frac{1}{46} \right)^2$$

$$= \frac{1}{1484}$$

$(N_e)_{\text{cam}} = 38.5 \text{ TV lines/mm.}$

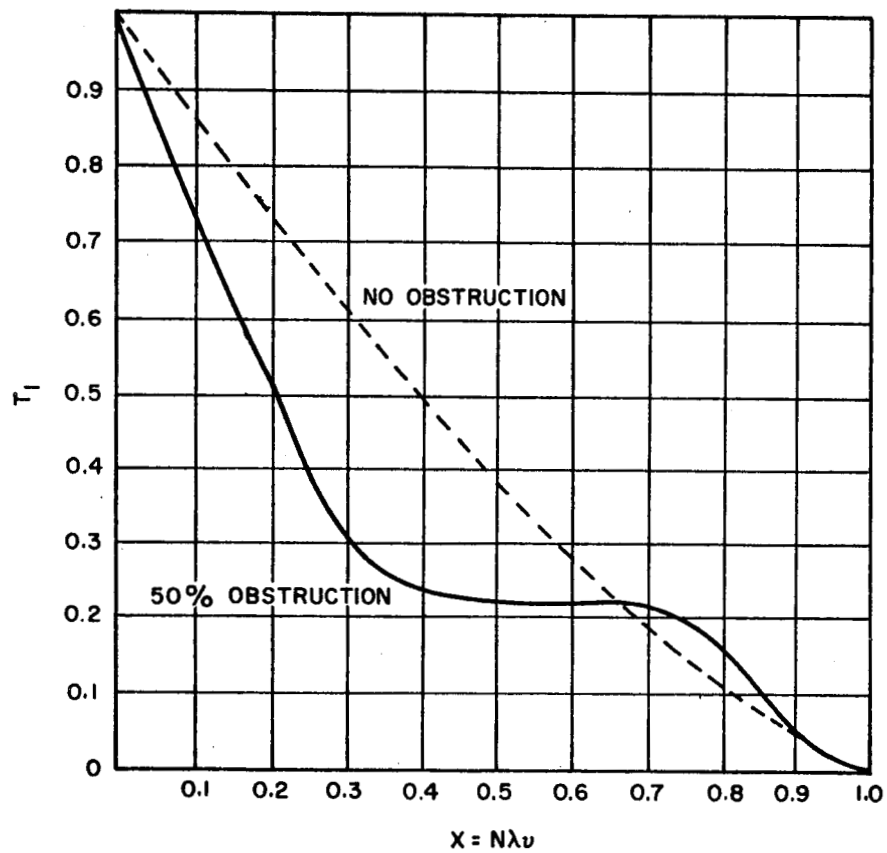


Figure III-14. Comparison of Theoretical Line-Wave Response of Obscured and Non-Obscured Optical Systems

C. OBJECTIVE LENS

Light-gathering and image-forming requirements establish the aperture and focal length for the optical objective lens. The dictum of low f-number and large aperture for high magnification lunar mapping limits the use of dioptric systems. For low magnification and wide field the dioptric system is preferable. The catadioptric systems have small fields but are capable of a high magnification. Obscuration, by the secondary optical members, reduces the sine wave response at low frequencies. Newtonian and Gregorian systems have the least obscuration but suffer from excess size and unsatisfactory off axis aberration correction balance. Cassagrainian systems are short in length with improved aberration coefficients. With the addition of an achromatized front element corrector plate and a dioptric back group, off-axis aberrations can be balanced.

Table III.C.1 is an outline of two system configurations. The 91.4 cm., F/2.5 catadioptric system was designed by Dr. James G. Baker. Both lens systems were built by Perkin-Elmer Corp. of Norwalk, Conn. The optical schematics of both lenses are shown in Figure III-15. The 30.5 cm., F/4 is an aspheric tessar type aerial camera lens, an improved version of the World War II camera lens. The 91.44 cm. focal length lens consists of a positive corrector lens, a primary concave mirror, a Mangin secondary mirror, and a dioptric lens group. Figure III-14, derived by Perkin-Elmer Corporation gives the sine wave response for the basic Baker Catadioptric system. To determine the transmission factor for a given level of resolution, consider the case of a periodic test object having a one meter period and imaged by the optical system from an altitude of 200 kilometers. The limiting resolution v_0 , is given by

$$v_0 = \frac{1}{N \lambda}$$

where $N = f/\#$, the relative aperture; and

$$\lambda = \text{average wavelength} = 6 \times 10^{-4} \text{ mm.}$$

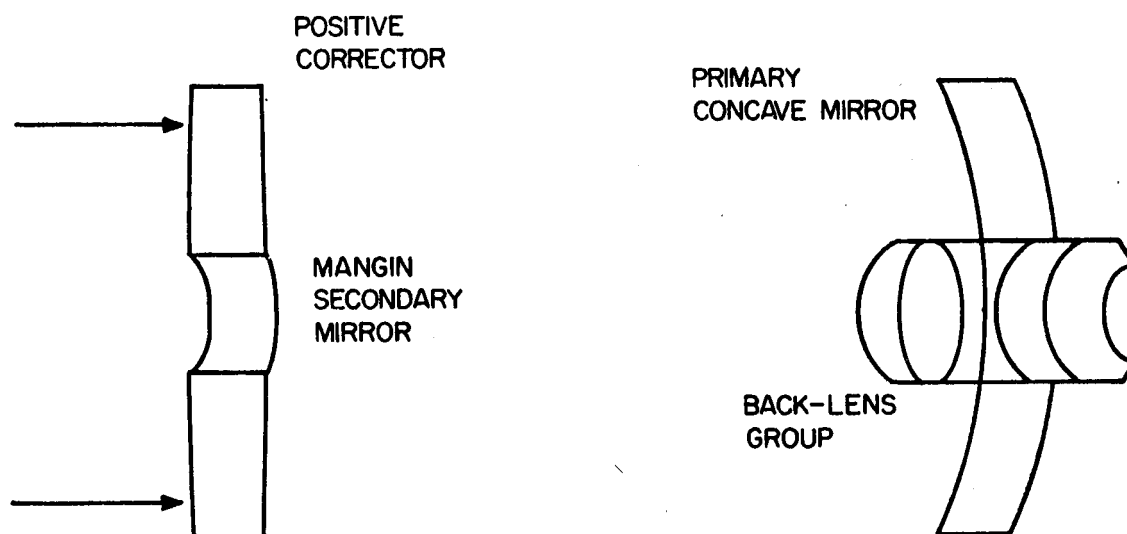
The frequency, v , in the image plane is given by

$$v = \frac{h}{df},$$

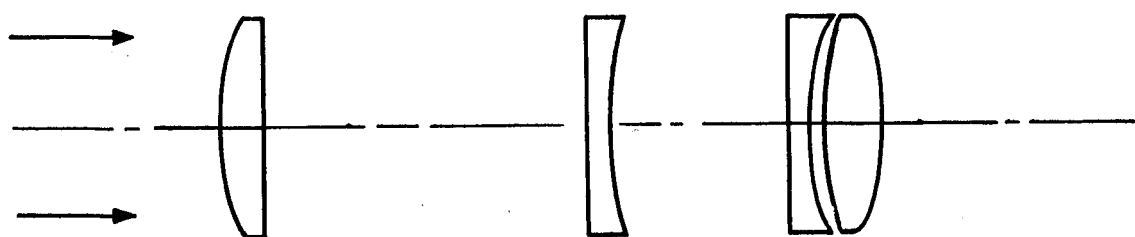
where $h = \text{object distance} = 200 \text{ km,}$

$d = \text{period of the test object} = 1 \text{ m, and}$

$f = \text{focal length of the object lens.}$



(A) BAKER CATADIOPTRIC F/2.5 36" F.L.



(B) PERKIN-ELMER 12" FL. F/4 TESSAR AERIAL LENS

Figure III-15. Optical Schematics

For $N = 2.5$ and a focal length of 91.44 cm, $v_o = 667$ cycles/mm and $v = 243$ cycles/mm. Computing the value for x (the abscissa of Figure III-16) we obtain

$$x = N \lambda v = \frac{v}{v_o} = 0.364$$

Entering the figure for this value of x , the sine-wave response of the lens system is found to be 25% using the 50% obscuration curve. The angular resolution of the optical system is 0.45 second of arc and is derived from the Rayleigh criterion as given by

$$\alpha = \frac{1.22 \lambda}{d},$$

where α is the angular resolution,

λ is the wavelength, and

d is the aperture diameter.

The angular subtense of 1 meter at 200 kilometers is 1 second of arc, which is above the theoretical diffraction limit of the optical system.

For decentration tilt and for focus control, an achromatized pair of wedges will be used. Development is required to determine an automatic technique for measuring foci variation. The dioptric section, of the Baker catadioptric system, permits smoother balancing of higher order aberrations with the lower order so that reasonably good off-axis image response is obtained. The optical system is rigid enough so that realignment after injection into lunar orbit is not required.

Lens Design Consideration for Electrostatic Tape Camera

Lens design parameters for the electrostatic tape camera differ somewhat from those required for photographic emulsions. Differences exist in the spectral sensitivity between these two sensors. Figure III-16 shows the spectral response curve for electrostatic tape.

A glass window is located between the lens and the electrostatic tape. The location of the window in respect to the camera is shown in Figure III-17. The glass window and its location in the optical path will influence the lens design in that corrective elements near the focal plane may be designed into the camera assembly.

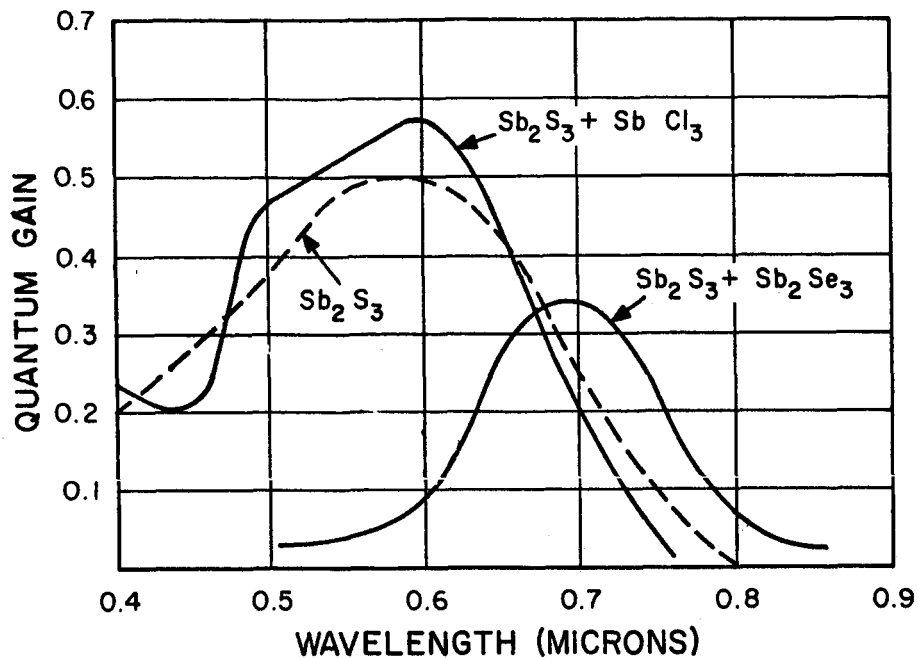


Figure III-16. Spectral Réponse Curves

The frequency response of a lens, for an electro-optical system, requires that the aberrations be balanced so that the aberration fringe surrounding the image of a point object is high in intensity but small enough in magnitude to yield high modulation at low frequency levels. This indicates that the relative illumination in the marginal zone regions should not be less than 40%.

The electrostatic tape is scanned horizontally by an electron beam. The sine wave response precludes that the tangential and radial residuals need to be balanced with respect to beam diameter as well as the linearity of the scan.

Dioptric systems having a focal length of 91.4 cm are within the state-of-the-art. Formidable problems arise when an f-number of 2.5 is required. These two requirements can be fulfilled in a catoptric or catadioptric type of design. As a high modulation response at low frequencies is necessary this means that obscuration, due to secondary mirrors, must be kept to a minimum.

Active image motion compensation systems require low error rotating optical members. This places an additional requirement on electrical power, size and weight for pressurization and thermal control. With a relatively 'fast' optical system IMC is adequate with a constant rate electrostatic tape transport system.

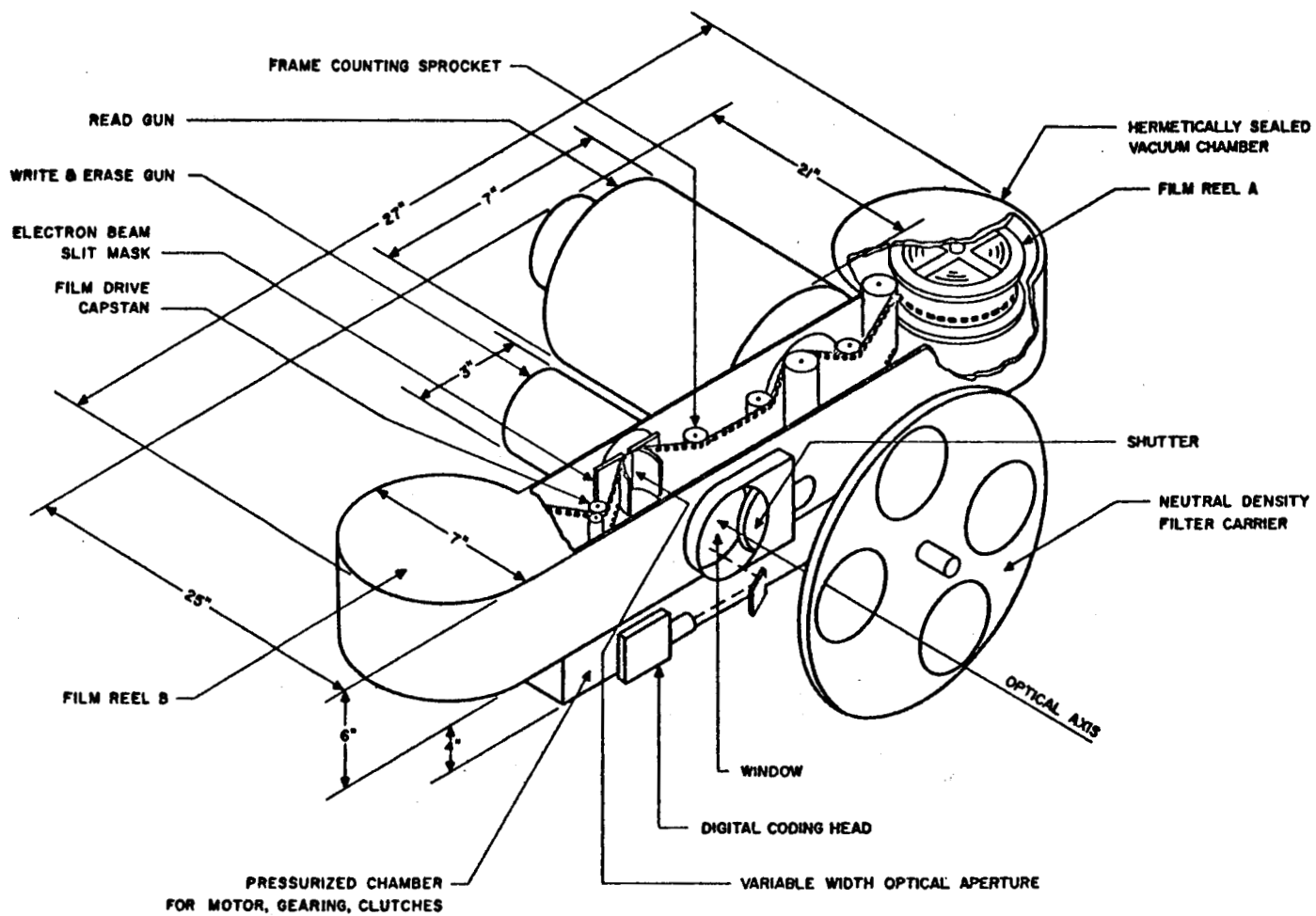


Figure III-17. Electrostatic Tape Camera Layout

Table III-C-1

Outline of System Configuration

	A	B	
Altitude (km)	200	250	250
Application	High Resolution Planimetric Mapping	Low Resolution Planimetric Mapping	High Resolution Planimetric Mapping
Altitude of Scan	Panoramic Normal to Orbit	Fixed Along Orbit	Fixed Along Orbit
Number of Lenses	1	1	1
E. F. L. of Lenses (cm)	91.44	30.5	91.44
Limit Resolution of object	1.1 meter	10 meters	1.4 meters
F/No	2.5	4	2.5
Field	3.5 ^o	11 ^o	3.5 ^o
Lens Type	Catadioptric	Dioptric	Catadioptric
Number of Cameras	4	2	2
Type of Shutter	Slit	Slit	Slit
Weight (Lens)*	109 lbs.	15 lbs.	109 lbs.
Size (Lens)(cm)	45.7 x 45.7	13 x 10.9	45.7 x 45.7
Power (Lens)	None	None	None

* Does not include the scan mirror or the scan mirror drive assembly.
Power requirements and weights are included in the section on structures.

D. STRUCTURE

The primary VOIS package contains a scanning mirror, a high-resolution optical system, four EST tape cameras, associated electronic equipment and servo-controlled drive units for indexing the rear mirror and making a single adjustment of the interlocked tape cameras for image compensation. (See Figure III-18).

The package is basically cylindrical in form and is a monocoque type structure. It consists of three reinforced steel cylindrical sections which permit the initial alignment of individual components before their integration in the package as a single unit.

Special emphasis has been placed on designing a vehicle which will minimize the shear and tensile forces acting on the mirror and lens surfaces as well as to provide suitable mountings for the optical components since it is necessary that the alignment of the optical system be maintained to a high degree of accuracy. To this end, all mirrors and lenses have been arranged so that their main surfaces will be in the plane of the thrust of the main rocket and retro-rocket motors. This means that they will be essentially in compression during the period of severe loading. (See Figure III-19). Glass is at least four times stronger in compression as in tension and if properly supported will not fail in compression.

Another major problem concerning the structure was that of possible damage or wrinkling of the optical surfaces as a result of thermal expansion of the optical components and warping of the structure with subsequent misalignment of the axis of the optical system. To prevent a detrimental stress build-up due to differential expansion, pre-loaded roller units are incorporated in the supports of the larger components. This will permit them to expand freely while being rigidly supported. In addition, structural materials having the same coefficient of expansion as quartz or glass will be utilized.

1. Primary Mirror Support

The primary mirror is supported by a series of pads which are bonded around the periphery of the mirror and connected to chrome molybdenum tubes by means of pre-loaded ball slides. The tubes are designed to distribute the load at the points of stress concentration and permit free expansion of the mirror.

Initial alignment of the mirror at assembly is effected by adjusting fine differential screws and flexure plates which are incorporated in the support. After final alignment by special methods using interferometers or other means, the mirror is riveted or otherwise permanently fastened in place.

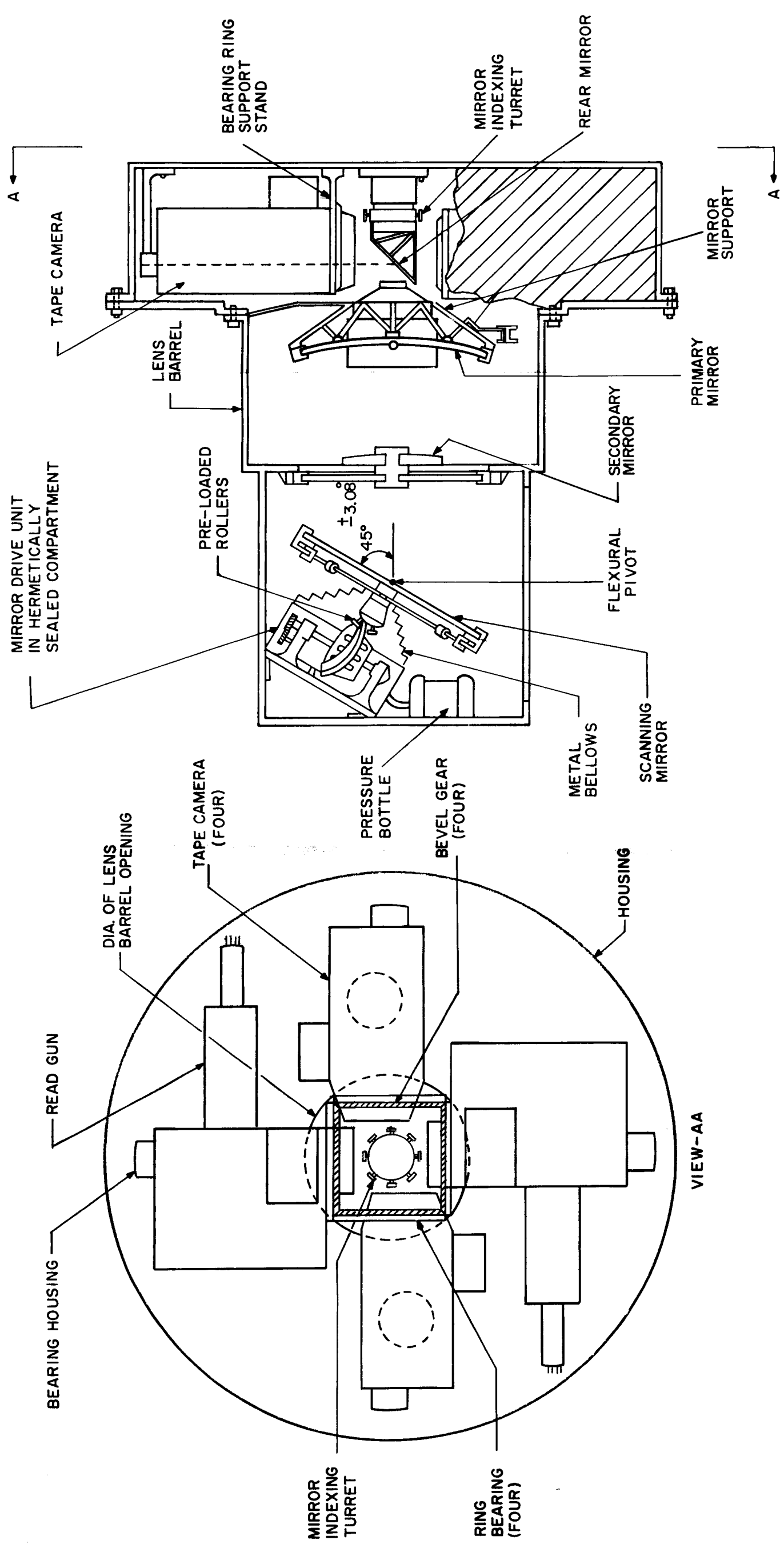


Figure III-18. Camera System Layout

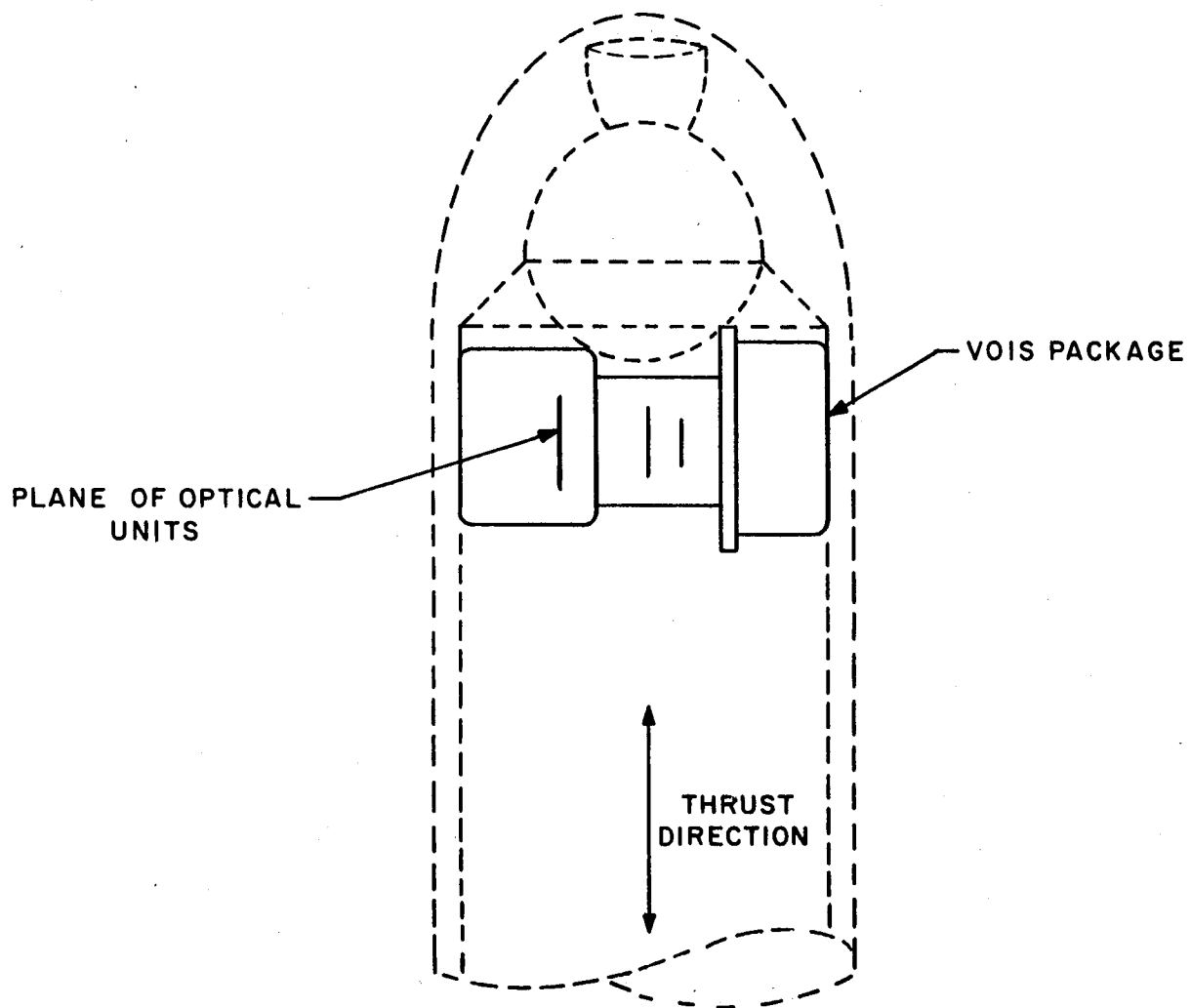


Figure III-19. Position of VOIS Package During Launch and Orbital Injection Phases

2. Scanning Mirror Support and Drive Unit

The scanning (wobble) mirror recommended by the Perkin-Elmer Corp. is a fused quartz mirror, elliptical in shape, with a 16" minor axis, a 24" major axis and a thickness of 4 inches. The unit weighs 25 - 35 pounds and is of the square cell sandwich type as shown in Figure III-20. It was further recommended that the mirror be provided with a back plate type of mounting such as shown in Figure III-21.

The present mirror is supported by chrome-molybdenum tubular members which permits it to expand freely. (See Figure III-22)

The mirror is pivoted on flexural pivots because of the small excursion (± 3 degrees) required and because it is desirable to avoid bearings whenever operating in a hard vacuum. These (crossed flexural) pivots are very accurate for rotations of up to 15 degrees.

The drive unit consists of a constant speed motor, a double ended cam and associated gearing. These cams have high accuracy, long life, low vibration and shockless performance even under high speeds. All bearings are pre-loaded to reduce the backlash to a minimum. See Figures III-18 and III-23.

The entire unit is enclosed in a hermetically sealed compartment where the pressure is monitored and maintained utilizing a pressure bottle. The pressure is sufficient to ensure operation throughout the period of operation. In addition, stellite bearings and dry film lubricants such as the CBS Labs lubricant CLD 5940 should provide additional reliability to the system in case of failure of the pressurization system.

3. Rear (Indexing) Mirror and Drive Unit

The rear (indexing) mirror is supported on an eight station indexing turret which itself is held very accurately by pre-loaded self-aligning angle bearings. See Figure III-23. Initial alignment of the mirror is accomplished by means of a standard flexural post and four differential screws. After final alignment by more exact means, the base is fixed permanently and the turret is left free to revolve about the optical axis.

The mirror is indexed by means of a multiple, double ended servo controlled cam. These cams can index a turret to 0.6 seconds of arc. As presently visualized, final and accurate positioning of the mirror will be made by a precisely ground locating pin driven by a face cam which is in turn driven, through gearing, by the indexing cam.

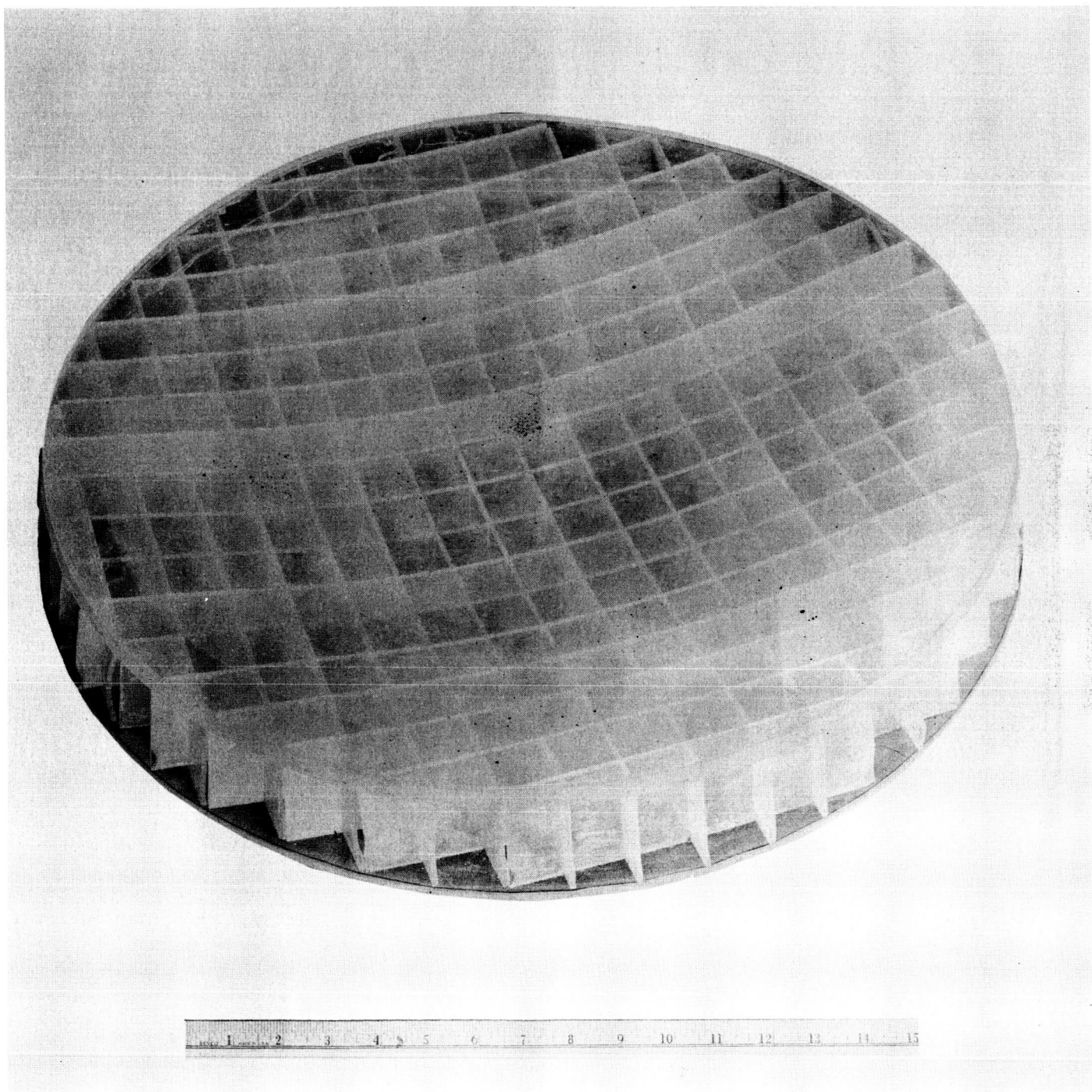


Figure III-20. Scanning (Wobble) Mirror

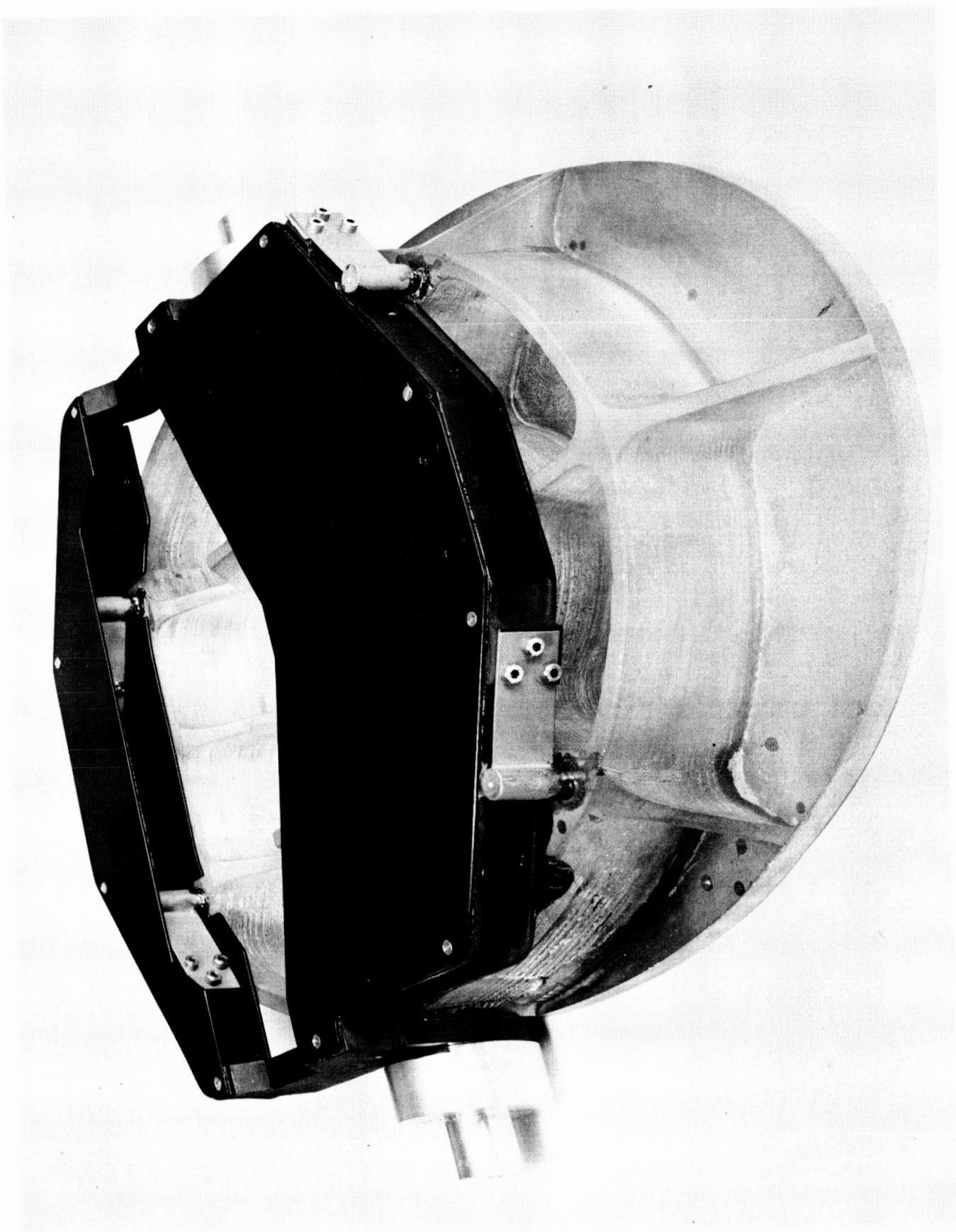


Figure III-21. Scanning Mirror Back Plate Mounting

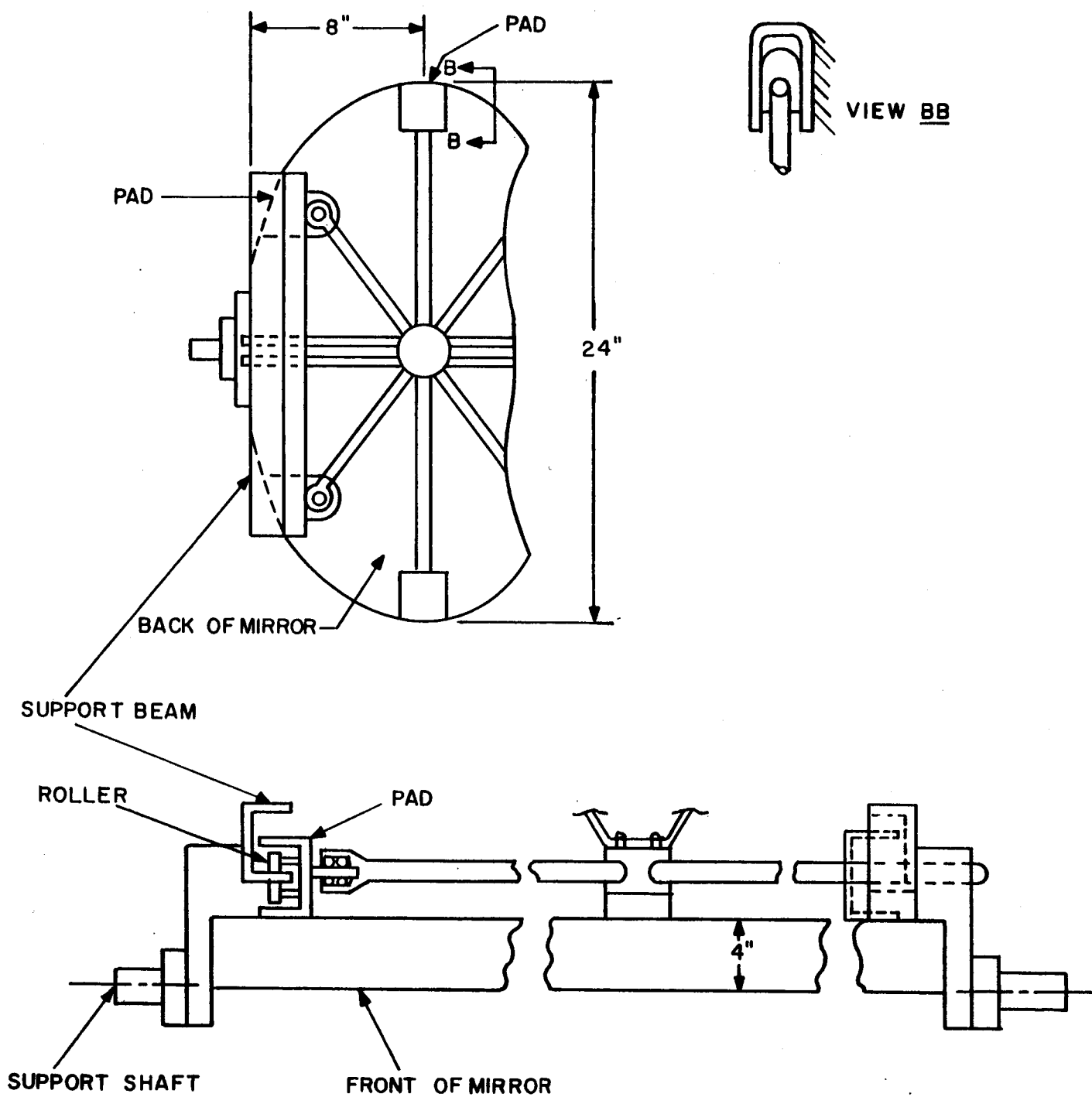


Figure III-22. Scanning (Elliptical) Mirror Details

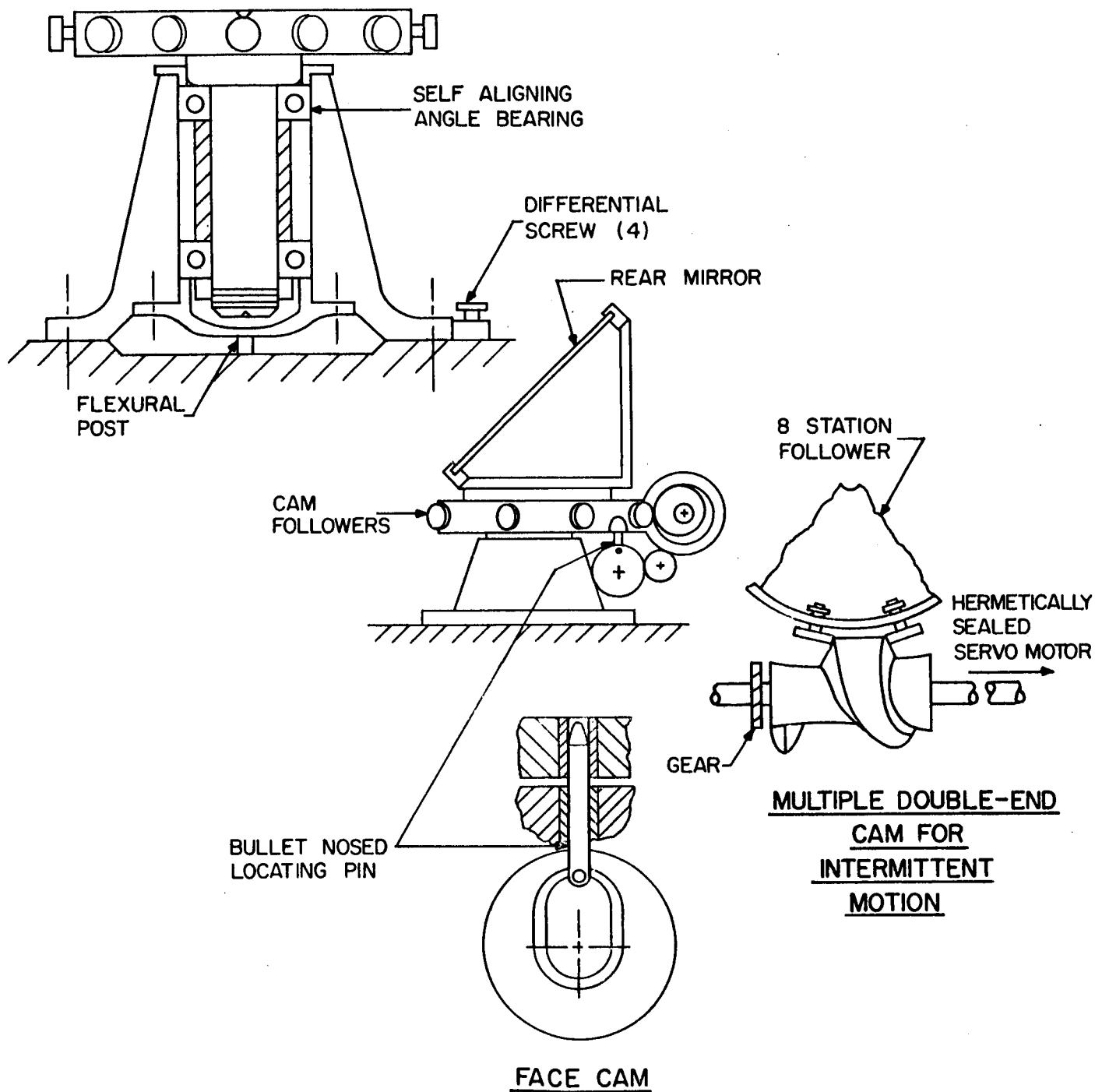


Figure III-23. Rear Mirror Drive and Support Details

These cams, etc. are not in pressurized compartments because the requirements are such that the turrent will be required to index only 180 times (approx.) during the entire period of operation and it is felt that dry film lubricated rollers etc. will withstand the rigors of a hard vacuum.

4. VOIS Dynamics

a. Scanning Mirror

The scanning mirror oscillates very precisely about a 45 degree line with a maximum excursion of approximately ± 3 degrees. The forward scan time is about 7.9 seconds and the return, dead time, is close to .9 sec. During this time the scanning angle swept through, on the terrain, is approximately 12.3 degrees. The cam drive used to accomplish this motion rotates at a speed of approximately 6.8 rev/min. and is made up of parabolic and straight line curves. These curves were chosen because they will not only accomplish the desired motion, but will drive the mirror with relatively low accelerations of a simple form. This will facilitate the cancelling of undesirable torques in the system.

For the mirror previously described, the moment of inertia is of the order of 5 lb-in-sec² resulting in a maximum torque of ± 2.88 in-lb, on the package, as shown in Figure III-24.

b. Indexing Cam Drive

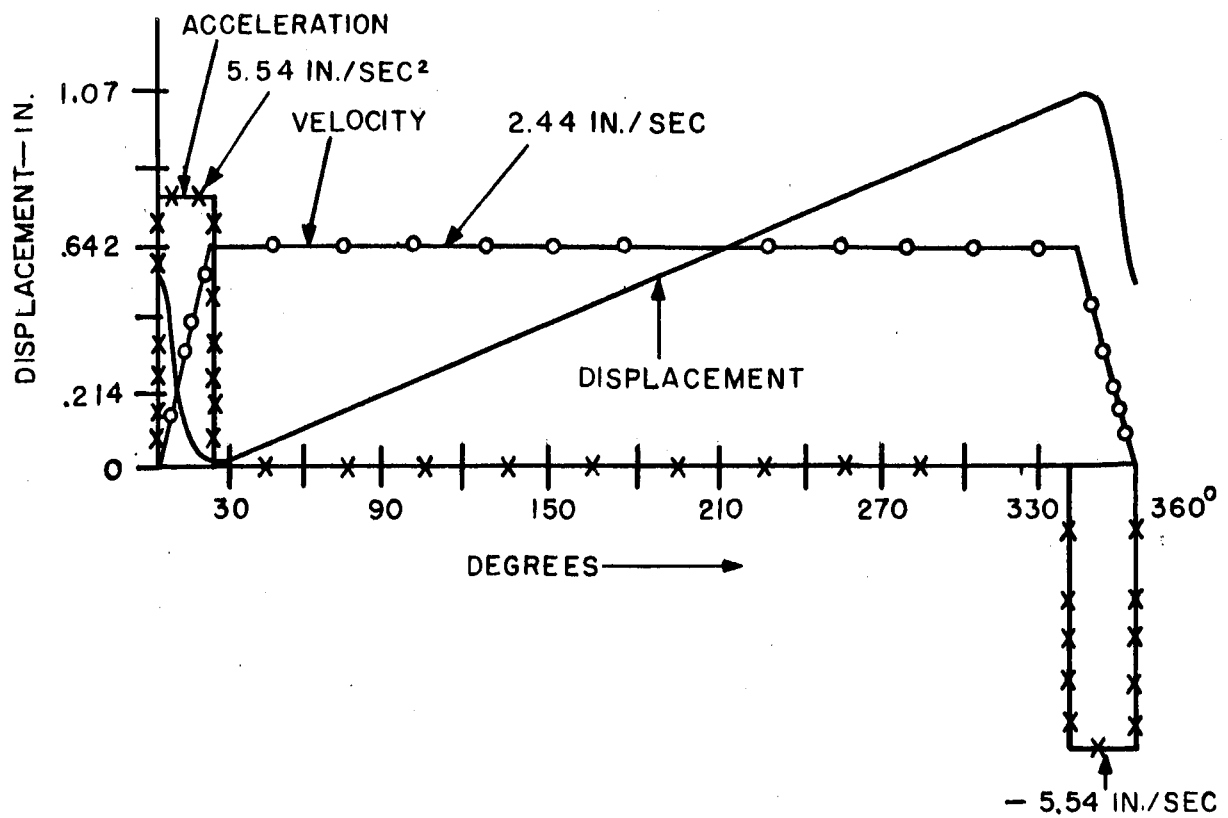
The indexing cam makes 2 revolutions for every 1/4 revolution of the turrent. This low indexing speed in conjunction with the parabolic and straight line curves selected for the cam surfaces results in accelerations and, vibrations of low magnitude and simple form. For a turrent of approximately .09 lb-in-sec², the resulting accelerations (max. .03 in-lb) etc are as shown in Figure III-25.

c. Angular Momentum of a Pair of Reels

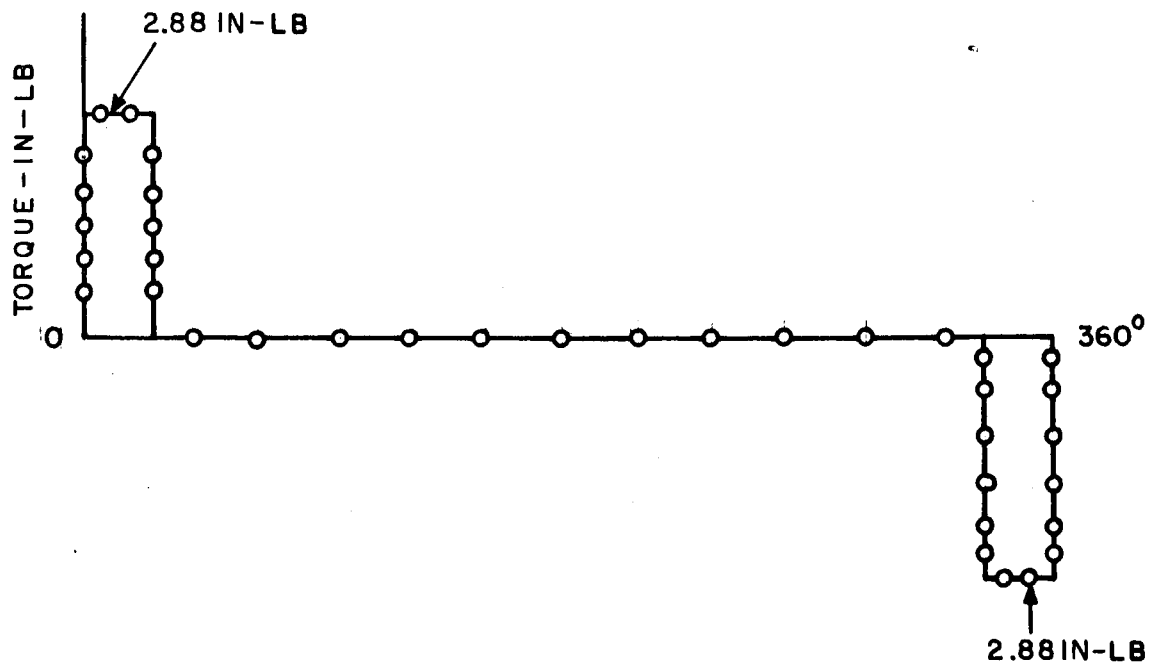
Each pair of reels (1 pair to each tape camera) is driven by a constant speed capstan. 1500 feet of tape (total weight 15 lb) are transferred between the reels at either the reading speed of 3.28 ft/sec or at the imaging speed of .092 ft/sec. This adds undesirable angular momentum to the system which must be eliminated. These disturbances may be considered random when all four tape cameras are considered and difficult to analyze. To determine the relative magnitude of angular impulse involved, two cases were considered:

Case 1: 1500 feet of tape on one reel and a few turns on the other reel.

Case 2: 750 feet of tape on each reel.

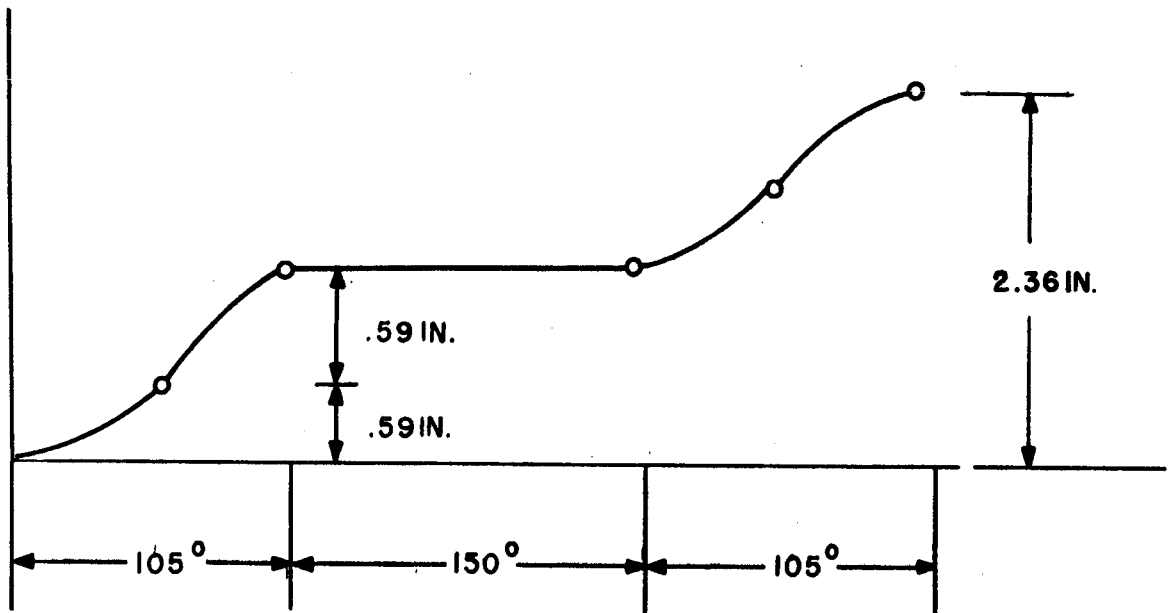


ACCELERATION-VELOCITY-DISPLACEMENT DIAGRAM

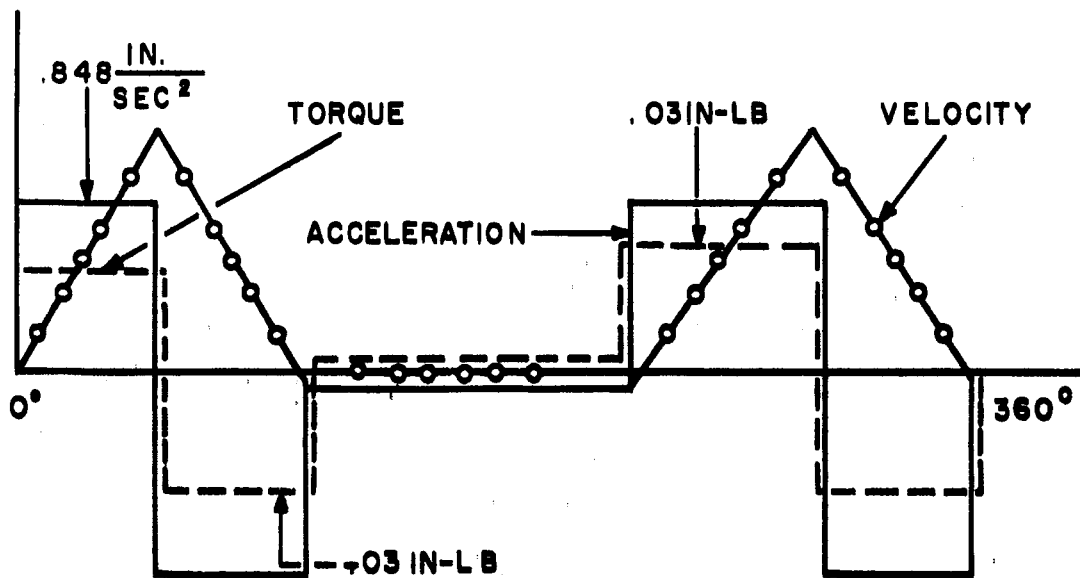


TORQUE CURVE

Figure III-24. (a) Acceleration - Velocity - Displacement Diagram,
(b) Torque Curve Diagram



DISPLACEMENT DIAGRAM



TORQUE-ACCELERATION-VELOCITY DIAGRAMS

Figure III-25. (a) Displacement Diagram, (b) Torque - Acceleration Velocity Diagram

For the two 12 inch, reels, the maximum angular impulse,

$$\left[\int_0^t M \, dt \right] = d(I\omega) = H_2 - H_1 = 4.68 \text{ in-lb-sec.}$$

where H_1 = angular momentum for case 1

H_2 = angular momentum for case 2

M = torque lb-in.

Summary:

- (1) Maximum torque about y axis due to scanning mirror = ± 2.88 in-lb
- (2) Maximum torque about Z axis due to indexing turrent = $\pm .03$ in-lb
- (3) Maximum impulse about y axis due to reels = $2(4.68) = 9.36$ in-lb-sec
- (4) Maximum impulse about Z axis due to reels = 9.36 in-lb-sec

Where the Z axis is parallel to the local vertical and the x axis is coincident with the optical axis. The center of the coordinate system is taken as the center of the back mirror (See Figure III-18).

IV. SUMMARY

The study program has covered the analysis of the various components included in the VOIS, and a set of specifications has resulted from this analysis. Table IV-1 lists these specifications. During the study it was found that an optimum altitude, as such, did not exist. In general, the higher the altitude the more alleviated were the problems in image motion compensation, optical field-of-view, and available transmission time. However, maximum resolution suffered from the requirements of higher altitudes. From the preceding analysis and considering the requirements for maximum resolution, altitudes in the range of 200 to 250 kilometers offer the best choice. It is not expected that perturbations to the orbit will affect the system characteristics over the operational lifetime of the vehicle.

Two separate systems have been considered in the study. The panoramic scan system offers the maximum resolution and complete coverage of the lunar surface at the expense of vehicle complexity and an increase in ground data processing. The alternate stripping system offers a more simplified system at the expense of high resolution coverage in the mid-latitudes. In both of the systems a Baker catadioptric optical system is utilized for high resolution imaging. This system offers the advantage of high lens resolution to take best advantage of the capabilities of the electrostatic storage tape camera.

The capabilities of the electrostatic storage tape camera required for the VOIS though not present state-of-the-art represent only modest advancements and should be representative of the EST capabilities in the 1963 to 1964 time periods.

The stereo capabilities of the systems differ. For the panoramic scan system viewing of the lunar surface at different angles is accomplished by the sidelap generated between successive orbits. In general, reasonably good stereo should be obtained between latitudes of 30 and 60 degree. However, the system is limited in angle of convergence since the maximum angle of convergence is approximately the angle of scan. The alternate system offers a better system for stereo viewing since two optical systems are employed and one optical system may be tilted off nadir in the orbital plane to generate the necessary convergence angle. On this basis good stereo could be obtained over most of the lunar surface. A convergence angle of approximately 15 degrees would not degrade the planimetric resolution to any great extent (the planimetric resolution is modified by the cosine of the convergence angle) and would offer reasonably good resolution in the third dimension.

The versatility of the EST camera and the techniques for obtaining high resolution and mapping data permit considerable variation in the operational programming for the system. In addition, the redundancy in design so that loss of a part of the system would only reduce its capabilities without complete loss of the system yields a high reliability to the overall payload.

Table IV-1

VOIS Characteristics

	Panoramic Scan System	Alternate System	
Average Orbital Altitude	200 km	250 km	
Orbital Period (seconds)	7656	7959	
Per Cent Transmission Time	60	60	
Sensor	70 mm EST camera (57 mm active surface)	70 mm EST camera (57 mm active surface)	
Limiting EST Resolution	200 TV lines/mm	200 TV lines/mm	
Sensitivity (ft-candle-secs.)	0.002	0.002	
Wavelength Response (microns)	0.5 to 0.7	0.5 to 0.7	
Tape Capacity/Camera (feet)	1500	1500	
Method of Exposure	Slit and moving Tape	Slit and moving Tape	
Optics		Mapping	High Resolu- tion
	focal length (mm)	305	914.4
	focal ratio	F/4	F/2.5
	exposure time (milliseconds)	13	3

	Panoramic Scan System	Alternate System
Resolution per T. V. line		
High Resolution (meters)	1. 1	1. 4
Mapping Resolution (meters)	10	10
Pointing Resolution (meters)	60	60
Storage Time (total 4 cameras)	2 days	2-4 days
Video Bandwidth (kilocycles/second)	500	500
Camera Weight (pounds)	80@	80@
Optics Weight (pounds)	140	140
Structure Weight (pounds)	100	100
Control Circuitry (pounds)	10	10
Average Power (watts)		
Camera (Tape Transport plus read-out)	85	85
Transmitter	25 - 50	25 - 50
Control Circuitry	5	5
Volume (Cubic feet)		
Camera (4)	~ 25	~ 25
Optics	~ 15	~ 5
Total Weight (pounds)	570	570
Total Average Power (watts)	150	150

	Panoramic Scan System	Alternate System
Total Volume (cubic feet)	~ 40	~ 30
Thermal Control		
Optics	$20^{\circ} \pm 5^{\circ}\text{C}$	$20^{\circ} \pm 5^{\circ}\text{C}$
Other Components	0 - 50°C	0 - 50°C